Petrology and Major Element Geochemistry of Basaltic Glasses from the Blanco Trough, Northeast Pacific.

A thesis presented to the Faculty

of the State University of New York

at Albany

in partial fulfillment of the requirements

for the degree of

Master of Science

College of Science and Mathematics

Department of Geological Sciences

Glenn A. Gaetani
1990

Petrology and Major Element Geochemistry of Basaltic Glasses from the Blanco Trough, Northeast Pacific.

Abstract of

a thesis presented to the Faculty

of the State University of New York

at Albany

in partial fulfillment of the requirements

for the degree of

Master of Science

College of Science and Mathematics

Department of Geological Sciences

Glenn A. Gaetani
1990

Abstract.

The original electron microprobe analyses of suite of basaltic glasses recovered in 1968 by W.G. Melson and co-workers from the Blanco Trough have extremely unusual characteristics. Their compositions plot in a region of the normative Ol-Di-Pl-SiO_2 tetrahedron which suggests that they represent liquids in equilibrium with an upper mantle assemblage of olivine + orthopyroxene at 10-15 kb. Given the present state of controversy surrounding the composition and depth of origin of primary MORB, natural examples of such liquids would be very important. The major element variations observed in the suite imply that the dominant phases are olivine and an iron-aluminum rich spinel. The crystal/melt partitioning data are consistent with an unusually large Fe_2O_3 component in the melt, which could help to explain the variation in liquidus phases, and thus the suite's position in Ol-Di-Pl-SiO_2 space.

New analyses of the original samples, performed on the microprobe at Rensselaer Polytechnic Institute, have failed to reproduce the original anomalies. The R.P.I. data does show that the glasses are slightly enriched in FeO* giving them unusually low Mg/(Mg + Fe) ratios for otherwise primitive looking mid-ocean ridge tholeiites. The new analyses plot near the Ol-Di join when projected from Pl onto the Ol-Di-SiO_2 plane, a region not uncommon for primitive MORB. The disagreement between the two data sets appears to be the result of a transposition of the FeO* and CaO abundances in the Smithsonian analyses prior to their publication by Melson et al. (1977), in addition to minor differences in calibration between the two laboratories.

All of the Blanco Trough glasses that were studied in thin section contain olivine, while 61.5% are saturated in chromian spinel. Some of the olivines display deformation bands and possible fluid inclusions, indicating that they are probably cumulate xenocrysts. In contrast with most other MORB suites, plagioclase is a major phenocryst phase in only one sample and is absent completely from 38.5% of the thin sections. Based on petrography, the first phase to appear is olivine, followed by assemblages of olivine + chromian spinel, olivine + chromian spinel + plagioclase and olivine + plagioclase. Although the appearance and disappearance of phenocryst phases agrees very well with

the phase equilibria in the system An-Fo-Di, no simple relationship exists between the Mg/(Mg + Fe) ratio of the liquid and the phenocryst assemblage.

Least-squares mixing models show that the primitive and evolved ends of the suite cannot be related simply by the fractional crystallization of an assemblage of olivine + chromain spinel + plagioclase. The best fit is obtained if clinopyroxene is added to the crystallizing assemblage, although it is not found as a phenocryst phase in any of the samples. The problem of needing to crystallize significant amounts of clinopyroxene to explain a suite of MORB which does not contain clinpyroxene is not unique to this study, but has been recognized by other workers for a number of years. The petrogenesis of the suite appears to involve several stages, in addition to fractional crystallization of olivine, chromian spinel and plagioclase in a shallow level magma chamber. Polybaric crystallization of several batches of parental magma, followed by homogenization during episodes of magma-mixing seems likely.

Acknowledgments.

Researching and writing a master's thesis is, more than anything else, an apprenticeship. In my three years here each member of the Department of Geological Sciences has contributed in some way to this process of learning and growth. In doing so they have all added to my development both as a scientist and a person. To each of the members of the faculty, staff and student body who have worked with me, helped me, or just put up with me I give my sincerest thanks. The members of my thesis committee, Steve DeLong, John Delano and Ed Mathez, are thanked for their careful reading of my work and for holding me to high standards. Thanks go to Dave Wark, at R.P.I., for his help in the microprobe lab, and Ian Carmichael, at Berkeley, for performing the FeO determinations. I benefitted greatly from the help and cooperation of Bill Melson, Tim O'Hearn and Sorena Sorensen, at the Smithsonian. Special thanks go to the two faculty members who have given me the most in terms of their time, advice and support. Steve DeLong has been a source of (very, very important) financial support and much encouragement. He has helped me to understand which questions need to be asked and has allowed me the freedom to try to answer them. His patience and gentle prodding whenever I was going off in the wrong direction has been greatly appreciated. The use of his least-squares mixing program made the petrogenetic modelling possible. John Delano has taught me, both in words and by example, how to be careful and thorough in all things, although I'm afraid that I will never be able to live up to his considerable abilities. His intensity and dedication to his work are truly unique.

I never would have survived the past three years without my fellow graduate students. The long hours never seemed half as bad when someone else was suffering along with me. Thanks. They have each contributed to this work in some way. Special thanks go to Dave Foster, Terry Spell, Greg Norrell and Pete Copeland for taking the time to help a lowly master's student learn the ropes. Ben Hanson has been a good friend and sounding board for ideas about basalt petrogenesis. Uli Eberle's infectious smile and kind words during stressful times were indispensable (even that damn giggling). The deepest, most heartfelt thanks possible go to Rob Alexander. He has been a close friend, trusted advisor, drinking buddy, and all around nice guy over the past three years. My words will never be able

to do justice to just how important his friendship has been to me. He has more kindness and insight than anyone else I know. He has been, and will always be, like a brother to me.

My wife Renee has been an endless source of love and friendship. She is something very special. I want to thank her for the patience and understanding that she has shown, especially over the past six months while we have been apart. She always seemed to know just when I needed a kind word and just when to kick me in the pants. She makes a difference in my life every day, and I love her very much. Robert and Carol Mandarano, my in-laws, are thanked for their friendship and support (which included quite a few free meals), and for letting their daughter marry a guy with no job.

None of this would have been possible without the love and support of my parents, Nick and Joan Gaetani, and my sister, Debbie Gaetani. They have helped in many ways, both large and small. Although I'm not sure if they always understood why I quit my job to look at rocks, they were always ready with whatever help I needed. Dad, this thesis is the answer to your frequently asked question "What have you been up to?"

This thesis was supported by NSF grant OCE8818315, and teaching assistantships from the Department of Geological Sciences of SUNY at Albany.

Table of Contents.

List of Tables.

List of Figures.

1. Mid-Ocean Ridge Basalts and the Blanco Trough Glasses.

1.1 Introduction.

Basaltic volcanism is a phenomenon that is known to have occurred on all of the terrestrial planets, the Moon, and some asteroids (BVSP, 1981). The ubiquitous nature of basaltic magmas indicates that they are of fundamental importance in the geochemical differentiation of planetary bodies. Mid-ocean ridge basalts (MORB) are believed to be the products of partial melting of a peridotitic upper mantle which segregate from their source region and reach the surface at the Earth's system of mid-ocean ridges. On a global scale this process leads simultaneously to the depletion of the oceanic upper mantle in elements which are strongly partitioned into the liquid during partial melting (incompatible elements) and the creation of an oceanic crust of basaltic composition approximately 10 kilometers thick. Due to their isolation from the continental crust, as well as the thin character of the oceanic crust at spreading ridges, MORB are thought to have erupted relatively unchanged from where they were segregated from their source regions. This has led many to believe that MORB can give insight into the composition, conditions and processes of the Earth's upper mantle, and that an understanding of their genesis and evolution is therefore fundamental to our knowledge of the geochemical evolution of the Earth's crust-mantle system.

Our understanding of the petrogenesis of MORB is constrained by the remarkably limited range of major element compositions displayed by samples recovered from spreading ridges and fracture zones throughout the world, with few examples of either very primitive or highly fractionated basalts (Engel et al., 1965; Walker et al., 1979; Stolper and Walker, 1980). Quenched MORB glass analyses cluster around the experimental one-atmosphere cotectic for liquids in equilibrium with olivine, plagioclase, and diopside in the olivine-diopside-plagioclase-silica tetrahedron (Walker et al.1979; Stolper, 1980) (Fig. 1). This places broad limits on the amount of heterogeneity, both in terms of bulk composition and oxidation state, which is possible in the MORB source regions. It also limits the range of possible processes, e.g., variations in degree of partial melting and range of polybaric fractional crystallization, that can lead to the generation of the large volumes of melt necessary to form

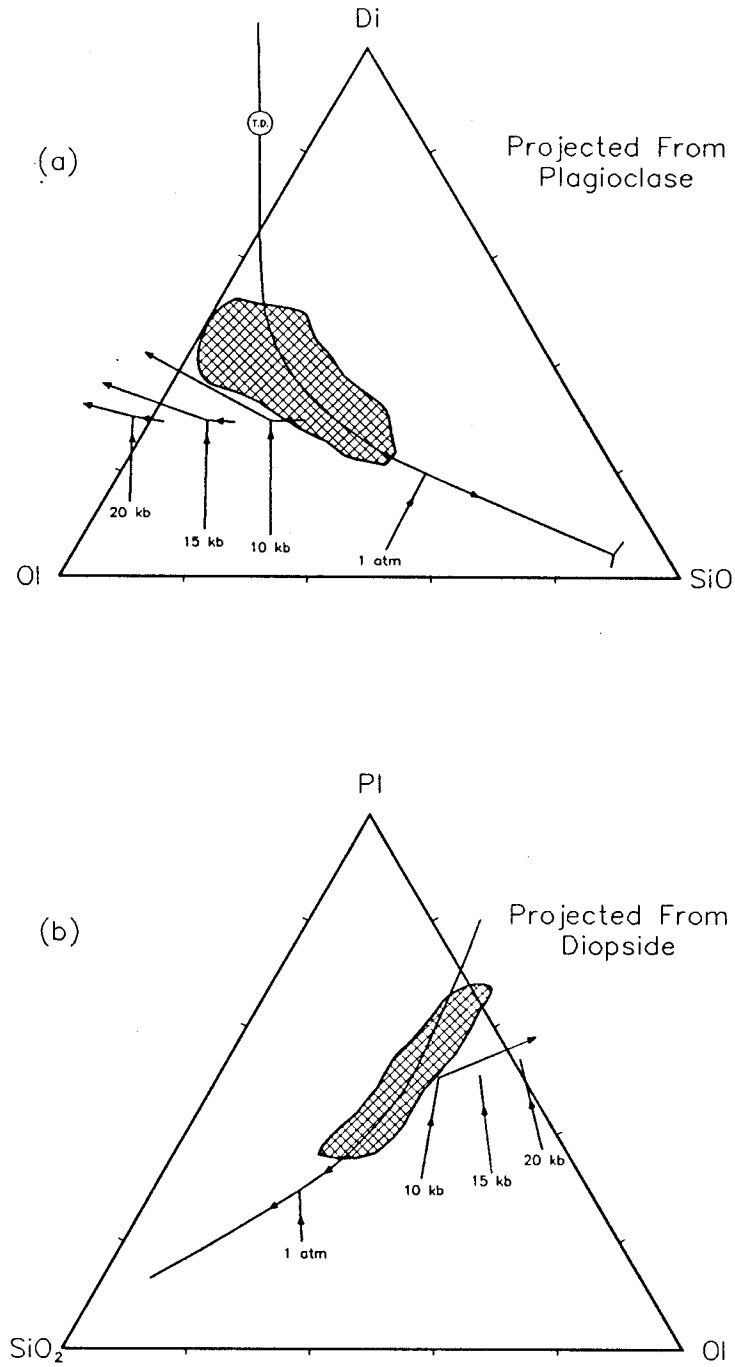

Figure 1. Clustering of MORB glass analyses at the 1-atmosphere cotectic of Walker et al. (1979) on (a) the projection from plagioclase onto the olivine-diopside-silica plane, and (b) the projection from diopside onto the olivine-plagioclase-silica plane in the Ol-Di-Pl-SiO_2 tetrahedron. After Stolper (1980).

the oceanic crust on a global scale.

In 1968 W.G. Melson and co-workers recovered a suite of basalts in a dredge haul from a 950 meter section of the north-facing wall of the Blanco Trough, in the northeast Pacific (Fig. 2). Glass chips from these samples were analyzed by electron microprobe at the Smithsonian Institution and although quite similar to normal abyssal tholeiites in some respects, the original analyses appear to show a number of extremely anomalous geochemical characteristics.

Section two of this chapter reviews the criteria by which primitive MORB are distinguished from those that are more evolved and summarizes the controversy surrounding the nature of primary MORB magmas. Section three discusses the anomalous location of the BT suite within the olivine-diopside-plagioclase-silica tetrahedron based on the original analyses, their location in the same system based on a new set of analyses, performed on the electron microprobe at Rensselaer Polytechnic Institute.

1.2 Primitive MORB and Primary Magmas.

The study of the quenched glass commonly found on the outer few millimeters of pillow basalts makes it possible for petrologists to avoid the problems inherent in studying crystalline basalt (e.g., mechanical enrichment or depletion due to flotation or settling of crystals, respectively, and xenocrystic contamination), giving a closer approximation to actual liquid compositions (Byerly et al., 1977; Staudigel and Bryan, 1981). Because the earliest crystallizing phases from MORB under a variety of conditions are known to be magnesian olivine, chromian spinel, calcic plagioclase, and magnesian clinopyroxene, some generally accepted criteria for distinguishing glasses which have undergone the least amounts of fractional crystallization have been established. Those liquids identified as having the highest $Mg/(Mg + Fe^{2+})$ ratio (Mg#) and $Ca/(Ca + Na)$ ratio (Ca#), as well as low concentrations of the incompatible elements (TiO_2,Na_2O, K_2O, etc.) must be closest in composition to a true mantle derivative, and so are taken as being the most primitive (Green et al., 1979; Presnall and Hoover, 1987).

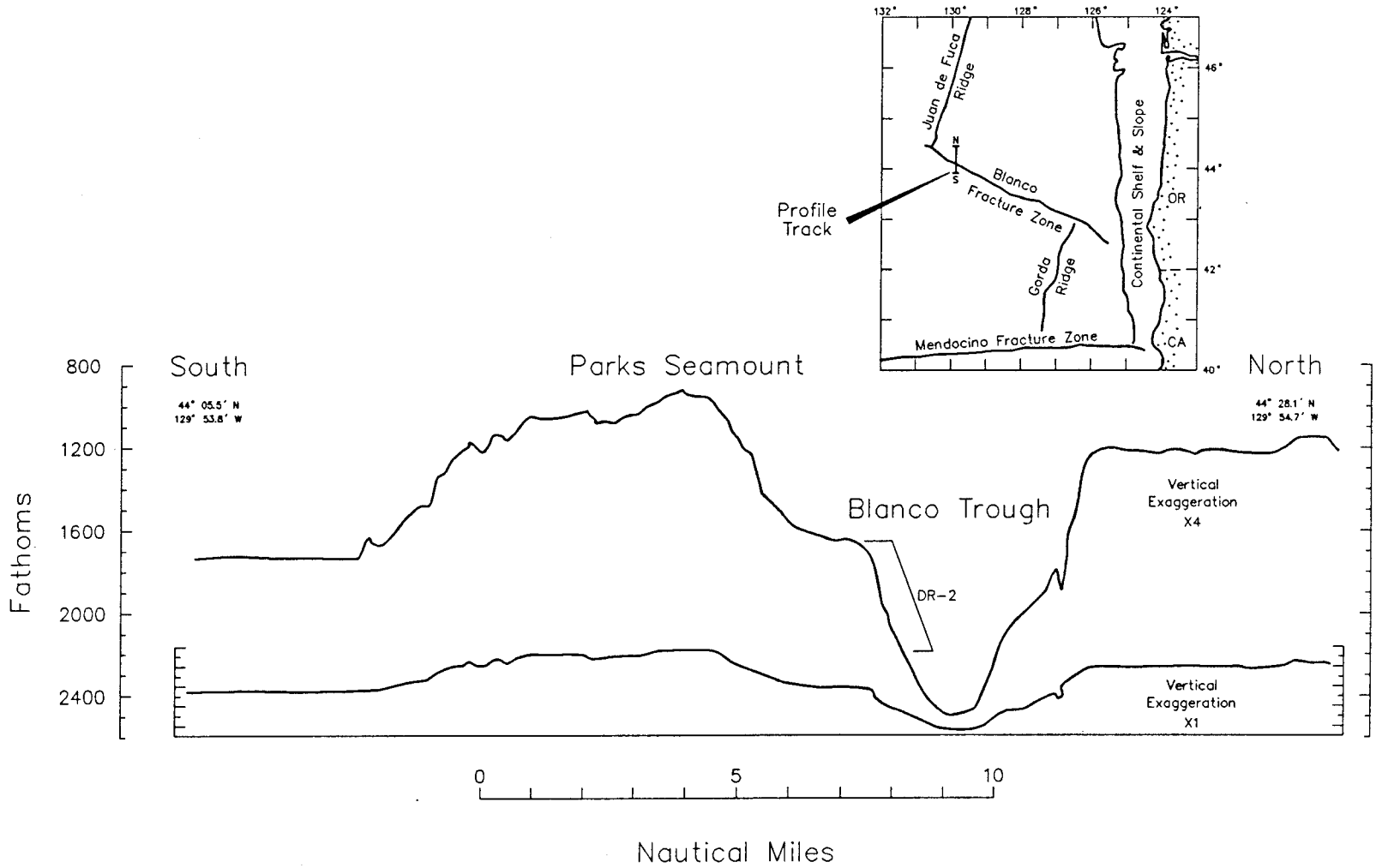

Figure 2. Bathymetric profile of the Blanco Trough and Parks Seamount showing the location of dredge #2. Inset gives location of profile. After Melson (1969).

Apart from simply identifying which basalts are the least evolved, a great deal of effort, and controversy, has gone into identifying MORB which are candidates for primary magmas. These are melts which segregate from their source region and reached the surface unchanged (Carmichael et al., 1974). In order to be able to understand in detail the processes involved in the petrogenesis of MORB, it is necessary to understand the phase relations of basaltic melts in their source regions as well as in near surface magma chambers. Given a magma composition which is primary, petrologists could identify the composition of the phases present in, as well as the depth of, the source region of MORB, and place limits on the degree of partial melting which took place prior to segregation.

Two models currently exist as to the composition and depth of origin of the primary magmas which give rise to mid-ocean ridge basalts. One model predicts the formation of primary liquids through partial melting of an assumed upper mantle composition at approximately 10 kilobars, or 30 km, the depth of a proposed cusp in the mantle solidus due to the coexistence of spinel and plagioclase. According to this model a primary magma is similar to the most primitive MORB recovered from the ocean floor (Presnall et al., 1979, Presnall and Hoover, 1984, 1986, 1987). The second model involves partial melting at pressures of 15-20 kb (Green et al., 1979; Jacques and Green, 1980; Falloon and Green, 1987; Falloon and Green, 1988; Falloon et al., 1988), or perhaps as high as 30 kb (O'Hara, 1968), whose product is a picritic magma which then undergoes fractional crystallization of olivine in order to give rise to primitive MORB.

Experimental petrologists have applied two approaches in using phase equilibria studies to put constraints on the composition of primary magmas, and the depths at which they form. The first approach involves the equilibration of a primitive MORB composition at mantle pressures and temperatures to determine which phases are on, or near, the liquidus (e.g. Bender et al., 1978; Green et al., 1979; Fujii and Bougault, 1983). A true primary MORB must have been in equilibrium with a residual assemblage of olivine + orthopyroxene ± clinopyroxene. The interpretation of results from this approach, however, have not been unanimously accepted (Thompson, 1987; Falloon and Green, 1987). An alternative approach is to melt a peridotite that is assumed to have had little history of basalt extraction (a "fertile" lherzolite) under a number of mantle pressure and temperature conditions

to determine the composition of liquids produced by various degrees of partial melting (Jaques and Green, 1980). Despite the directness of this approach, there are difficulties in producing enough glass to overcome the problem of quench modification in simple peridotite melting experiments. This has been largely overcome through the use of the "sandwich" technique, in which a layer of basaltic glass is placed between two layers of peridotite and then the entire assemblage is equilibrated at upper mantle pressure and temperature conditions (e.g. Stolper, 1980; Takahashi and Kushiro, 1983; Fujii and Scarfe, 1985; Falloon and Green, 1987; Falloon and Green, 1988; Falloon et al., 1988).

Although application of the sandwich technique in several different studies has led to a fairly consistent picture of the phase relations of peridotite and primitive basalt under mantle conditions, there is little consensus as to the nature of primary MORB. The controversy arises largely from the fact that primitive MORB display a range in silica saturation from nepheline normative to silica normative. An experimental study by Stolper (1980) was the first to show that the pseudo-invarient point for primitive MORB in equilibrium with a lherzolite residua moves toward progressively more olivine rich compositions with increasing pressure, as shown in Fig. 1a. Many of the phase equilibria studies performed since Stolper's (e.g. Takahashi and Kushiro, 1983; Falloon and Green, 1987) have given qualitatively the same results, although the precise position of cotectics for a given pressure has changed slightly. Based on these findings, many believe that the simplest explanation for the observed range in silica saturation is melting at pressures ranging from 8 to 20 kilobars, followed by olivine fractionation (Falloon and Green, 1988).

1.3 The Blanco Trough Suite.

When projected onto the Ol-Di-SiO_2 and Ol-Pl-SiO_2 faces of the Ol-Di-Pl-SiO_2 tetrahedron (Walker et al., 1979), the Smithsonian microprobe analyses of the BT glasses fall along a trend which conforms broadly with the 10 to 15 kb olivine + orthopyroxene cotectics as defined by the experiments of Stolper (1980) (Fig. 3). This trend is distinct from both the general clustering of mid-ocean ridge glass compositions in general (Fig. 1), and the trends observed within individual MORB suites from the FAMOUS, Gorda, and Tamayo regions (Fig. 4). If accurate these analyses would seem to imply

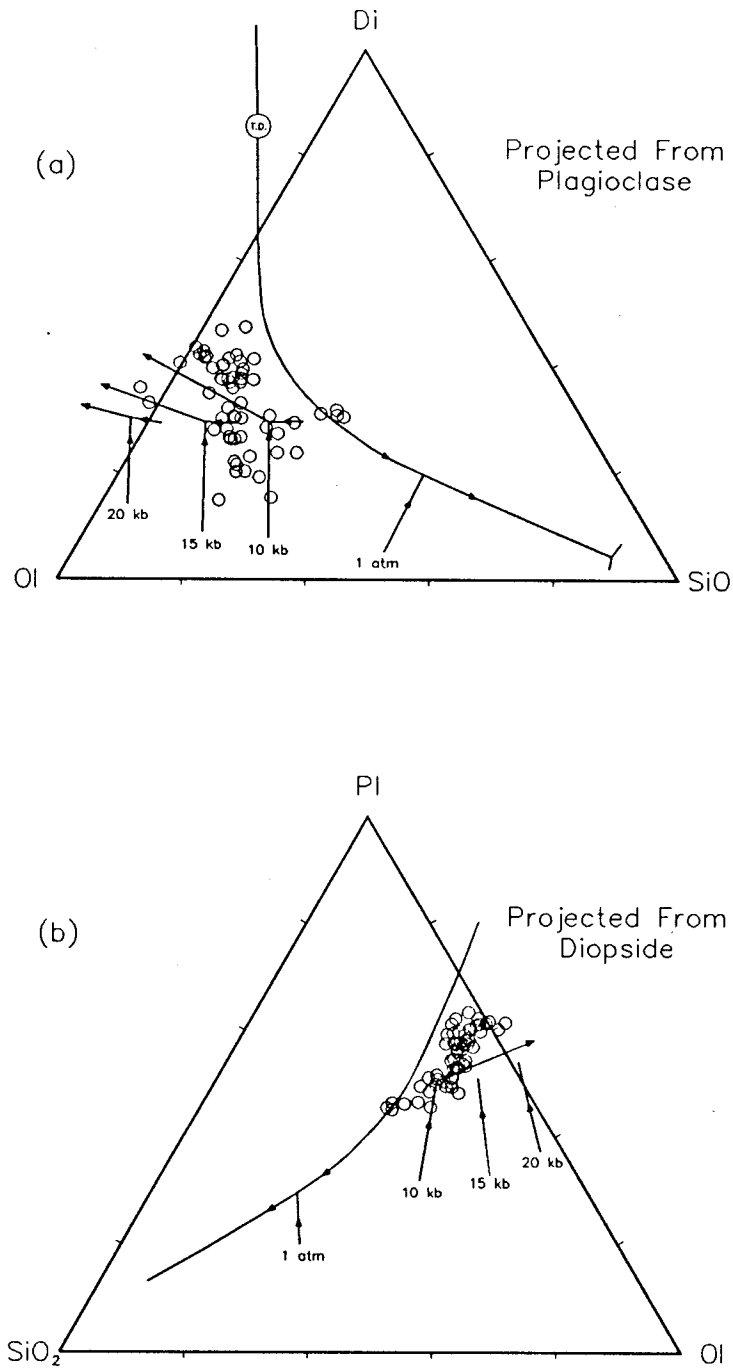

Figure 3. Smithsonian analyses of the Blanco Trough glasses projected (a) from plagioclase onto the olivine-diopside-silica plane, and (b) from diopside onto the olivine-plagioclase-silica plane in the Ol-Di-Pl-SiO_2 tetrahedron. Note the location of the glass compositions with respect to the 10 and 15 kb cotectics of Stolper (1980).

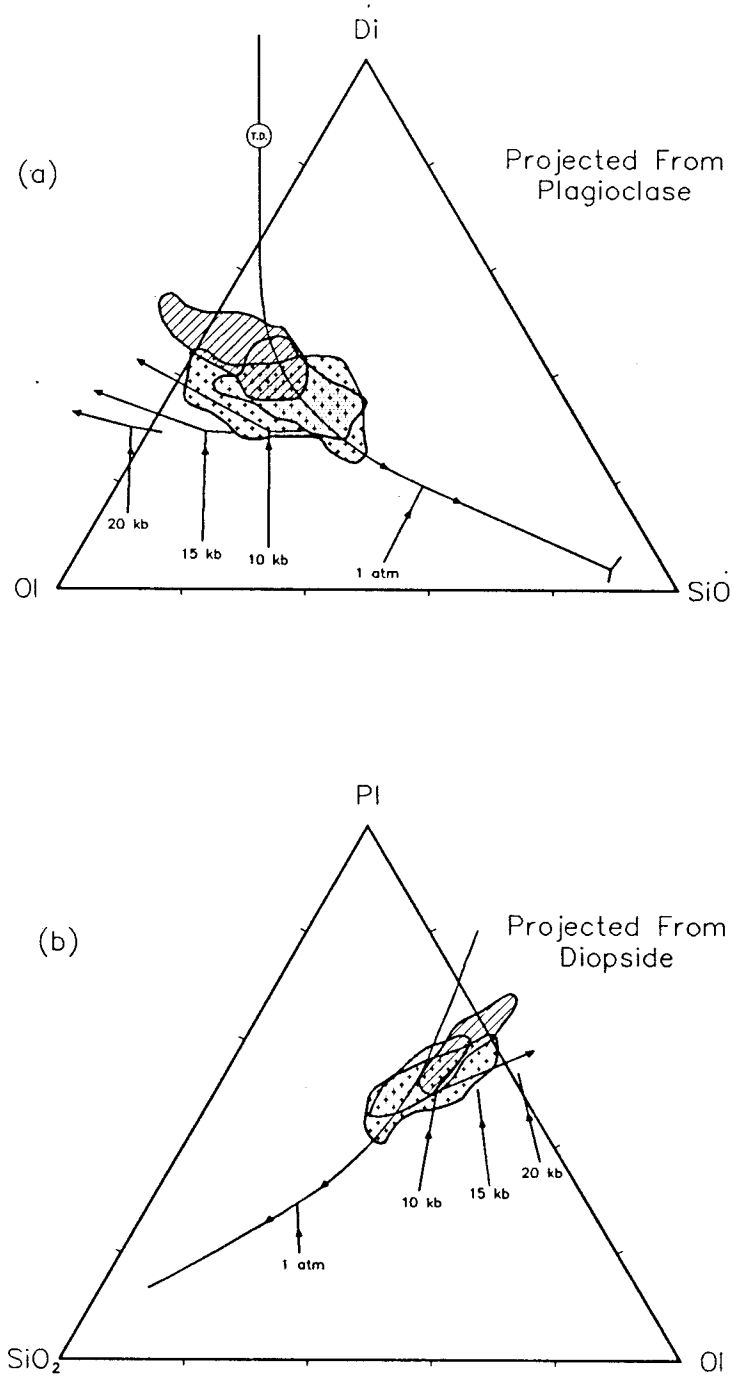

Figure 4. Fields for MORB glass compositions from FAMOUS region (crosses), Gorda Ridge (dots) and Tamayo Fracture Zone (diagonal lines) projected (a) from plagioclase onto the olivine-diopside-silica plane, and (b) from diopside onto the olivine-plagioclase-silica plane in the Ol-Di-Pl-SiO_2 tetrahedron.

that the Blanco Trough glasses could represent a liquid trend produced by high pressure partial melting or fractional crystallization of olivine + orthopyroxene.

The compositional anomalies observed in the Smithsonian analyses, whatever their origin, seem to contradict the conventional definitions for primitive MORB. When compared with analyses of glass samples from the Lamont seamount chain (F-2-1), and the Mid-Atlantic Ridge (525-5-1), as well as the 10 and 20 kilobar experimental liquids of Stolper (Table I; Fig. 5), it can be seen that for similar concentrations of TiO_2, Na_2O, and K_2O, the BT glasses appear to be depleted in CaO and MgO, while being enriched in FeO*. This leads to their appearing quite primitive, yet having unusually low Ca/(Ca + Na) and Mg/(Mg + Fe) ratios , an indication that they could have undergone an unusual modification during their ascent, or that their source region exhibited unusual geochemical characteristics. In addition to being unusually low, the Mg/(Mg+Fe) ratios for the entire suite show a very limited range of values. Forty seven of the fifty samples have Mg/(Mg + Fe) x 100 between 50 and 56, while the remaining three fall between 60 and 61 (Fig. 6).

New microprobe analyses of the original glass samples from the Smithsonian, performed at Rensselaer Polytechnic Institute, have failed to reproduce the original compositional anomalies. Based on the new data, the glasses plot with other primitive MORB at higher normative diopside (Fig. 7). The Mg / (Mg + Fe) x 100 values for the new analyses show a more even distribution, with the suite showing a continuous range from 51 to 62 (Fig. 6). The new analyses bring into the question the correct composition of this suite of MORB glasses, and call for a very different interpretation of their petrogenesis. Evidence supporting the validity of the new analyses, as well as a probable explanation for the seeming compositional anomalies present in the original ones, will be discussed in Chapter 4.

1.4 Summary.

Although primitive MORB exhibit a very limited range in composition, so that simple criteria for degree of fractional crystallization can be applied to samples recovered from spreading centers throughout the world, the Smithsonian microprobe analyses of basaltic glasses recovered from the Blanco Trough do not seem to fit these criteria. If these anomalies are due to fractional crystallization,

Table I

Comparison of Smithsonian analysis of primitive basaltic glass from the Blanco Trough with analyses of primitive MORB glasses from the Pacific and Atlantic, as well as liquids from high pressure phase equilibria studies.

Sample	*1*	*2*	*3*	*4*	*5*
SiO_2	48.34	48.40	49.19	48.96	47.50
TiO_2	0.83	0.86	0.85	0.77	0.86
Al_2O_3	17.56	17.38	16.12	17.27	16.67
FeO*	12.42	8.33	8.74	8.32	10.06
MgO	8.80	9.44	10.41	10.74	10.18
CaO	9.71	13.16	11.91	10.90	10.74
Na_2O	2.37	2.18	2.35	1.92	2.50
K_2O	0.06	0.02	0.09	0.10	0.13
Total	100.15	99.77	99.88	98.98	98.64
Mg#[6]	55.8	66.9	71.2	69.7	64.3
Ca#	69.4	76.9	73.7	75.8	70.4
CaO/Al_2O_3	0.553	0.757	0.739	0.631	0.644

(1) Smithsonian analysis of VG-348.
(2) F-2-1 from Lamont seamount chain (Allan et al., 1989).
(3) 525-5-1 from the Mid-Atlantic Ridge (Bryan and Moore, 1977).
(4) Average of 10 kb experimental liquids 519-7 & 519-10 (Stolper, 1980).
(5) 20 kb experimental liquid 519-14 (Stolper, 1980).
(6) Mg-number calculated with total Fe as FeO for comparative purposes.

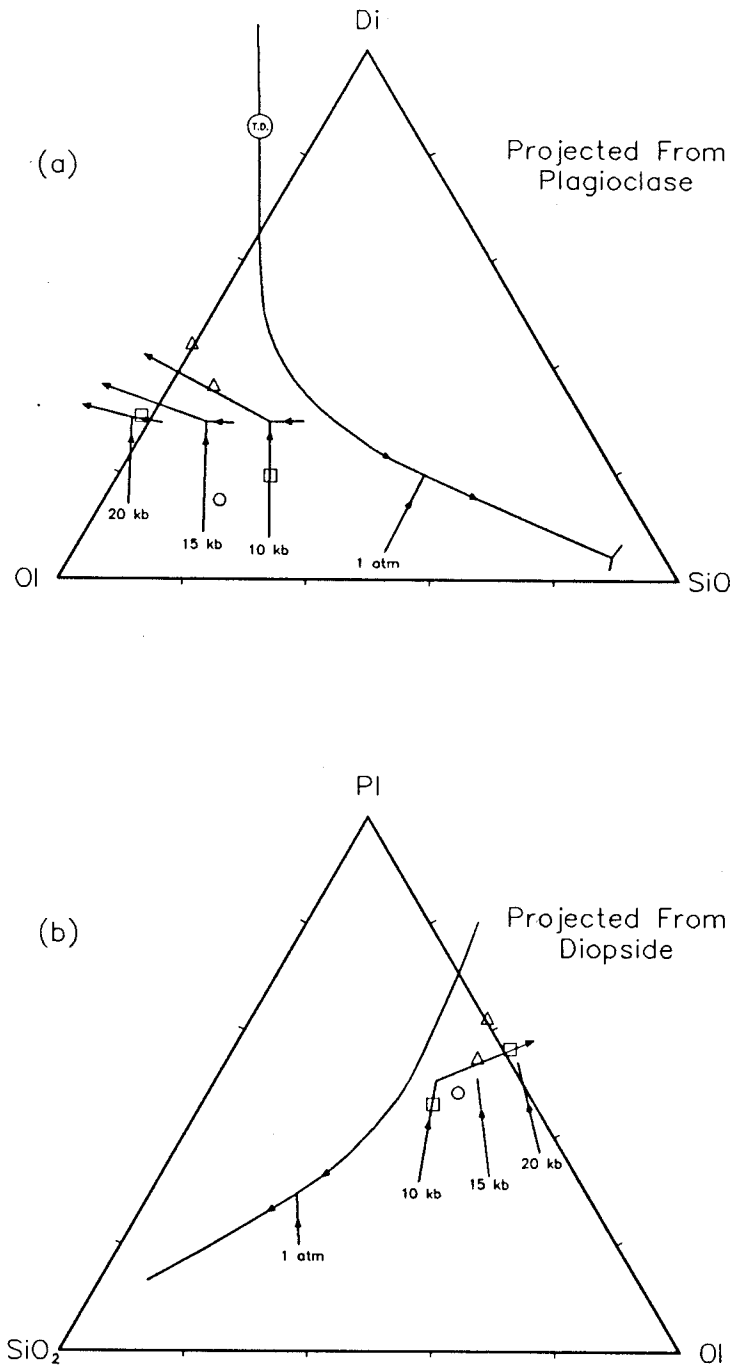

Figure 5. Projection of MORB glass compositions in Table I (a) from plagioclase onto olivine-diopside-silica plane, and (b) from olivine-plagioclase-silica plane in the Ol-Di-Pl-SiO_2 tetrahedron. Circle is VG-348, squares are high pressure melts and triangles are primitive glasses from Atlantic and Pacific.

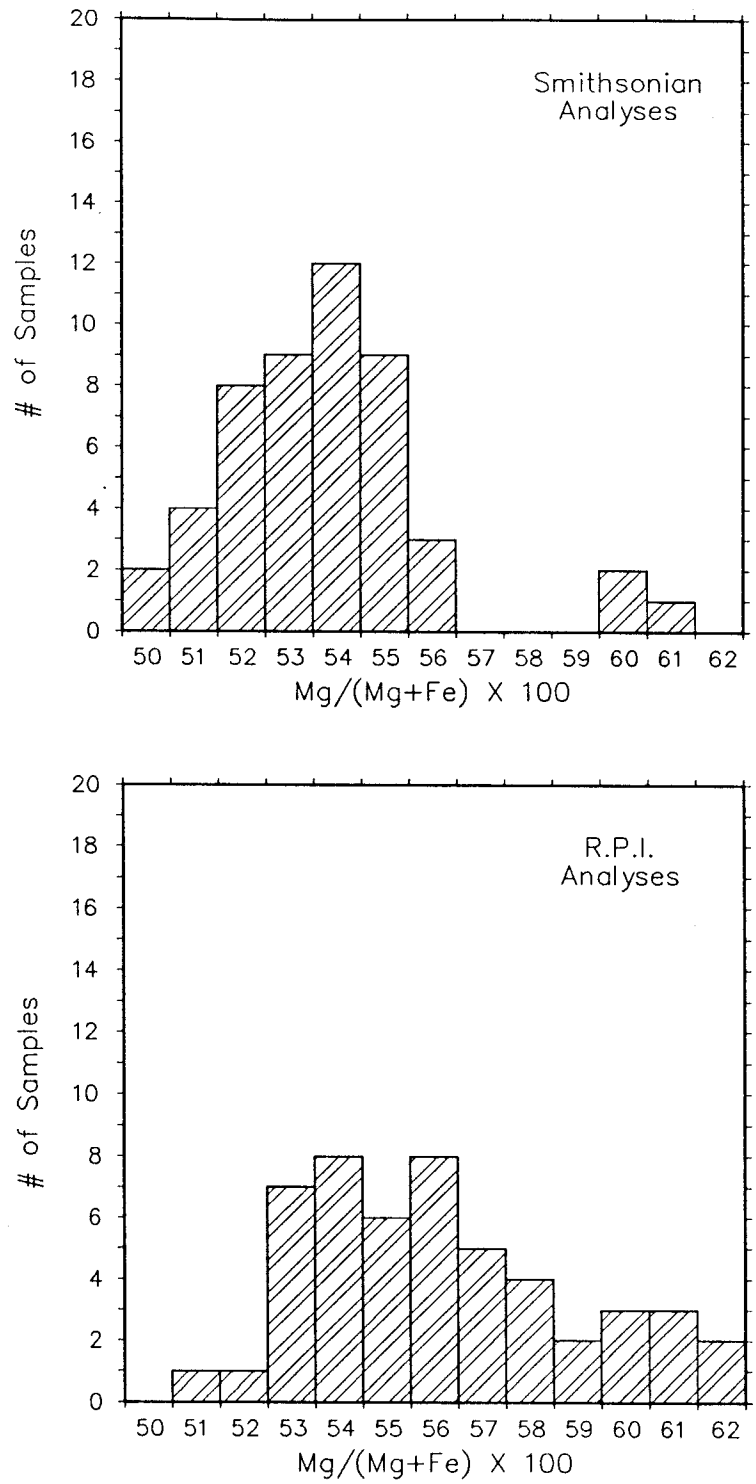

Figure 6. Histograms comparing the distribution of Mg/(Mg + Fe) for Smithsonian and R.P.I. analyses of the Blanco Trough glasses.

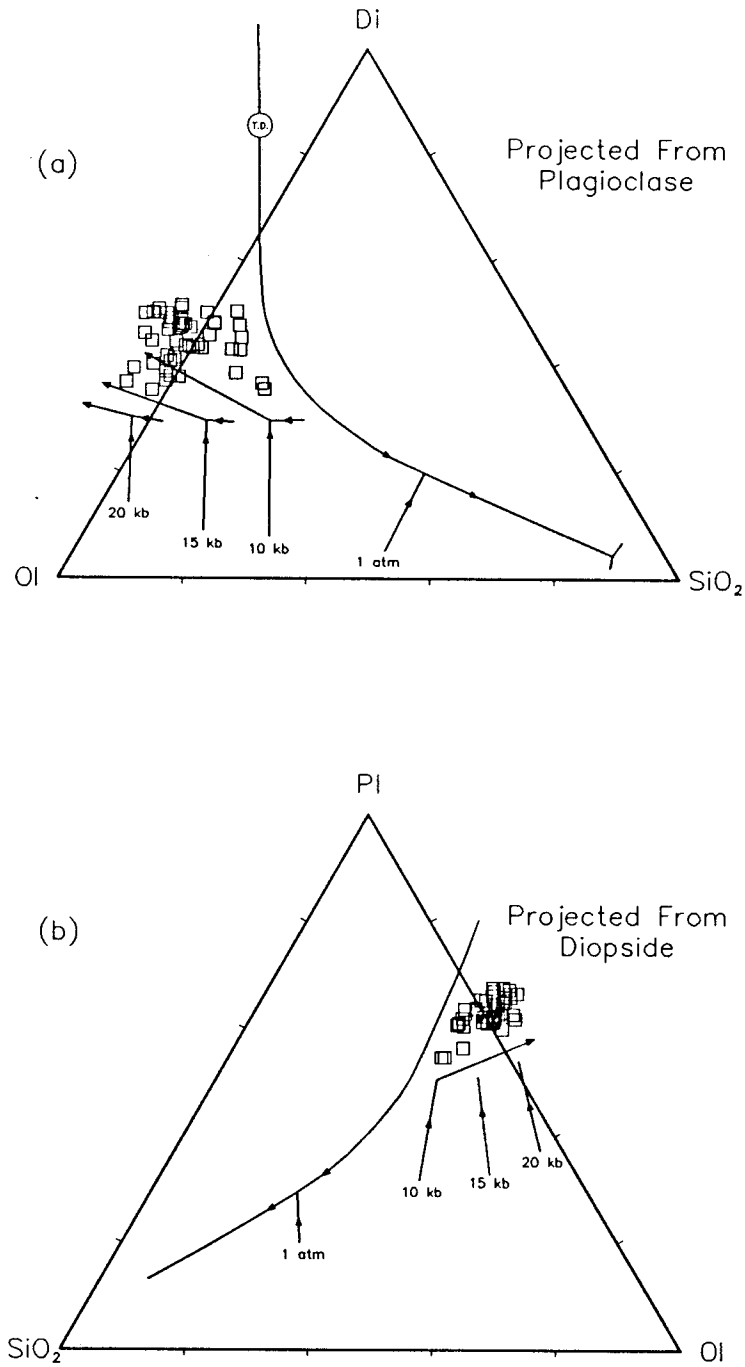

Figure 7. R.P.I. analyses of the Blanco Trough glasses projected (a) from plagioclase onto the olivine-diopside-silica plane, and (b) from diopside onto the olivine-plagioclase-silica plane in the Ol-Di-Pl-SiO_2 tetrahedron.

this would seem to necessitate a variation in the liquidus phases, and their order of appearance, from what is generally observed for normal MORB melts. If they are a product of variations in the degree of partial melting, the source rock must be different from the type of peridotite normally associated with the oceanic upper mantle. New analyses of the original samples, however, have failed to reproduce the original chemical anomalies, indicating instead that these samples may represent primitive normal MORB (Fig. 7). Subsequent chapters will discuss the tectonic setting of the area from which these samples were recovered (Chapter 2), their petrography (Chapter 3), and the question of the major element chemistry of the glasses and phenocrysts (Chapter 4).

2. Tectonics of the Northeast Pacific.

2.1 Introduction.

The Blanco Fracture Zone trends west-northwest between the Gorda Ridge to the southeast and the Juan de Fuca Ridge to the northwest (Fig. 8) and is characterized by a series of parallel to subparallel rises and basins (Melson, 1969). The Juan de Fuca Ridge is approximately 490 km in length, but is composed of at least six segments, ranging in length from 50 to 150 km, with highly variable morphology. The total spreading rate for the ridge is roughly 6 cm/yr (Johnson and Holmes, 1989). Spreading rates along the northern segment of the Gorda Ridge are comparable to those of the Juan de Fuca Ridge (Riddihough, 1988), while in the south they are significantly lower, with a total rate of approximately 2 cm/yr (Atwater and Mudie, 1973). Consistent with a slower spreading rate, the southern segment also shows ample evidence of block faulting (Atwater and Mudie, 1968). The Blanco Trough, which represents the westernmost of the basins along the fracture zone, is located southeast of the Juan de Fuca Ridge-Blanco Fracture Zone intersection, adjacent to the Parks Seamount, in an area that has had a complex tectonic history. Section two of this chapter briefly reviews the early studies of the northeast Pacific, and how they made seminal contributions to modern plate tectonics theory. Section three gives a short synopsis of our present understanding of the development of the northeast Pacific as a whole, based on the magnetic lineations found on the Pacific plate. Section four reviews the current models for the development of the region surrounding the Blanco Fracture Zone, including the Juan de Fuca and Gorda ridges. Section five discusses the association of iron and titanium enriched MORB with areas of active ridge propagation.

2.2 Early Studies of the Northeast Pacific and Modern Plate Tectonics Theory.

The complexity of the northeast Pacific was first seen in the magnetic surveys performed aboard the *USS Pioneer* in the late 1950's (Raff and Mason, 1961). The resulting anomaly maps show a series of north-south to northeast-southwest trending magnetic anomalies that are fairly continuous along strike, except where offset by fracture zones (Fig. 8)(Vacquier, 1959; Vacquier et al., 1961).

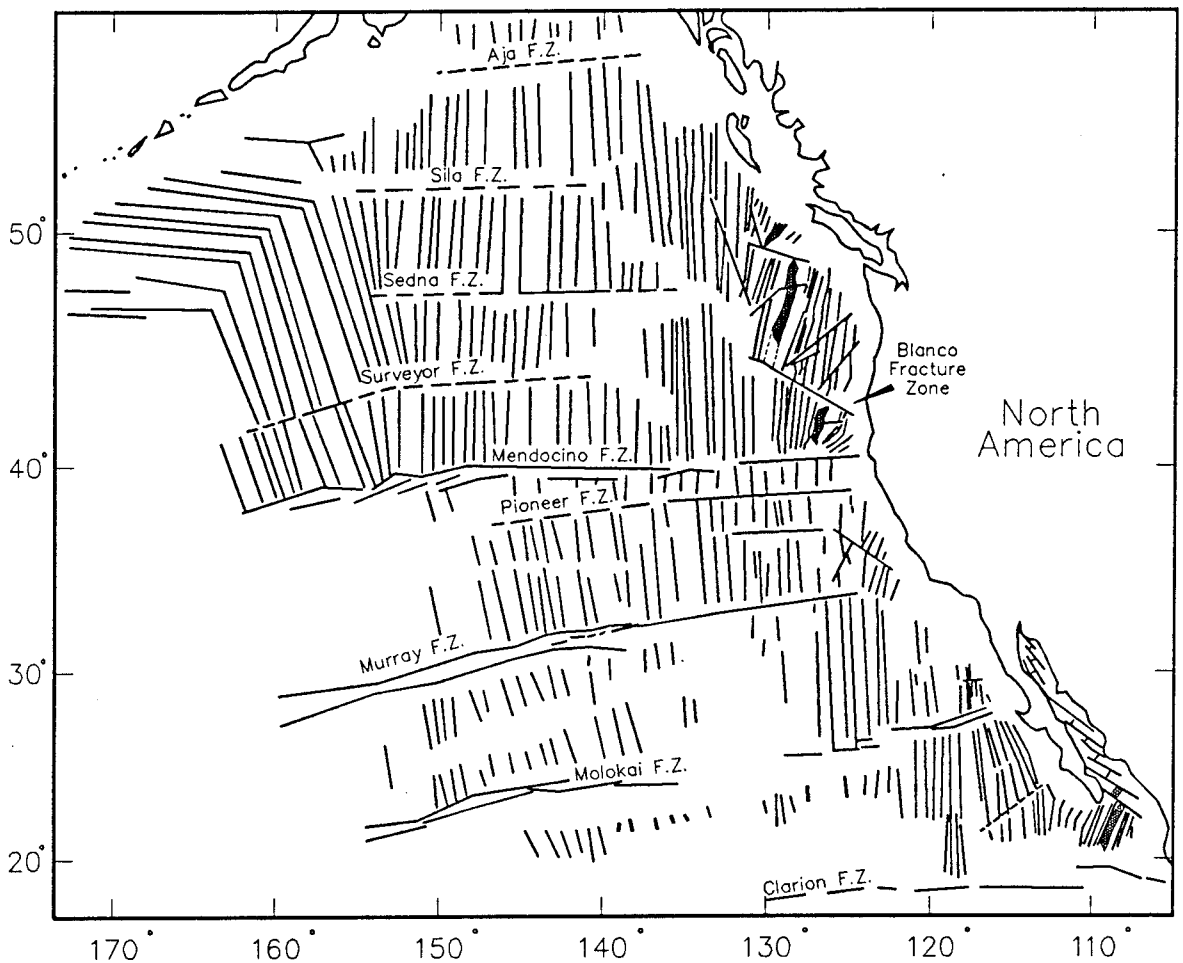

Figure 8. The pattern of linear magnetic anomalies in the northeast Pacific. After Atwater and Menard (1970).

These early studies eventually led to the recognition of two fundamental things about the nature of the ocean floor. First that there is a process operating in ocean basins to create linear anomalies having remarkably uniform orientations over substantial distances, and second that large scale horizontal movements of the oceanic crust take place.

Marine magnetic anomalies were found to exist over ocean ridges throughout the world, but their origin remained controversial until 1963, when it was proposed that they are produced when the Earth's ambient magnetic field is recorded in the crust formed at ocean ridges during times of both normal and reversed polarity (Vine and Matthews, 1963). This was supported by studies which showed that synthetic anomalies created using an independently derived time scale for a series of reversals over the last 4 million years match very well the anomaly patterns observed across the Juan de Fuca Ridge (Vine and Wilson, 1965; Vine, 1966). An equally important tenet of plate tectonics was demonstrated by the fact that the offset of anomalies seen at fracture zones in the northeast Pacific is the product of transform, rather than transcurrent, faulting, in which the true sense of motion is opposite to that which had been assumed based on the apparent offset seen in continental faulting (Wilson, 1965).

In the late 1960's, the consistent geometric relationships observed between fracture zones, linear anomaly patterns, and spreading direction in presently active ridges led to the development of theories dealing with changes in spreading direction over time. The complicated pattern of the anomalies formed at the Juan de Fuca and Gorda ridges, combined with the oblique orientations of fracture zones in the area played a prominent role in the development and substantiation of much of this work (Menard and Atwater, 1968).

2.3 Regional Tectonic Development.

The tectonic development of the northeast Pacific over much of the last 150 million years is thought to be tied to the convergence of the Farallon, Kula, and Pacific plates with the western margin of the North American plate. Reconstruction of the evolution of these plates is difficult due to the fact that most of the evidence pertaining to their geometry and relative motion, with the major exception of the magnetic lineations remaining on the Pacific plate, has been subducted (Riddihough, 1988).

The reconstruction of past plate motions in ocean basins can generally be accomplished with a good degree of accuracy across spreading ridges using magnetic anomaly patterns, with no absolute reference frame (Stone, 1977). With the exception of the Juan de Fuca and Gorda ridges, however, the spreading centers which formed the crust in the northeast Pacific no longer exist, and the paleomagnetic record is incomplete. The reconstructions that have been proposed for the evolution of the region are therefore greatly dependent on the frame of reference that is chosen to discern the relative motions of the Pacific and North American plates through time. Histories based on a hot spot reference frame, combined with magnetic data and the assumptions of symmetrical spreading and constant motion between the plates, have proven to be the most consistent with known plate margin geometries (Stone, 1977; Riddihough, 1988). Reconstructions are generally considered to be (1) reliable over the last 40 million years, during which the motion of the Pacific plate has been constant, (2) less accurate during the period from 40 to 80 million years ago, or the time between the change in Pacific plate motion and the formation of the oldest seamount in the Hawaii-Emperor chain, and (3) highly speculative before 80 million years ago.

2.3.1 Events Older Than 80 Million Years.

The earliest reconstruction possible for the Pacific basin is 145 million years, before which no magnetic data are available. At this time the northeast Pacific was dominated by the Farallon plate, although it is possible that minor plates were present which left no record. The Izanagi plate was to the southwest, while the Pacific plate was in the south (Engebretson, 1982) (Fig. 9). The Pacific-Izanagi and Pacific-Farallon boundaries were spreading centers, while the Farallon-Izanagi boundary is believed to have been dominantly transform in character. At 135 million years there was a change in relative plate motions, after which the Farallon-Izanagi boundary became dominated by subduction (Engebretson et al., 1985). Due to the fact that the Earth's magnetic field did not change polarity during the period from 118 to 84 Ma, relatively little is known about the region's spreading history (Atwater, 1989).

At about 85 million years, relative motions changed again causing the Farallon plate to break,

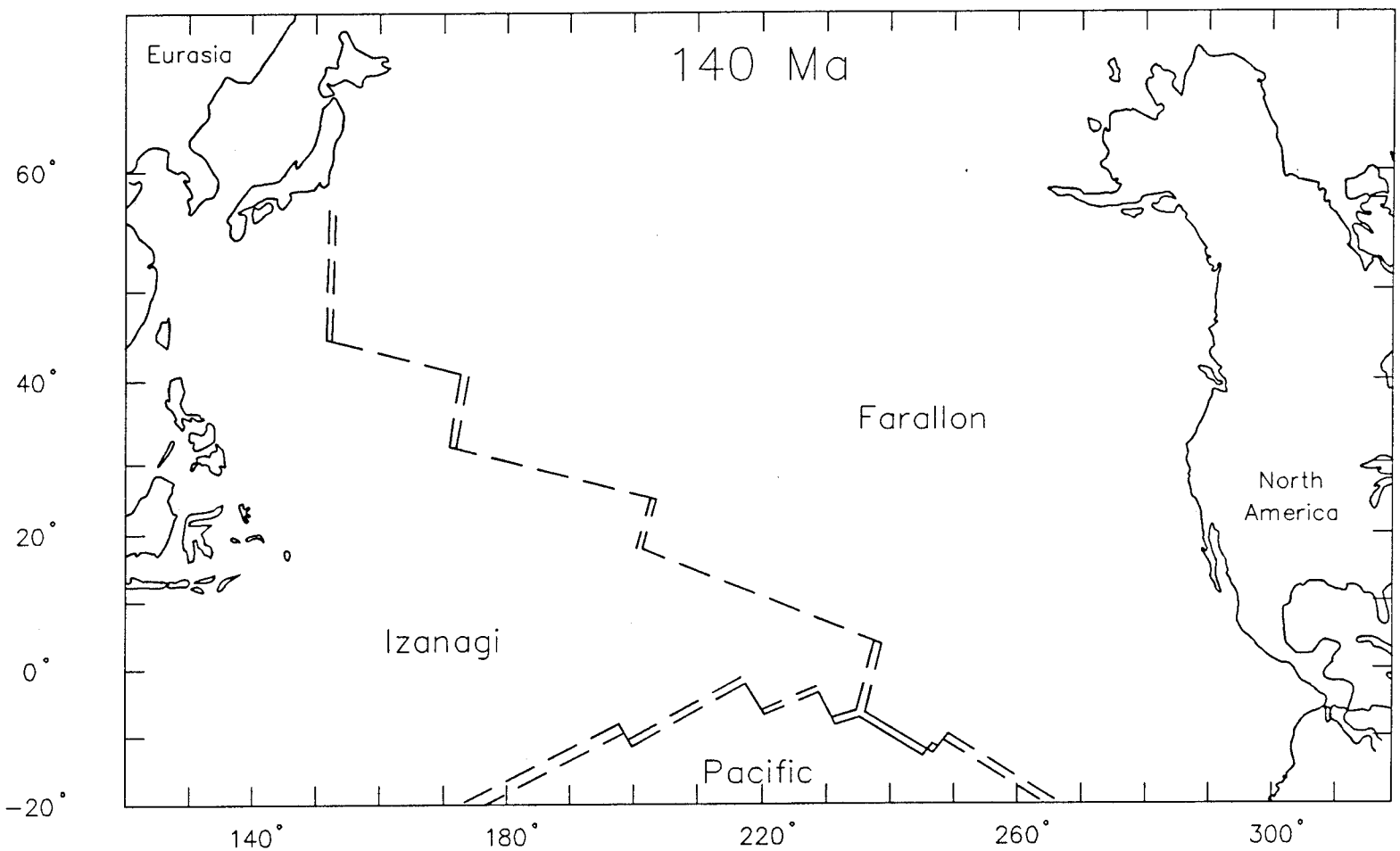

Figure 9. Reconstruction of the plates in the Pacific at approximately 140 Ma. Dashed double lines represent spreading centers, dashed single lines represent transform boundaries. After Engebretson et al. (1985).

forming the Kula plate and initiating the Kula-Farallon spreading center (Engebretson et al., 1985). Whether this break took place in the northern or southern portion of the Farallon plate is uncertain. It is believed that the Pacific, Farallon, and Kula plates met at a triple junction formed by three spreading ridges. The existence of the Kula plate and the triple junction, both of which have been completely destroyed, is inferred from the fact that east-west trending magnetic lineations are found south of the Aleutian trench, forming an approximate 120° angle with the north-south trend which characterizes most of the Pacific plate (Fig. 8) (Grow and Atwater, 1970). The geometry of this "magnetic bight" requires that the spreading center which formed the crust be bent, and that a third ridge be present to stabilize the configuration (Stone, 1977). The true form of the ridge which separated the Kula and Farallon plates is unknown, and was likely made up of a number of ridge segments connected by transforms, similar to the Pacific-Farallon plate boundary, but for convenience it is usually approximated in reconstructions as a simple linear ridge system (Riddihough, 1988), leading to uncertainties in the location of the ridge with respect to North America. The existence of additional, smaller oceanic plates adjacent to North America cannot be ruled out, but for simplicity only three are assumed to have been important.

Prior to 80 million years ago, it is thought that the Kula-Pacific-Farallon triple junction lay farther south than the present location of the magnetic bight (Atwater, 1970). The Farallon and North American plates were converging along much, or perhaps all, of their boundary (Riddihough, 1982). The boundary between the two plates was probably complex, dominated by subduction, but with transform motion possible, depending on local geometries.

2.3.2 Events from 80 to 40 Million Years Ago.

The Kula-Farallon ridge is thought to have been in contact with North America off the coast of southeast Alaska and western Canada forming a triple junction by 80 million years ago, although the exact nature and location of the interaction is dependent on the shape of the ridge. Between 80 and 60 million years ago the Farallon and Kula plates are thought to have been converging with North America in a northeasterly direction (Riddihough, 1982).

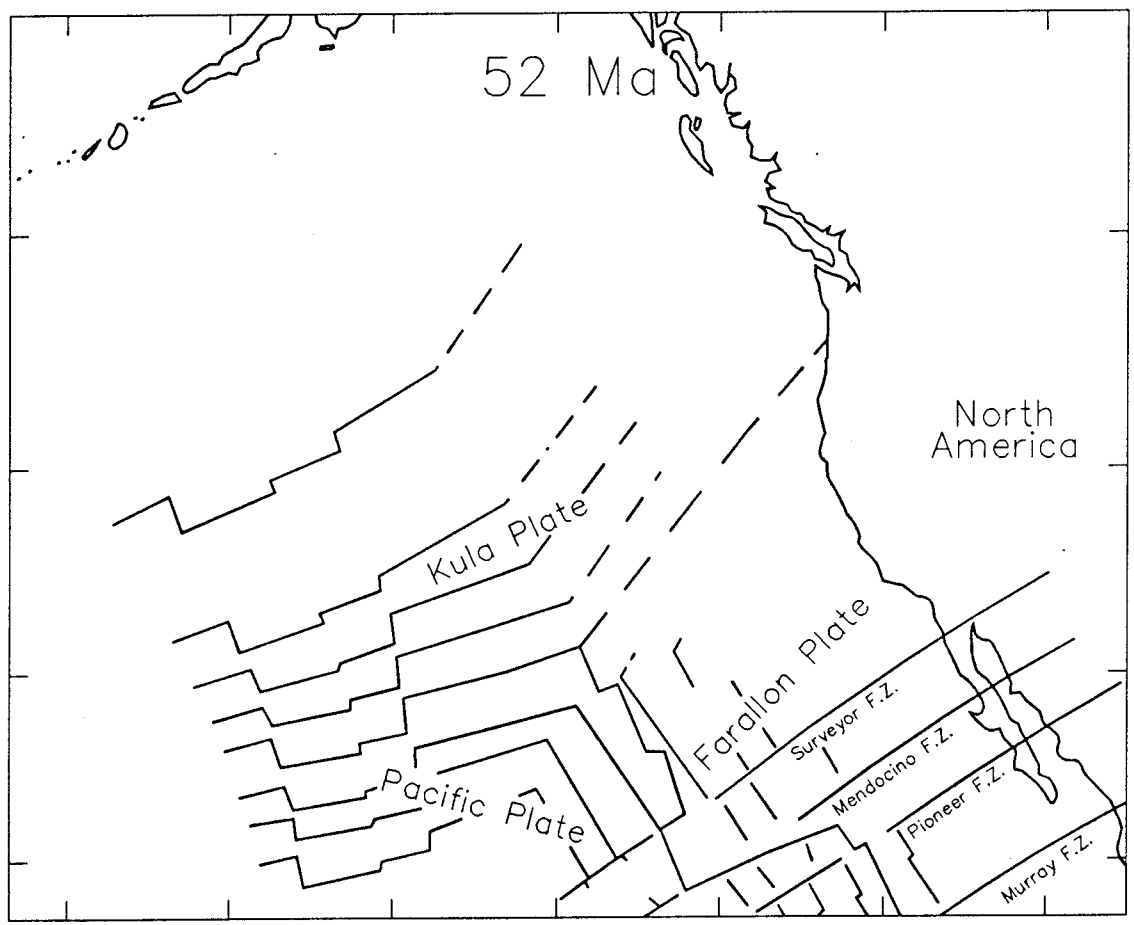

Figure 10. Reconstruction of the plates in the northeast Pacific at 52 Ma, including magnetic anomalies. After Engebretson et al. (1985).

Between 60 and 40 million years ago, many believe that the triple junction probably was moving southward along the coast (Fig. 10), reaching as far as Queen Charlotte Island, or perhaps Vancouver Island (Coney, 1978; Cooper et al., 1976; Stone, 1977). Atwater (1970) proposed, however, that it started in the south 80 million years ago, near what is now southern California, and migrated north until 40 million years ago. Byrne (1979) suggests that by 55 million years ago the Kula-Pacific spreading ridge had become inactive, so that the Kula plate was no longer independent, however some reconstructions have it separate from the Pacific plate until 43 million years (Engebretson et al., 1985), or even as recently as 20 million years ago (Grow and Atwater, 1970).

2.3.3 Events from 40 Million Years Ago to the Present.

The change in the trend on the Hawaii-Emperor seamount chain, which is dated at approximately 43 million years, marks a major shift in Pacific plate motion. It appears that there was a major plate re-orientation, during which the motion of the Pacific plate, relative to the Hawaiian hot-spot, changed by approximately 50° and the rates of interaction with the North American plate were reduced by one half (Riddihough, 1982). The Pacific-Farallon spreading ridge is thought to have collided with North America approximately 37 million years ago (Engebretson et al., 1985). Continued convergence and subduction, along with the establishment of the San Andreas fault system, is believed to have created the large scale features observed today in the northeast Pacific.

2.4 Tectonics of the Blanco Trough Area.

The oblique orientation, with respect to both relative and absolute plate motion, of magnetic anomalies surrounding the Juan de Fuca Ridge has been reconciled with the rigidity of lithospheric plates through the concept of ridge propagation (Hey, 1977). The present spreading geometry is believed to have been established in response to shifts in the direction of spreading at 8.5 and 5.0 million years ago. These shifts resulted in a change in motion of the Juan de Fuca plate relative to the Pacific plate, from parallel to the Mendocino Fracture Zone to parallel to the Blanco Fracture Zone (Hey and Wilson, 1982).

Propagation of the Juan de Fuca Ridge, north to the Cobb Offset and south to the Blanco Fracture Zone, is believed to be the mechanism which enabled the change in spreading direction to take place (Hey and Wilson, 1982; Johnson et al., 1983). The model which best fits the observed anomaly pattern involves seven propagation sequences, two northward and five southward (Fig. 11) (Wilson et al., 1984). The distorted lineation pattern and high seismicity of the Gorda plate seem to indicate that this shift has caused convergence along the Mendocino Fracture Zone, as well as deformation of the Gorda plate (Stoddard, 1987).

The Blanco Fracture Zone is thought to have been established during a shift in the pole of rotation at 5.0 Ma, at which time the southernmost propagator stopped moving. The transform was subsequently lengthened twice, as two of the other three southward propagating segments reached it and also stopped. It was the arrival of the third segment that created the area containing the Blanco Trough and the Parks Seamount (Fig. 12) (Hey and Wilson, 1982).

2.5 Propagating Rifts and the Occurrence of Iron and Titanium Enriched MORB.

The process of rift propagation at the Galapagos, Juan de Fuca, and Explorer Ridges is associated with the eruption of relatively unusual MORB. The composition of glasses recovered from dredge hauls and submersible dives in these relatively restricted areas ranges from primitive (MgO > 9%; FeO* ~ 8-9%; TiO_2 ~ 0.9-1.1%) to relatively more evolved, iron and titanium enriched (FeTi basalt) (MgO < 6.5%; FeO* ~12-16%; TiO_2 ~ 1.5-2.5%), with occasional examples of such highly evolved magmas as tholeiitic andesites and rhyodacites (Byerly et al., 1976; Byerly, 1980; Clague et al., 1981; Hey et al., 1989). This diversity can be correlated with proximity to the propagator tip at the time of eruption, the most primitive MORB occurring immediately behind the tip, and FeTi basalts being caused by fractional crystallization in shallow magma chambers emplaced into relatively cool crust slightly farther behind. A gradation to "normal" MORB compositions presumably occurs as the chambers become well established, and are regularly recharged with primitive melts after a period of fractional crystallization, thus approaching a relatively steady state of magma production (Christie and Sinton, 1981).

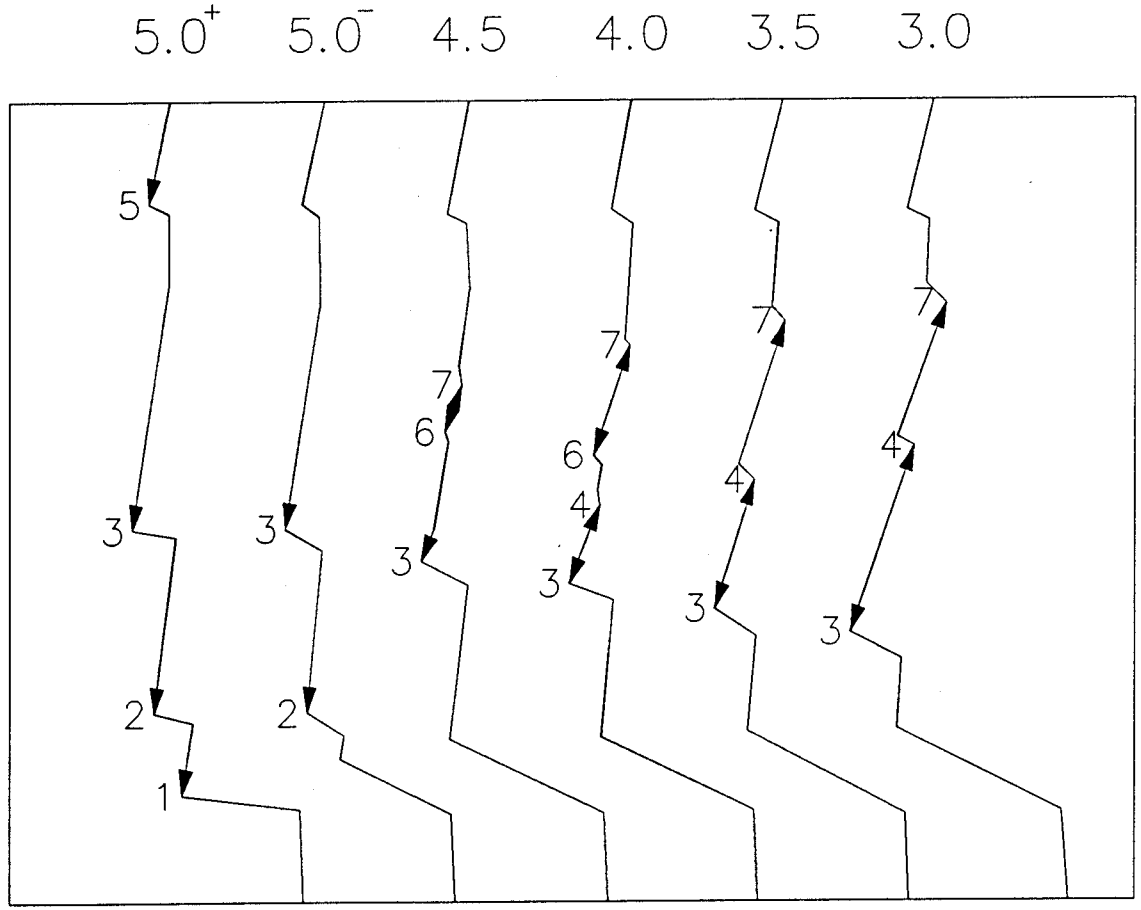

Figure 11. Schematic representation of the reorientation of the Juan de Fuca Ridge from 5.0 to 3.0 Ma, with propogators numbered. After Wilson et al. (1984).

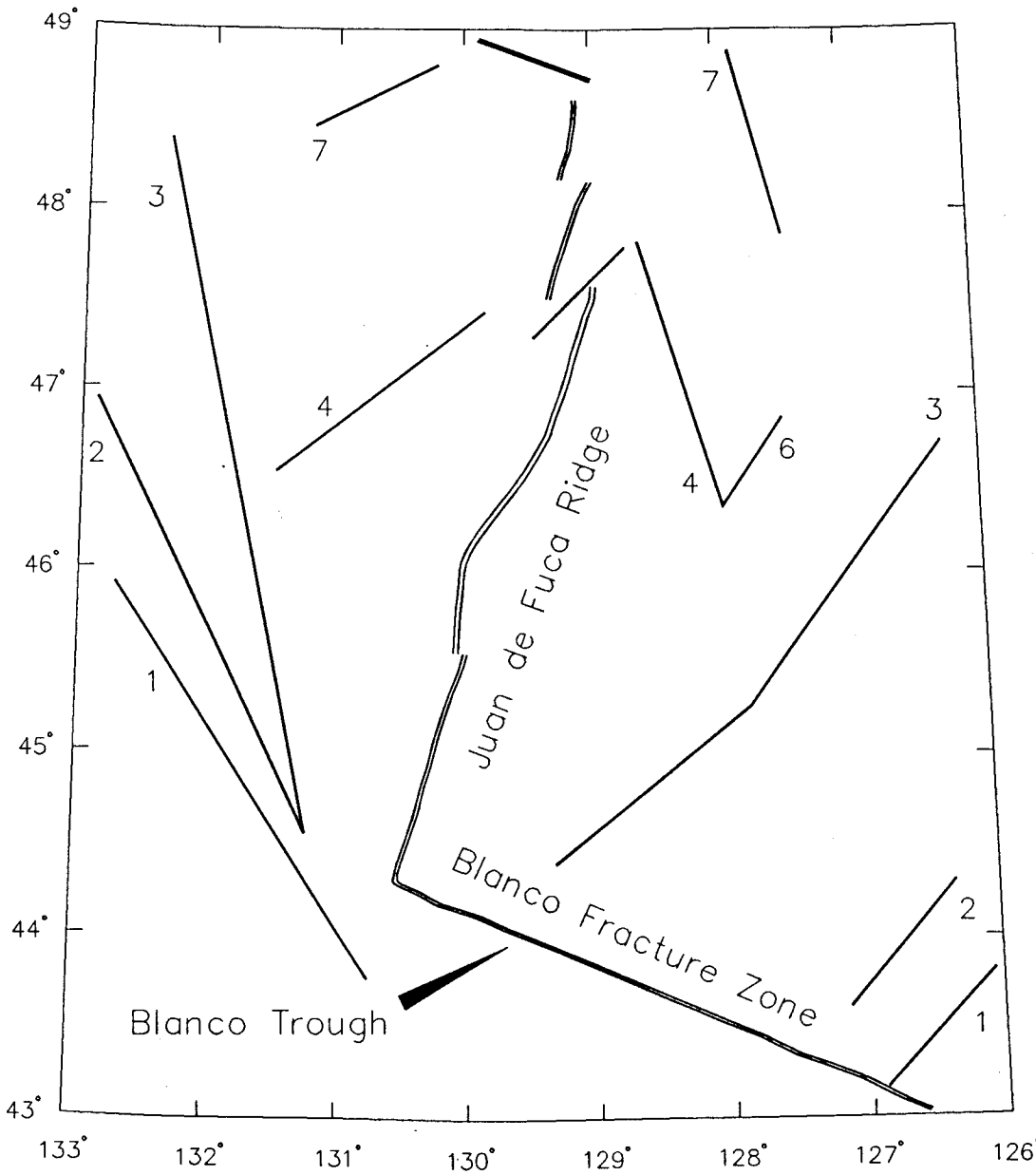

Figure 12. Location of proposed propogator wakes in the Juan de Fuca Ridge-Blanco Fracture Zone area. After Johnson and Holmes (1989).

FeTi enrichment is especially prominent along the Juan de Fuca Ridge south of the Cobb Offset at 48° N., with FeO* values commonly exceeding 10% (Delaney et al., 1981), and reaching as high as 15% near the Blanco Fracture Zone (Vogt and Byerly, 1976). North of the Cobb Offset, MORB compositions change drastically, with normal FeTi enrichment, but greater than normal enrichment in potassium (Delaney et al., 1981; Delaney et al., 1982; Sinton et al., 1983; Karsten and Delaney, 1985; Johnson and Holmes, 1989).

2.6 Summary.

The dynamic tectonic history of the area surrounding the Blanco Fracture Zone has led to the production of varied and unusual MORB compositions, including the FeTi basalts commonly associated with propagator tips (Sinton et al., 1983; Johnson and Holmes, 1989). Given the proximity of the Blanco Trough to the Juan de Fuca Ridge, as well as propagator tip 3 (Fig. 12), it is not surprising that the Smithsonian analyses characterize a suite of basalts recovered there as unique . Despite the fact that they show the glasses to be enriched in total iron, there is not a complementary enrichment of titanium, and the chemical variations found within the suite are distinct from those observed in FeTi basalts, seeming to rule out a simple genetic relationship between the two. The analyses performed at R.P.I. seem to indicate that these glasses are only slightly enriched in total iron, and have affinities with some of the more primitive MORB recovered from FeTi basalt localities.

3. Petrography of the Blanco Trough Glasses.

3.1 Introduction.

Basalts extruded onto the ocean floor experience perhaps the most rapid cooling rates attainable under terrestrial conditions. When a melt experiences such high degrees of supercooling the dominant control on the crystal growth rate becomes the rate of diffusion of components through the melt. The liquid at the crystal boundary becomes depleted in the elements preferentially partitioned into the solid, and a compositional gradient develops. Under these conditions planar crystal faces tend to become unstable and morphologies such as dendrites and spherulites are favored as the growing crystal attempts to "reach out" into the portion of the liquid enriched in the components necessary for continued growth (Kirkpatrick, 1981).

Because pillow basalts experience a large variation in cooling rate as a function of distance from the pillow rim, the crystalline phases found in them display a range of morphologies that reflects the changing growth rate. The outer few millimeters of the pillow, where the cooling rate is so high that the liquid is quenched, commonly consists of glass which may contain sparse skeletal or euhedral phenocrysts of olivine and/or plagioclase, the majority of which were presumably present in the melt. A variolitic zone is generally found just inside the quenched rim, where the cooling rate is slightly lower. This is characterized by olivine dendrites, commonly with non-dendritic cores, and plagioclase spherulites, often with skeletal cores. There is commonly a gradation into a zone of coalesced olivine dendrites and partially coalesced plagioclase spherulites, with small amounts of residual glass. As the cooling rate continues to decrease there is a zone of coalesced plagioclase spherulites and skeletal olivine, with pyroxene commonly found between the arms of plagioclase spherulites. Next is a zone of skeletal olivine, "bow-tie" spherulite plagioclase, again with pyroxene commonly found between the plagioclase arms. The core of the pillow generally consists of skeletal olivine and plagioclase microlites, with dendritic pyroxene and some opaques in between (Bryan, 1972; Kirkpatrick, 1978).

The glasses recovered from the Blanco Trough contain phenocrysts of olivine, chromian spinel, and plagioclase. The suite can be divided into plagioclase-bearing and plagioclase-free samples

(Table II), although this grouping is somewhat arbitrary due to the fact that chromian spinel is absent in some samples from each group. Because the phases of interest are those that were present in the melt at the time of extrusion, the petrographic descriptions concentrate on phenocrysts present in the glassy rim. Where microphenocryst-sized euhedral to subhedral plagioclase laths were found only in the outer few millimeters of a microcrystalline portion of the thin section, they were considered to be representative of plagioclase in the melt. This chapter contains a generalized description of the petrography of the suite as a whole, while a brief description of the phases observed in individual thin sections can be found in Appendix 3.

3.2 Petrography.

Doubly-polished thin sections were prepared from samples supplied by the Smithsonian for twenty-six of the fifty glasses which make up the suite . Phenocryst phases are divided, on the basis of size and morphology, into phenocrysts (diameter $\geq$ 0.5 mm), microphenocrysts (0.5 mm > diameter > 0.05 mm) and microlites (diameter $\leq$ 0.05 mm). Grain size estimates are based on an average of ~10 grains that display good euhedral morphology.

Ten of the samples for which thin sections were prepared (38.5%) contain no plagioclase. The approximate width of the glass rind present on the plagioclase-free samples ranges from 1.0 to 7.5 mm. Olivine is the dominant phenocryst phase in all of these samples, while an assemblage of olivine + chromian spinel is found in only 3 (Table II).

The remaining 16 samples contain plagioclase. The approximate width of the glass rind present on these samples ranges from 2.0 to 4.0 mm. Olivine is again the dominant phenocryst phase in all samples, with plagioclase being abundant in only one (VG-169). An assemblage of olivine + chromian spinel + plagioclase is found in 13 of the 16 samples in this group (Table II).

3.2.1 Olivine.

Olivine is colorless under plane-polarized light in all thin sections. Grains are commonly euhedral to subhedral, but may also exhibit skeletal or bladed morphology (Fig. 13, 14, 15). VG-383

Table II

Phenocryst phases observed in thin sections of the Blanco Trough glasses.

Sample	*Olivine*	*Chromian Spinel*	*Plagioclase*
VG-169	X	X	X
VG-172	X	X	
VG-178	X		
VG-340	X		
VG-342	X	X	X
VG-345	X	X	X
VG-347	X	X	X
VG-348	X	X	X
VG-355	X		X
VG-356	X	X	X
VG-357	X	X	X
VG-358	X		
VG-360	X	X	X
VG-368	X	X	
VG-370	X	X	X
VG-372	X		
VG-373	X	X	X
VG-376	X	X	X
VG-378	X	X	
VG-380	X		
VG-381	X		
VG-382	X		
VG-383	X		X
VG-384	X	X	X
VG-385	X	X	X
VG-387	X		X
% of Total	100%	61.5%	61.5%

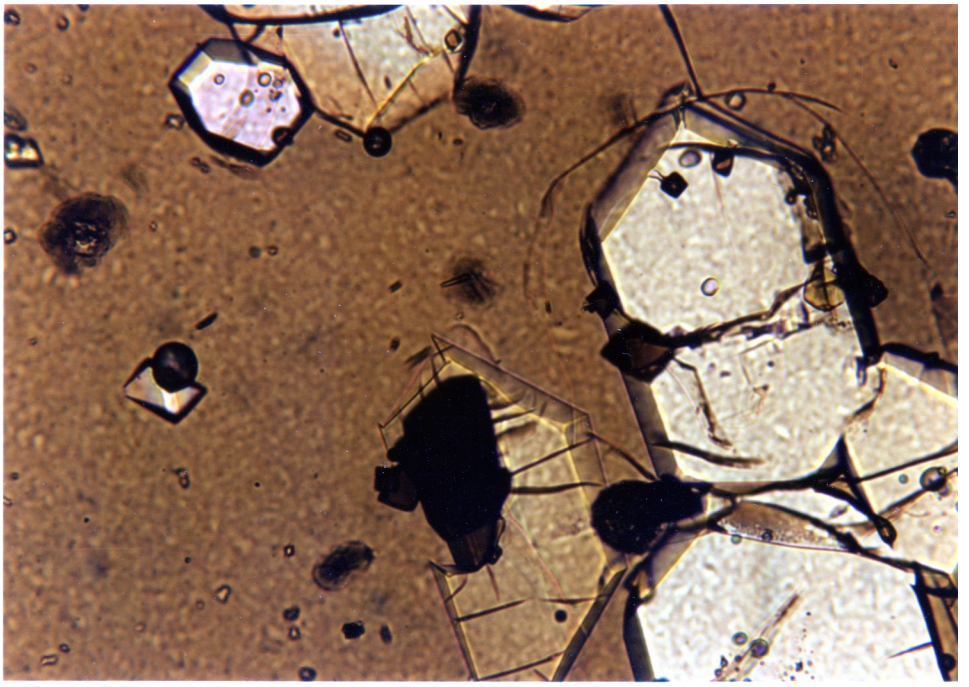

Figure 13. Photomicrograph of olivines displaying euhedral to subhedral morphology in a matirx of basaltic glass from VG-348. Brown inclusions are chromian spinel. Long dimension of photo is equal to 0.64 mm.

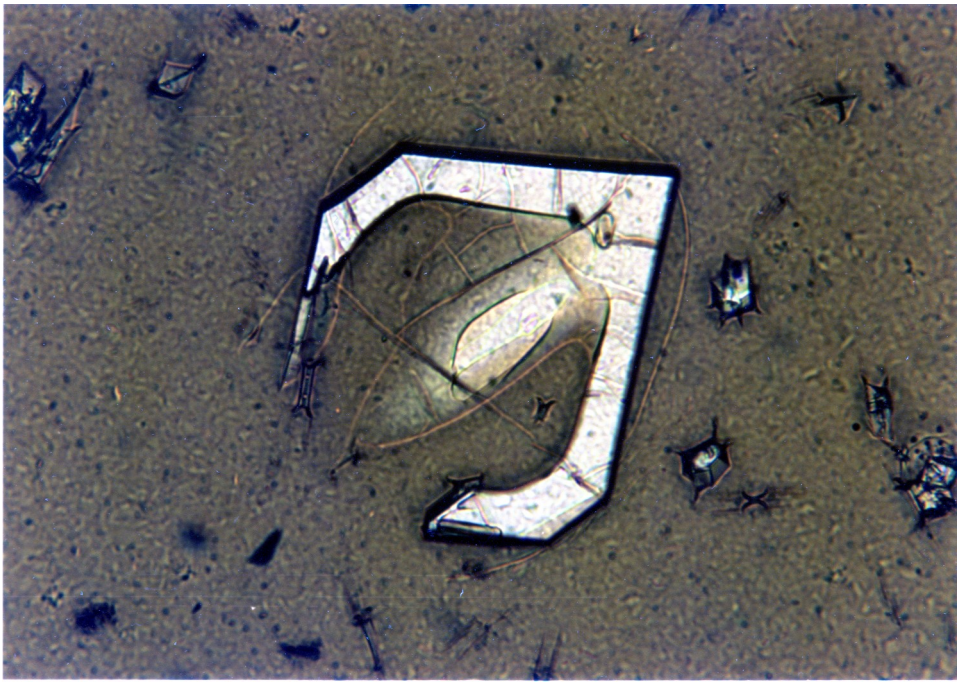

Figure 14. Photomicrograph of olivine displaying skeletal morphology in a matrix of basaltic glass from VG-372. Long dimension of photo is equal to 0.64 mm.

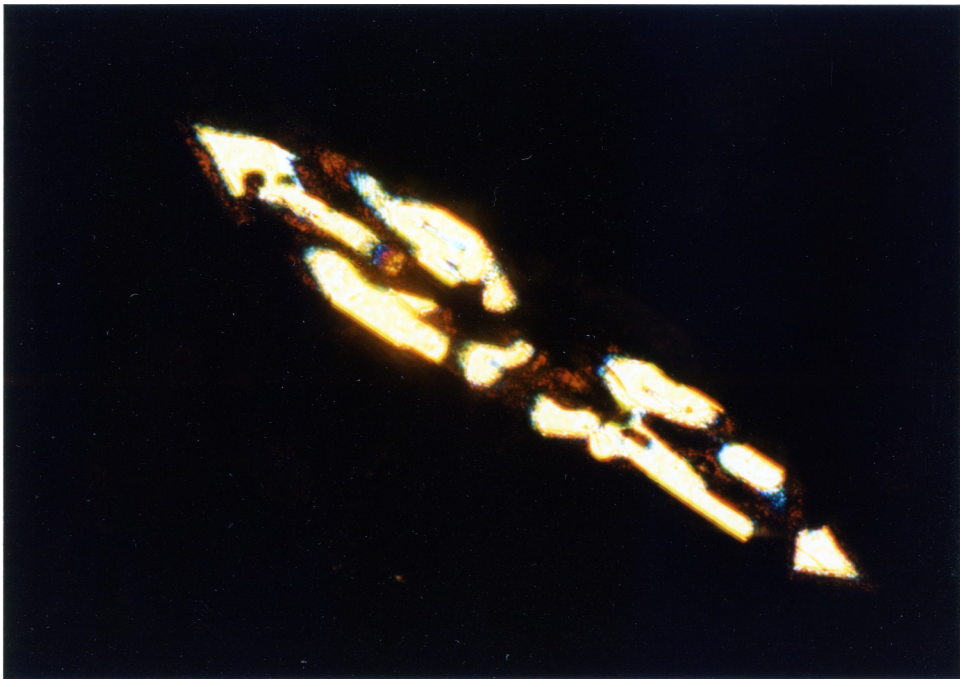

Figure 15. Photomicrograph, taken in cross-polarized light, of olivine displaying bladed morphology in the crystalline zone of VG-381. Long dimension of photo is equal to 0.64 mm.

contains deeply embayed, reversely zoned grains (Fig. 16). Some samples contain large subhedral grains, commonly in the crystalline portion of the pillow, which display deformation bands and possible fluid inclusions, indicative of a xenocrystic origin (Fig. 17). Electron microprobe analysis of some of these grains (Ol-385.24, Ol-385.25 in Appendix 2) show them to have nearly the same composition as the phenocrysts, indicating that they probably have a cumulate origin.

Olivine is most abundant as microphenocryst-sized grains in samples in both groups, tending to be slightly larger in the plagioclase-bearing samples, with an average grain size of 0.22 x 0.35 as compared to 0.15 x 0.26 mm. Microlites occur in most plagioclase-free samples but are not generally abundant, while they are found in every sample of the plagioclase-bearing group, and tend to be more abundant within individual samples. No grains large enough to be classified as phenocrysts occur in the plagioclase-free samples, however phenocryst-sized grains are present in two samples from the plagioclase-bearing group, VG-342 and VG-373.

A few samples contain arcuate chains of olivine grains similar to those reported in samples from the Oceanographer Fracture Zone (Fig. 18). The structures in the Oceanographer basalts were attributed to the mechanical disruption of the inner portion of the pillow skin, forming globules that are cool relative to the surrounding magma. Olivine grains that adhere to theses globules appear as circular chains in thin section (Walker et al. 1980).

3.2.2 Chromian Spinel.

Chromian spinel is translucent red-brown to brown under plane-polarized light. Grains are commonly euhedral to subhedral in morphology, occurring in the glass, as inclusions in olivine and embedded in olivine grain boundaries (Figs. 13, 19, 20). No spinel inclusions were observed in plagioclase. A few spinels with worm-like embayments were observed, but only in one sample (VG-373).

Grains are generally small (~0.03 x 0.03 mm) in all thin sections, although a range of grain sizes is present in some samples (e.g. VG-373). In general the grain size of spinels seems to diminish in the more evolved samples.

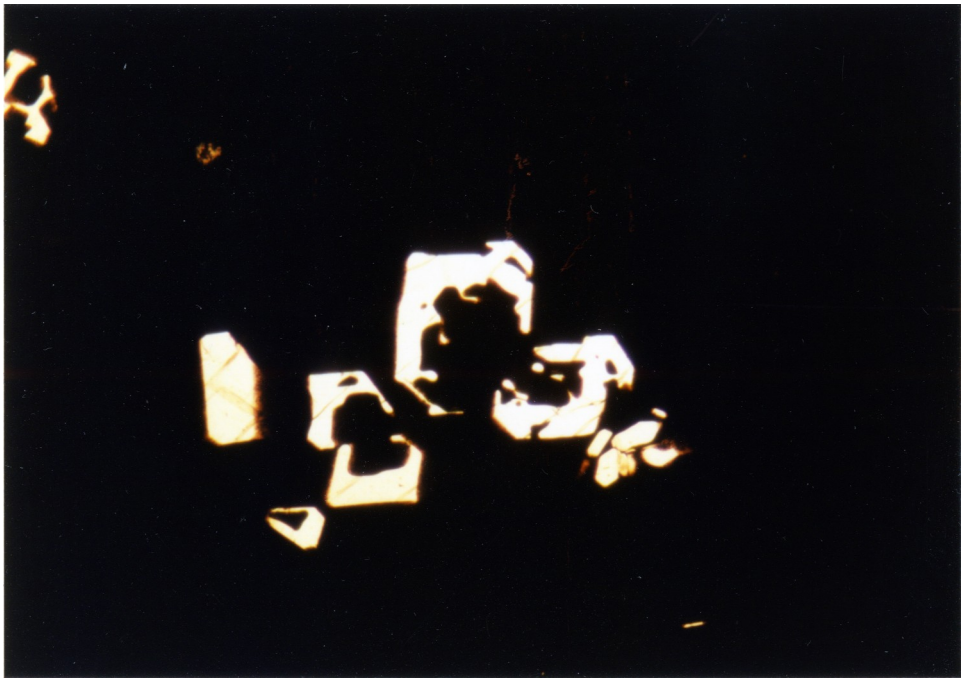

Figure 16. Photomicrograph of deeply embayed, reversely-zoned olivines from the crystalline zone of VG-383. Long dimension of photo is equal to 2.5 mm.

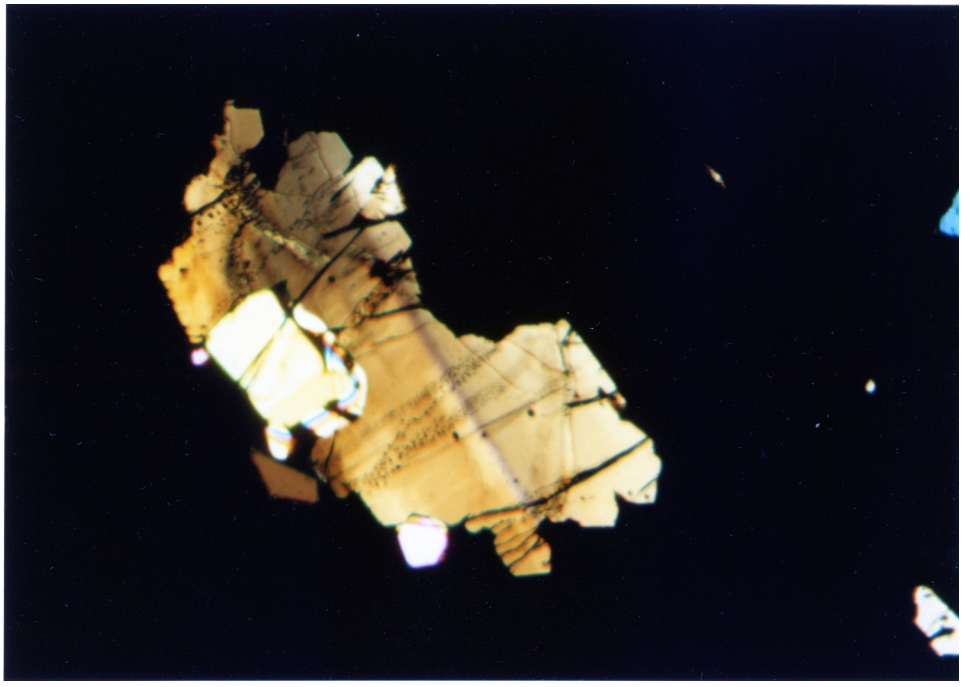

Figure 17. Photomicrograph, taken in cross-polarized light, of xenocrystic olivine showing deformation bands and possible fluid inclusions from VG-357. Long dimension of photo is equal to 2.5 mm.

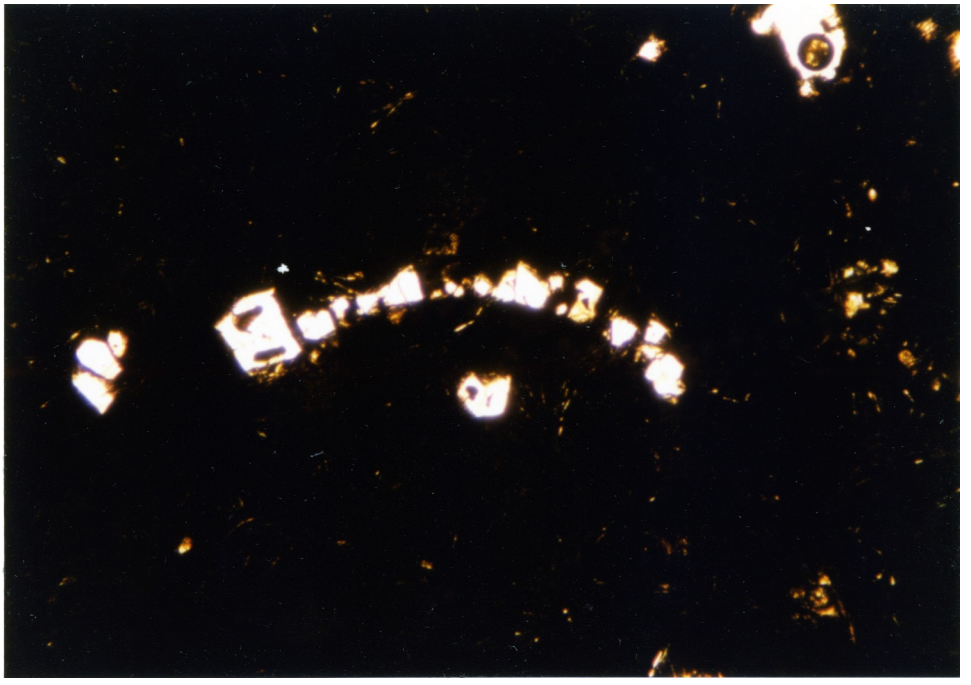

Figure 18. Photomicrograph of arcuate olivine chain from the crystalline zone of VG-387. This feature is similar to the ring-structures reported in MORB from the Oceanographer Fracture Zone by Walker et al. (1980). Long dimension of photo is equal to 2.5 mm.

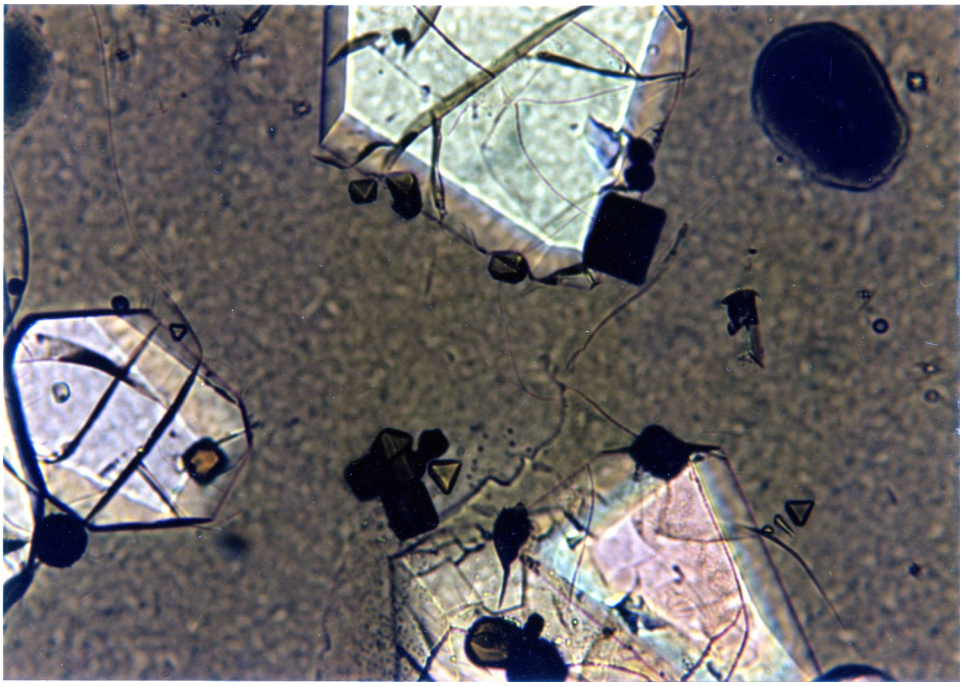

Figure 19. Photomicrograph showing euhedral to subhedral chromian spinels as inclusions in olivine, embedded in olivine grain boundaries, and in basaltic glass matrix from VG-348. Long dimension of photo is equal to 0.64 mm.

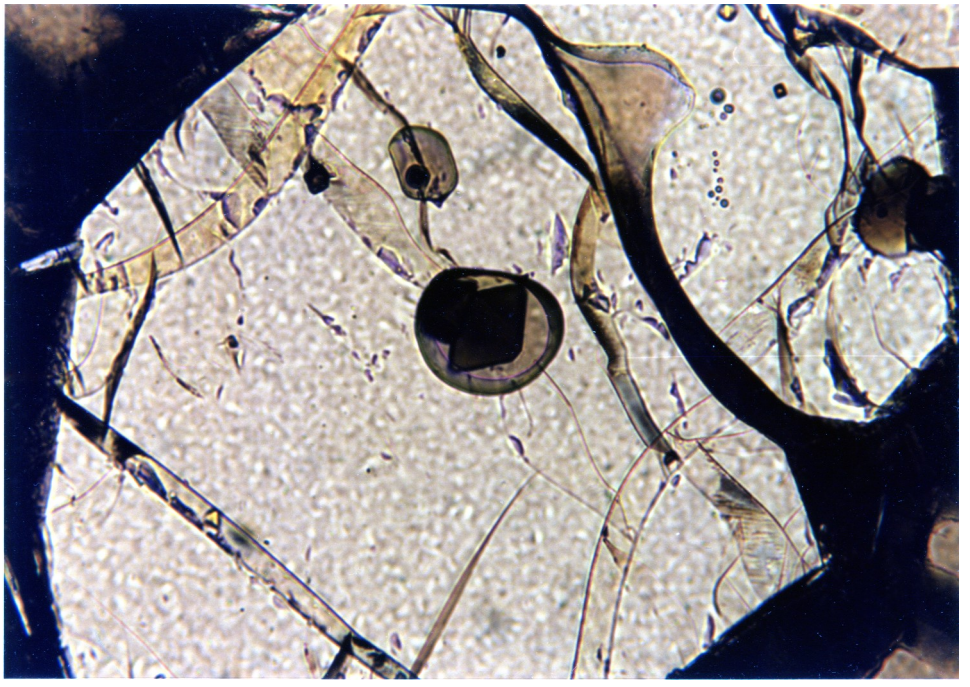

Figure 20. Photomicrograph showing melt inclusion with chromian spinel in olivine from VG-376. Long dimension of photo is equal to 0.64 mm.

3.2.3 Plagioclase.

Plagioclase is a minor phase in the majority of samples in which it occurs. It is colorless under plane polarized light, and albite twinning is ubiquitous under cross-polarized light. Grains usually take the form of laths, and may occur either alone in the glass, intergrown with other plagioclase grains or with olivine. The grain size in most samples is small, averaging 0.04 x 0.20 mm.

Plagioclase is abundant in VG-169, forming laths with a larger average size than in any other sample (0.10 x 0.25 mm), with considerably larger grains occurring in the crystalline zone. It commonly forms plagioclase glomerocrysts, as well as intergrowths with olivine (Fig. 21). Some grains display zoning (Fig. 22), a feature which is absent in all but one (VG-342) other sample.

3.3 Crystallization Sequence.

The order of appearance of phenocryst phases can be inferred based on petrography. Given that the samples containing only olivine show no sign of ever having been saturated in chromian spinel (i.e. no spinel inclusions are found even in the resorbed-looking grains), it would seem that olivine was the first phase to appear on the liquidus. The order of appearance of phases as the melt cooled would then be (1) olivine, (2) olivine + chromian spinel, (3) olivine + chromian spinel + plagioclase, and (4) olivine + plagioclase. This is a commonly observed crystallization sequence in mid-ocean ridge tholeiites, and it can be understood qualitatively by looking at the iron-free system anorthite-forsterite-diopide (e.g. Morse, 1980). Figure 23a shows that melts whose bulk composition start in the forsterite + liquid field close to the forsterite-anorthite join (hexagon), will have olivine as the first phase on the liquidus. The composition of the melt will move directly away from the forsterite corner of the ternary until it reaches the forsterite + spinel + liquid cotectic. Crystallization of olivine + spinel will move the liquid along this cotectic until it reaches the spot at which the forsterite, anorthite and spinel fields meet. At this "reaction point" a four phase assemblage of forsterite + anorthite + spinel + liquid will exist. Equilibrium crystallization would cause the liquid to remain at the reaction point until all of the spinel is eliminated through the reaction:

Spinel + Liquid = Forsterite + Anorthite

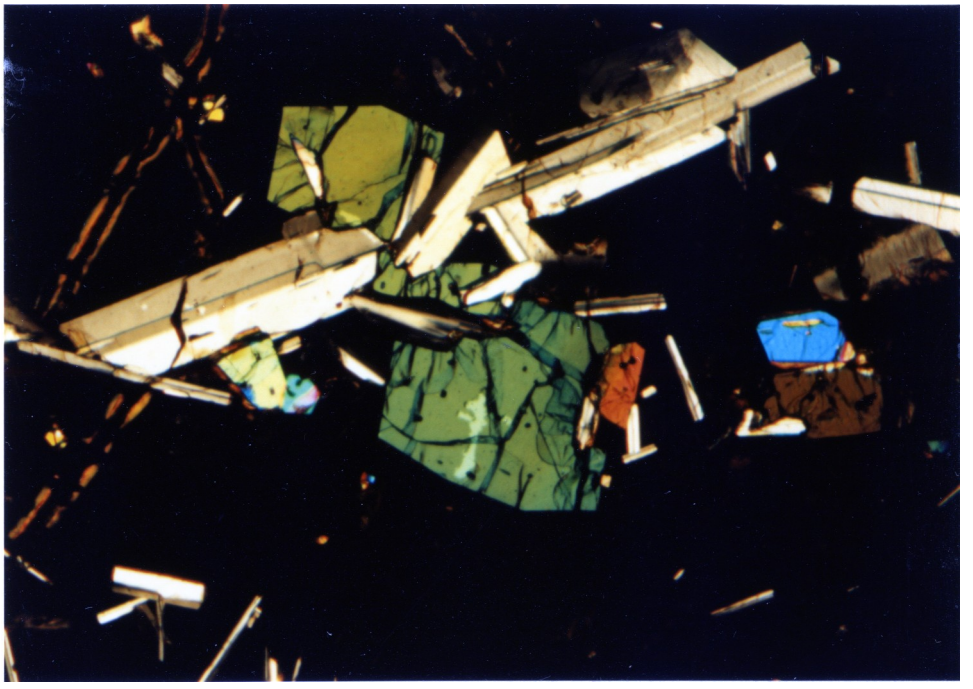

Figure 21. Photomicrograph, taken in cross-polarized light, showing plagioclase-olivine intergrowth from crystalline zone of VG-169. Long dimension of photo is 2.5 mm.

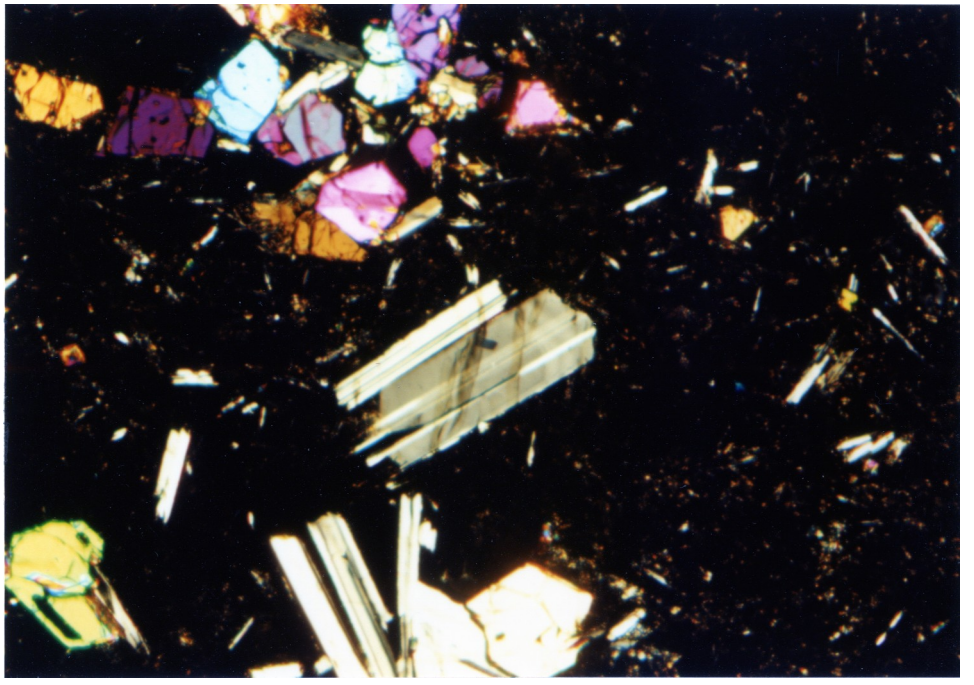

Figure 22. Photomicrograph, taken in cross-polarized light, showing zoned plagioclase (center) from crystalline zone of VG-169. Long dimension of photo is equal to 2.5 mm.

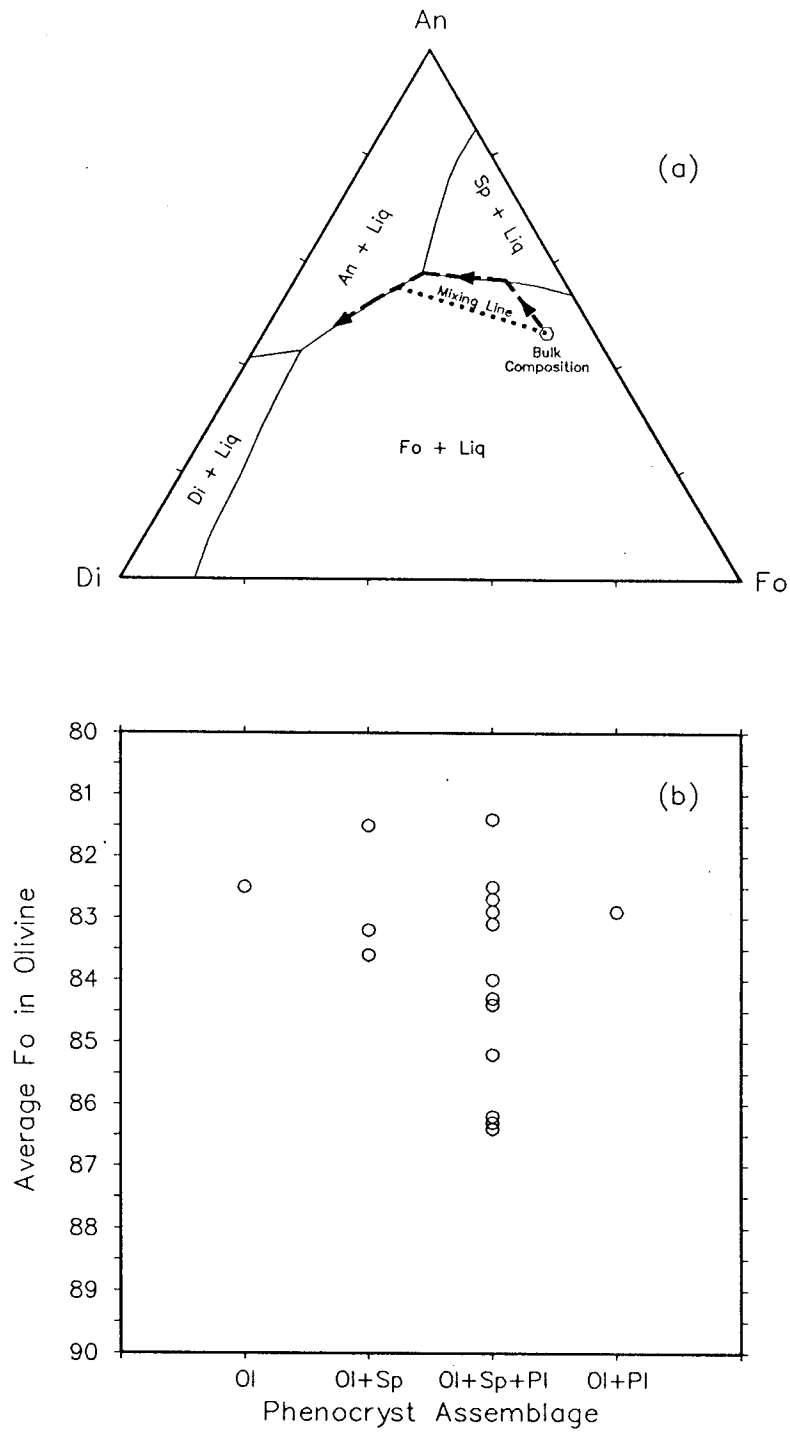

Figure 23. (a) Phase relations in the iron-free system An-Fo-Di, after Morse (1980). Heavy dashed line shows crystallization path for a magma with an initial bulk composition (hexagon) in the Fo + Liq field. Dotted line shows the effect of mixing an evolved composition with the parental liquid. (b) Average olivine compositions for samples grouped by observed phenocryst assemblage.

Fractional crystallization will not allow the reaction to take place, so that the liquid will continue through the reaction point with spinel simply stops crystallizing. Once spinel has disappeared, the liquid moves along the the forsterite + anorthite + liquid cotectic, crystallizing anorthite and forsterite.

Although the appearance and disappearance of phases observed in the Blanco Trough suite are consistent with the well characterized phase equilibria in the anorthite-forsterite-diopside system, no simple relationship exists between the observed phenocryst assemblage and the liquid composition. Figure 23b shows that as the phenocryst assemblage changes, the $Mg/(Mg + Fe^{2+})$ of the liquid as shown by the average forsterite content of the olivines does not change systematically. This implies that the more than one batch of parental magma must have been involved in the petrogenesis of the suite, because magma mixing would cause the liquid compositions to leave the three-phase cotectics (Fig. 23a), and start the crystallization sequence over in the forsterite + liquid field at different values of $Mg/(Mg + Fe^{2+})$ for the magma.

3.4 Summary.

Petrographic evidence shows that all of the Blanco Trough glasses for which thin sections are available are saturated in olivine, while 61.5% are saturated in chromian spinel. Some of the olivines display deformation bands and trails of what appear to be fluid inclusions, indicating that they are probably cumulate xenocrysts. Plagioclase is a major phenocryst phase in only one sample, and is absent completely from 38.5% of the thin sections. Based strictly on petrography, and assuming that all samples are genetically related, the inferred crystallization sequence is:

olivine
olivine + chromian spinel
olivine + chromian spinel + plagioclase
olivine + plagioclase

This indicates that most of the the Blanco Trough glasses represent primitive MORB that have undergone relatively little plagioclase crystallization. Although the appearance and disappearance of phenocryst phases agrees very well with the phase equilibria in the system anorthite-forsterite-diopside, no simple relationship exists between the liquid composition and the phenocryst assemblage. This

implies the existence of several batches of parental magma, and that magma mixing, in addition to fractional crystallization, is involved in the petrogenesis of the suite.

4. Major Element and Phase Chemistry of the Blanco Trough Glasses.

4.1 Introduction.

Basalts recovered from mid-ocean ridges throughout the world, both in dredge hauls and during submersible dives, are dominantly tholeiitic. They have a characteristic low pressure crystallization sequence of olivine ± chromian spinel, olivine + plagioclase ± chromian spinel, and olivine + plagioclase + augite with decreasing temperature (Bender et al., 1978; Walker et al., 1979; Bryan, 1983). The ubiquity of this sequence leads to predictable chemical variations within a cogenetic suite of MORB which can be quantitatively evaluated using mass balance or least squares mixing calculations (Bryan, Finger and Chayes, 1968). In addition, a pronounced enrichment in total iron with increasing degrees of fractional crystallization is a definitive characteristic of primitive tholeiitic basalts.

There are several processes, in addition to fractional crystallization, which can affect the compositional variations found in basalt suites, and their influence can complicate the interpretation of chemical data obtained from MORB glasses. Mixing of primitive with relatively more evolved melts in sub-axial magma chambers during episodes of recharge (Dungan and Rhodes, 1978; Rhodes et al., 1979; Walker et al., 1979), and variation in degree of partial melting of a source region (Langmuir and Bender, 1984; Bender et al., 1984; Davis and Clague, 1987) are potentially the most important of these processes . The release of volatiles, such as H_2O and CO_2, and the separation of immiscible sulfide liquids (Mathez, 1976; Czamanske and Moore, 1977) occur with decreasing temperature, and assimilation of wall rock can sometimes be discerned using trace element and isotopic data, but the overall effect of these processes on the concentration of major elements is probably negligible.

The chemistry of phenocrysts found in the glass can be used to help constrain the petrogenesis of MORB. Because the glass composition is very close to that of the original liquid, assuming that quench modification is negligible, partition coefficients determined in phase-equilibira experiments can be used to quantitatively assess the degree of mineral-melt equilibrium. The presence or absence of zoned or embayed crystals can help in assessing the relative importance of such processes as magma mixing and xenocrystic contamination.

The Smithsonian analyses of the basaltic glasses recovered from the Blanco Trough stand out among MORB in some of the correlations observed among the major elements on variation diagrams. These anomalous trends were not reproduced in the analyses performed at R.P.I. The new analyses indicate major element variations more consistent with normal primitive MORB. This chapter will discuss the correlations found among the major elements, compare them to suites recovered from other areas, and attempt to reconcile the two data sets. The phase chemistry of the phenocrysts found in the glass, and the partitioning of major elements between phenocrysts and glass will also be discussed.

4.2 Analytical Procedures.

The original microprobe analyses of the glasses were performed by the Smithsonian Institution (Byerly et al., 1977; Melson et al., 1977) on fresh-looking chips less than 1 millimeter in diameter mounted in 5 millimeter holes on the perimeter of a 25 millimeter diameter by 6 millimeter thick lexan disc. Analyses were performed on either a three spectrometer ARL-EMX electron microprobe or a nine spectrometer ARL-SEMQ electron microprobe. A 50 micron defocused beam was used at 15 kilovolts accelerating potential and a beam current reported as 0.30 microamps, with 10 second counting times. Data reduction consisted of background and Bence-Albee correction procedures. Each analysis represents an average of five spots, with each oxide normalized to a VG-2 standard.

The new analyses were performed using a five spectrometer JEOL 733 Superprobe in the Department of Geology at Rensselaer Polytechnic Institute. Forty second counting times were used, with an accelerating potential of 15 kilovolts and a beam current of 20 nanoamps. The original mounts, supplied by the Smithsonian, were analyzed using a beam width of 20 microns. Reported glass analyses represent an average of approximately 5 spots, with standard deviations reported in Appendix 1. The VG-2 basaltic glass standard was analyzed after every five samples to ensure that calibrations did not drift. Averages of the VG-2 analyses, along with standard deviations, from each microprobe sessions are listed in Appendix 1. All phenocryst analyses were performed on doubly-polished thin sections, prepared from samples supplied by the Smithsonian, with a beam width of up to 20 microns, depending

on phenocryst size. On-line data reduction consisted of background and Bence-Albee correction procedures. Relative errors are generally less than 1% for major elements (SiO_2, Al_2O_3, FeO*, MgO, CaO), and less than 15% for minor elements (TiO_2, MnO, Na_2O, K_2O).

Determination of ferrous iron was performed on glass separates from twelve samples by Dr. I.S.E. Carmichael at the University of California at Berkeley using a colorimetric technique (Wilson, 1960; Lange and Carmichael, 1989). The separates were prepared at S.U.N.Y. at Albany by chipping glass off of the rind of the same samples used for thin sectioning, after first cleaning in a beaker of distilled water placed in an ultrasonic cleaner. The chips were then hand-ground in a boron-carbide mortar so as to pass through 60-mesh screen and catch on 100-mesh. The samples were then put through a Frantz magnetic separator to remove crystalline material. The resulting separates were hand-picked to remove any remaining crystalline material. During the dissolution process Dr. Carmichael reported that several samples (VG #'s 172, 345, 348, 384) contained an undissolved residue, presumably small chromian spinel grains that had been in the glass. Despite their presence, no systematic variations in $Fe^{3+}/(Fe^{2+} + Fe^{3+})$ were observed. The glass separate from sample VG-360 appeared to contain a large proportion of quench crystals (i.e. olivine dendrites and spherulites), but again no systematic variation in $Fe^{3+}/(Fe^{2+} + Fe^{3+})$ was observed.

4.3 Chemical Variations in MORB Suites Recovered from Other Areas.

The nature of the chemical trends to be expected in a normal MORB glass suite can be evaluated by comparing samples from several different areas. Compositions reported in the literature of basaltic glasses recovered from the Gorda Ridge (Davis and Clague, 1987), the Tamayo Fracture Zone (Bender et al., 1984), the FAMOUS area (Bryan and Moore, 1977), and the Galapagos (Fornari et al., 1983) will be used to represent well characterized glass suites from widely separated regions. In addition, the results of phase-equilibria studies on compositions recovered from the Oceanographer Fracture Zone (Walker et al., 1979) will be presented in order to further constrain the relative importance of fractional crystallization in producing the observed chemical variations.

The samples from the Gorda Ridge were recovered from 17 sites between 43° N and 40.8° N.

They represent normal MORB whose chemical characteristics are best explained by different degrees of partial melting and subsequent modification by varying degrees of fractional crystallization and magma mixing (Figs. 24, 25, 26). The phenocryst phases present in the glass are abundant plagioclase, less abundant olivine ± chromian spinel (Davis and Clague, 1987).

The Tamayo Fracture Zone samples were recovered from a 75 kilometer section of the East Pacific Rise, up to the area where it intersects the Tamayo Fracture Zone. Variation in degree of partial melting best explains the variations seen in this suite of samples also, with high and low pressure fractional crystallization playing a minor role (Figs. 24, 25, 26). The phenocryst phases found in the glasses are olivine and plagioclase, with rare chromian spinel and clinopyroxene (Bender et al., 1984).

The samples from the FAMOUS region were collected by the submersible Alvin from the median valley of the Mid-Atlantic Ridge near 36° 49'. The compositional variations observed in the suite can be qualitatively explained by fractional crystallization of calcic plagioclase with magnesian olivine and/or calcic pyroxene, although some component of variation in degree of partial melting is probably also present (Figs. 24, 25, 26). The phenocryst phases found in these glasses are olivine, plagioclase, clinopyroxene and chromian spinel (Bryan and Moore, 1977).

The Galapagos samples were collected by the submersible Alvin in the Ecuador and eastern Galapagos rifts, as well as along the Inca transform which connects them. The samples represent rock types ranging from MORB to FeTi basalts, andesites, and rhyodacites, including compositions thought to be transitional between the groups. It is thought that much of the chemical diversity found in these glasses can be attributed to fractional crystallization in small, shallow-level magma chambers (Fornari et al., 1983) (Figs. 24, 25, 26).

4.4 Major Element Chemistry of the Blanco Trough Glasses.

The major elements whose concentrations appear to be the most anomalous in the Smithsonian analyses are FeO* and CaO. In the samples with the lowest concentration of incompatible minor elements (TiO_2, Na_2O, K_2O), the concentration of FeO* is the highest found in the suite, while the concentration of CaO is the lowest, the opposite of what is commonly observed in

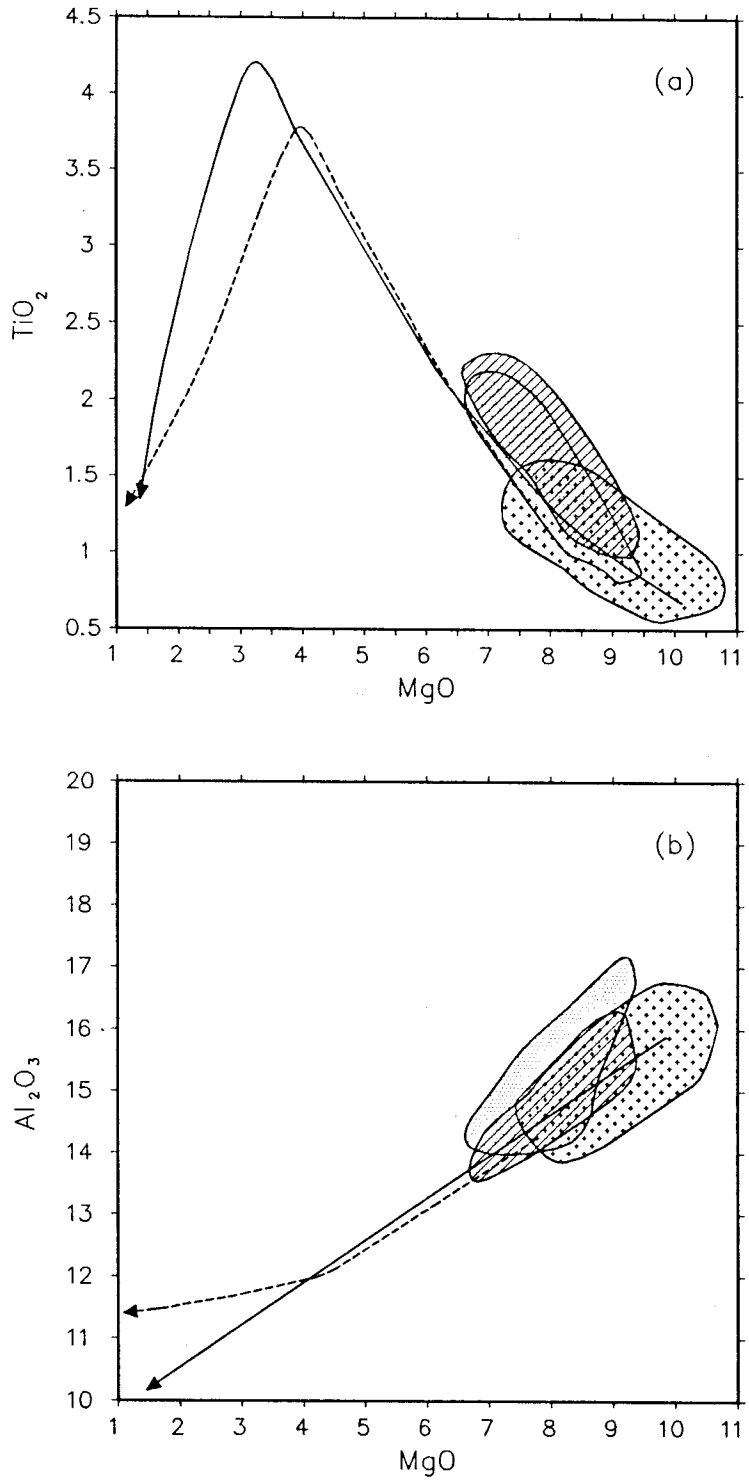

Figure 24. Plots of MgO vs. (a) TiO_2 and (b) Al_2O_3 showing MORB glass compositions from the FAMOUS region (crosses), Gorda Ridge (dots), Tamayo Fracture Zone (diagonal lines), Galapagos region (dashed line) and Oceanographer Fracture Zone experiments (solid line).

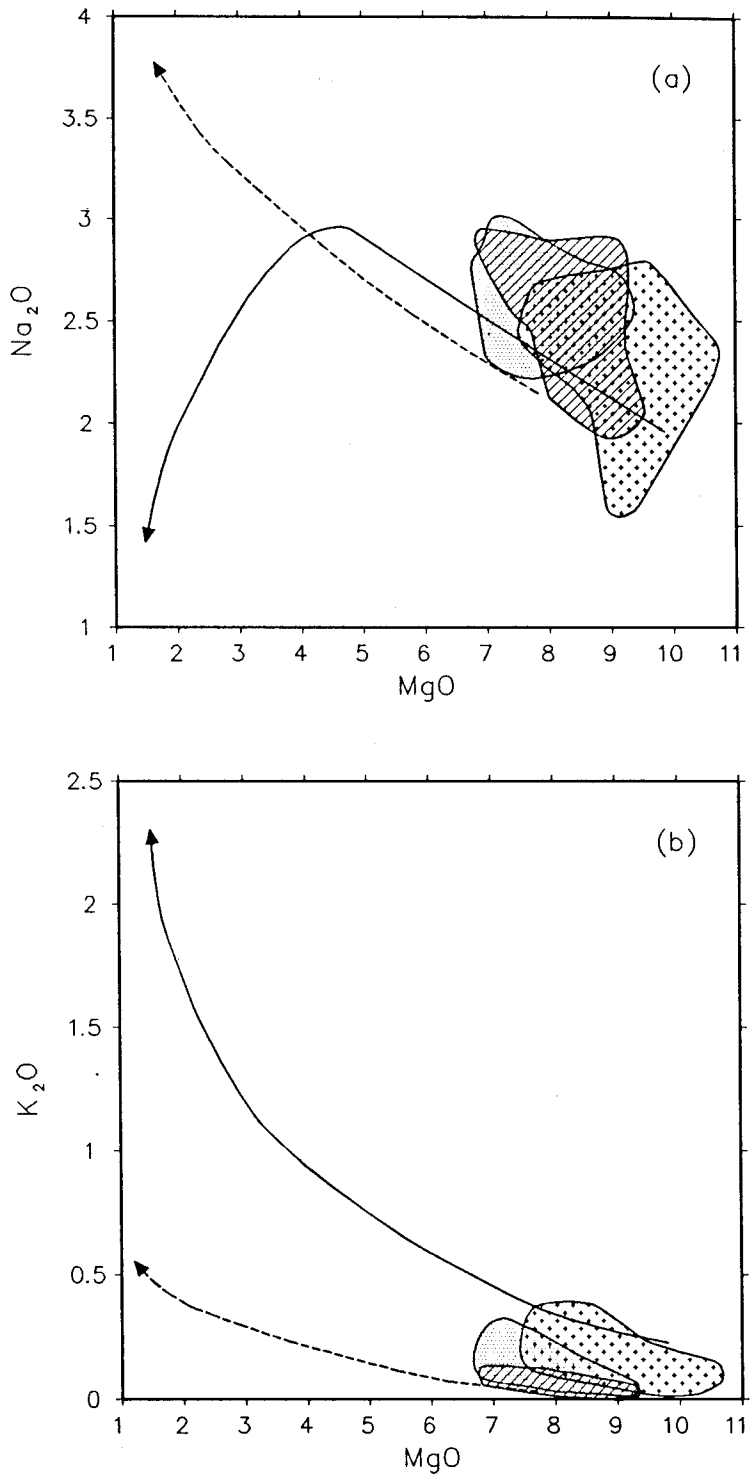

Figure 25. Plots of MgO vs. (a) Na_2O and (b) K_2O showing MORB glass compositions from the FAMOUS region (crosses), Gorda Ridge (dots), Tamayo Fracture Zone (diagonal lines), Galapagos region (dashed line) and Oceanographer Fracture Zone experiments (solid line).

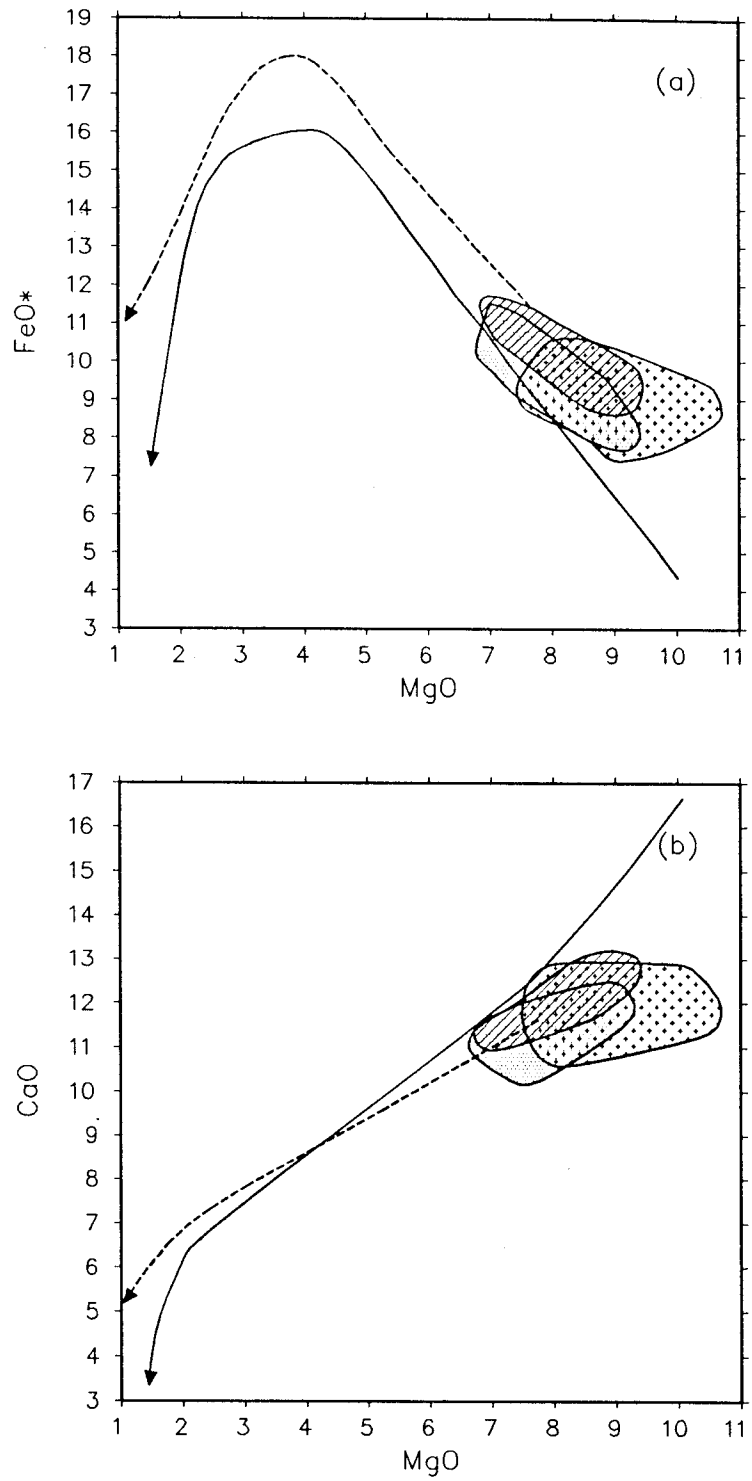

Figure 26. Plots of MgO vs. (a) FeO* and (b) CaO showing MORB glass compositions from the FAMOUS region (crosses), Gorda Ridge (dots), Tamayo Fracture Zone (diagonal lines), Galapagos region (dashed line) and Oceanographer Fracture Zone experiments (solid line).

MORB glasses (Table III). The microprobe analyses performed at R.P.I. do not show these anomalies, however, and thus seem to imply that these glasses represent more normal mid-ocean ridge tholeiites (Table IV).

During pressure-release partial melting of a peridotitic upper mantle it is expected that the incompatible elements would show the highest concentrations in the first increments of melt, while the concentration of the compatible elements would be the lowest. Subsequent melting would serve to enrich the compatible, while diluting the incompatible elements, causing a negative correlation between members of the two groups. During an episode of fractional crystallization the process would be reversed and, assuming that the crystallizing phases are relatively similar to those that melted in the source region, the negative correlation should be preserved.

Given these assumptions, it is difficult to explain the primitive compositions represented by the Smithsonian analyses by partial melting of the type of lherzolite normally associated with the oceanic upper mantle. If the apparently high concentration of FeO*, and low concentration of CaO in those samples which have low concentrations of the incompatible elements are to be accepted, then melting of a modified peridotite must be invoked. However, the types of metasomatic processes believed to alter portions of the upper mantle (i.e. silicate melt migration and fluid related metasomatism) tend to cause a pronounced enrichment in the large ion lithophile elements (e.g. K_2O) which is not seen in these samples (Le Roèx, 1987).

Sections 4.4.1 and 4.4.2 will discuss the chemical variations as defined by each data set in detail. If the original analyses are in error, then an explanation for its cause must also explain the systematic behavior of FeO* and CaO that they display, as well as the good match found for the other elements between the two data sets.

4.4.1 Chemical Variations from Smithsonian Analyses.

The chemical variations observed in the Smithsonian analyses are broadly similar to the Gorda, Tamayo and FAMOUS suites in some respects, and quite distinct in others. Among the incompatible minor elements (TiO_2, Na_2O, K_2O), the expected negative correlation with MgO is

Table III

Comparison of Smithsonian analyses of relatively "primitive" and "evolved" samples from the Blanco Trough.

Sample	*VG-345*	*VG-347*	*VG-348*	*VG-360*	*VG-383*
SiO_2	49.55	49.36	48.34	50.15	50.35
TiO_2	1.38	1.53	0.83	2.54	2.21
Al_2O_3	16.27	16.53	17.56	14.73	14.86
FeO*	12.57	12.23	12.42	11.08	11.43
MnO	n.d.	n.d.	n.d.	n.d.	n.d.
MgO	8.04	7.63	8.80	6.56	7.60
CaO	8.98	10.27	9.71	11.27	10.92
Na_2O	2.65	2.70	2.37	2.98	2.88
K_2O	0.10	0.16	0.06	0.39	0.31
P_2O_5	0.10	0.14	0.06	0.29	0.20
Total	99.63	100.55	100.15	99.99	99.27
Mg#	53.3	52.7	55.8	51.3	51.0
Ca#	65.2	67.8	69.4	67.6	63.9
CaO/Al_2O_3	0.552	0.621	0.553	0.765	0.693

Table IV

Comparison of R.P.I. analyses of relatively "primitive" and "evolved" samples from the Blanco Trough.

Sample	*VG-345*	*VG-347*	*VG-348*	*VG-360*	*VG-383*
SiO_2	49.26	48.75	48.09	50.41	50.42
TiO_2	1.58	1.66	0.91	2.63	2.18
Al_2O_3	16.13	16.12	17.41	14.72	14.90
FeO*	9.52	10.80	10.35	11.90	11.71
MnO	0.19	0.20	0.22	0.22	0.21
MgO	8.66	8.02	9.22	6.90	7.68
CaO	11.67	11.15	11.52	10.25	10.74
Na_2O	2.81	2.88	2.60	2.93	2.94
K_2O	0.12	0.19	0.09	0.43	0.31
P_2O_5	n.d.	n.d.	n.d.	n.d.	n.d.
Total	99.94	99.77	100.41	100.39	101.09
Mg#	61.9	57.0	61.3	50.8	53.9
Ca#	69.6	68.1	71.0	65.9	66.9
CaO/Al_2O_3	0.723	0.692	0.662	0.696	0.721

present in all four suites (Figs. 27a, 28). In addition, the concentration of these elements for a given MgO content in the Blanco Trough glasses is very similar to those from Gorda Ridge and the Tamayo Fracture Zone, but all three are distinct from the FAMOUS samples. The FAMOUS glasses appear more primitive, with higher MgO coupled with lower TiO_2 and Na_2O (Figs. 27a, 28a), but similar concentrations of K_2O (Fig. 28b). This seeming difference in the behavior of the K_2O concentration may be due, at least in part, to the higher relative errors associated with electron microprobe determination of elements with low concentrations.

The major elements do not behave quite as regularly as the minor elements. Al_2O_3 shows the expected positive correlation with MgO, consistent with crystallization or melting of an Al-bearing phase, although the Blanco Trough glasses appear to be slightly enriched at higher MgO contents compared with the other suites (Fig. 27b).

In contrast, a plot of MgO vs. FeO* shows an abnormal positive correlation, with the exception of a few samples which plot at lower FeO* for a given concentration of MgO (Fig. 29a). This indicates that FeO* is behaving compatibly in the majority of samples, indicating the presence of an Fe-bearing phase, again either crystallizing from the melt or as a residual in the source region.

A plot of MgO vs. CaO shows that the behavior of Ca is just as abnormal as Fe. In this case a negative correlation is observed, once again with the exception of a few samples that plot in the range expected based on the other MORB suites (Fig. 29b). This means that Ca is behaving incompatibly in these melts, indicating that neither plagioclase nor clinopyroxene can be playing a large role in either fractional crystallization or partial melting.

Based on the concentrations of FeO* and CaO from the Smithsonian analyses, it seems that the Blanco Trough glasses can be divided into a group with normal MORB affinities, and a group with unique FeO* and CaO characteristics (Table V). The chemical trends seen in the abnormal group are consistent with the controlling influence of an Fe-bearing phase, as well as the fact that plagioclase is not controlling the Al_2O_3 variations. These observations are consistent with the conclusion that magnesian olivine and an Fe,Al-rich spinel phase are responsible for the compositional variations observed in these basalts. Figure 30 illustrates the effect of removing olivine and chromian spinel of

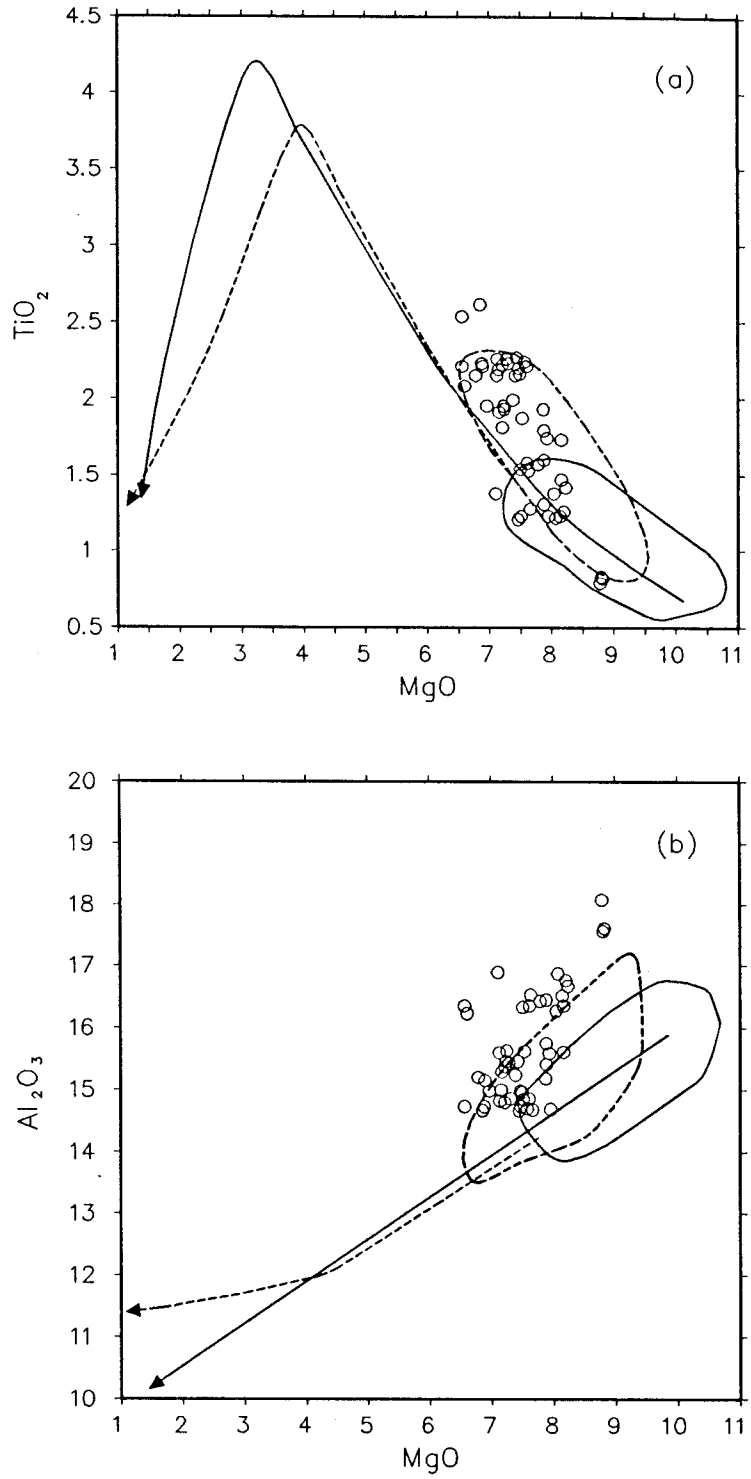

Figure 27. Plots of MgO vs. (a) TiO_2 and (b) Al_2O_3 comparing the Smithsonian analyses of the Blanco Trough glasses with MORB glass compositions from the FAMOUS region (field bounded by solid line), Gorda Ridge and Tamayo Fracture Zone (field bounded by dashed line), Galapagos region (dashed line) and Oceanographer Fracture Zone experiments (solid line).

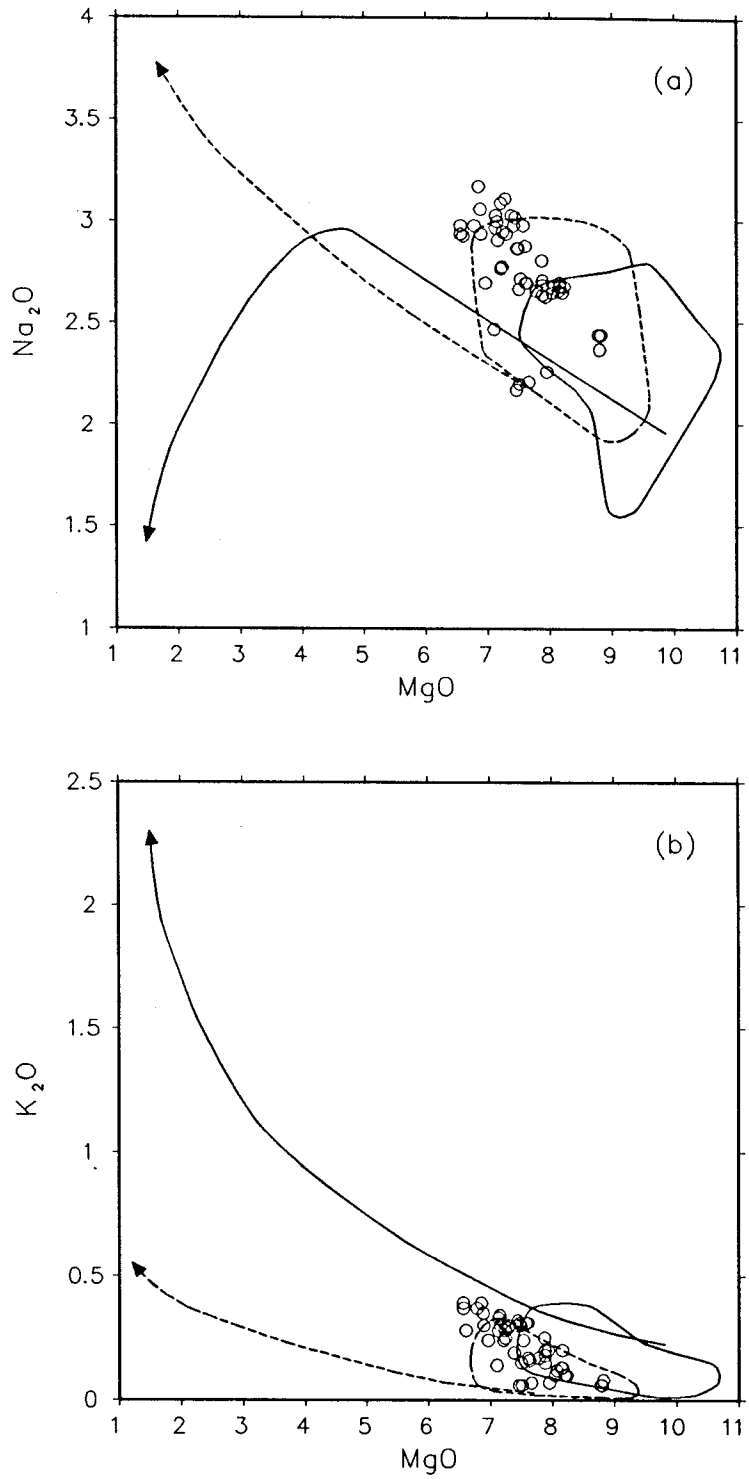

Figure 28. Plots of MgO vs. (a) Na_2O and (b) K_2O comparing the Smithsonian analyses of the Blanco Trough glasses with MORB glass compositions from the FAMOUS region (field bounded by solid line), Gorda Ridge and Tamayo Fracture Zone (field bounded by dashed line), Galapagos region (dashed line) and Oceanographer Fracture Zone experiments (solid line).

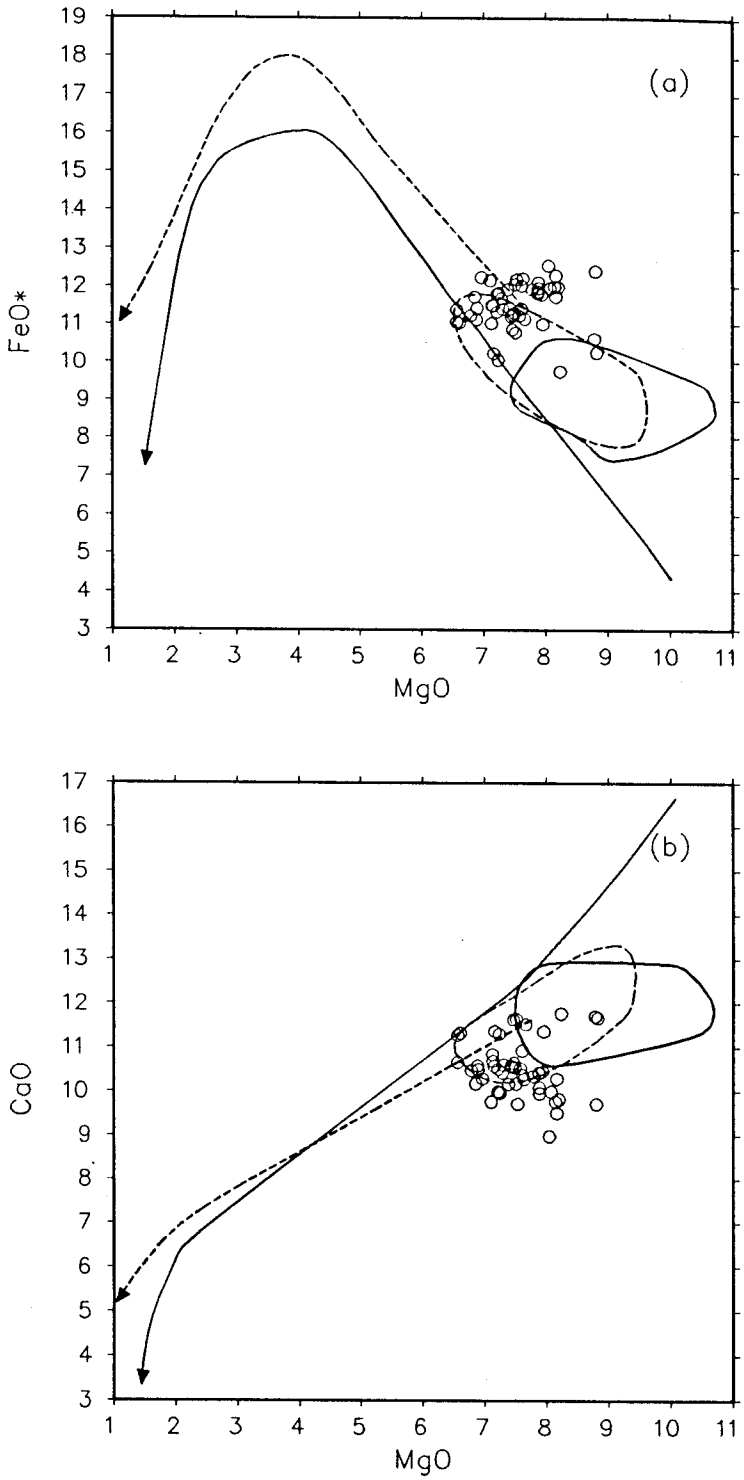

Figure 29. Plots of MgO vs. (a) FeO* and (b) CaO comparing the Smithsonian analyses of the Blanco Trough glasses with MORB glass compositions from the FAMOUS region (field bounded by solid line), Gorda Ridge and Tamayo Fracture Zone (field bounded by dashed line), Galapagos region (dashed line) and Oceanographer Fracture Zone experiments (solid line).

Table V

Blanco Trough glasses showing normal MORB affinities and anomalous FeO and CaO characteristics in the Smithsonian analyses.*

Normal MORB	*Anomalous FeO*, CaO*	
VG-169	VG-170	VG-353
VG-173	VG-172	VG-354
VG-368	VG-178	VG-355
VG-369	VG-332	VG-356
VG-370	VG-337	VG-357
VG-371	VG-338	VG-358
VG-373	VG-339	VG-359
VG-376	VG-340	VG-360
VG-377	VG-341	VG-372
VG-379	VG-342	VG-374
	VG-343	VG-375
	VG-344	VG-378
	VG-345	VG-380
	VG-346	VG-381
	VG-347	VG-382
	VG-348	VG-383
	VG-349	VG-384
	VG-350	VG-385
	VG-351	VG-386
	VG-352	VG-387

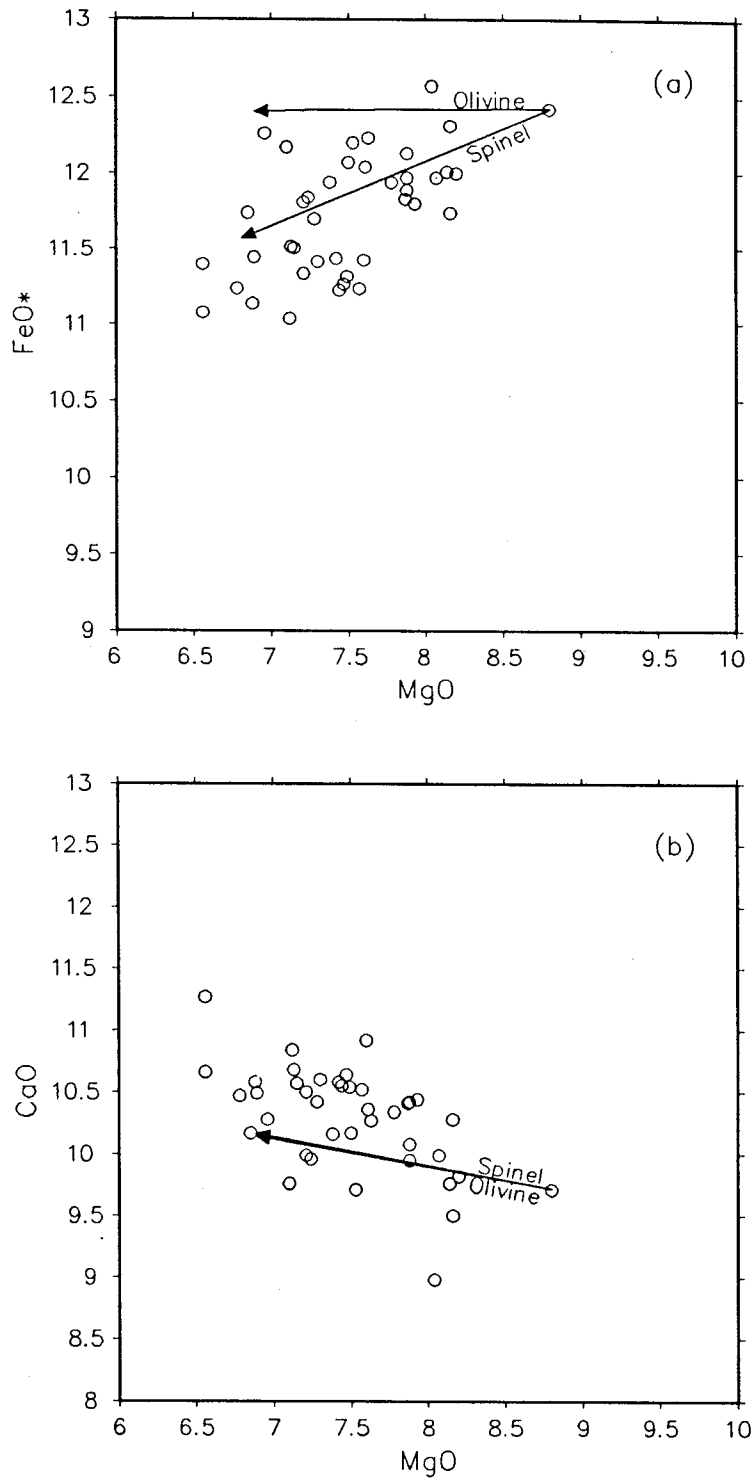

Figure 30. Plots of MgO vs. (a) FeO* and (b) CaO for the samples which appear anomalous in the Smithsonian analyses (Table V), illustrating the effect of removing olivine and chromian spinel of the composition found in VG-348.

the appropriate composition from VG-348. Because the observed partition coefficient for FeO* between olivine and melt is ~1, and between chromian spinel and melt is ~1.3 for this glass, fractional crystallization of large amounts of the latter would produce a trend approximating what is actually observed. Because neither olivine nor chromian spinel contain any substantial amounts of CaO, its distribution coefficient in a melt saturated in only these phases would be very small, and it would be enriched in the melt. Partial melting of a source region rich in an Fe-rich spinel phase could produce trends approximating those seen in this suite by similar arguments.

It can be seen that although the variations in FeO* and CaO reported in the Smithsonian analyses are anomalous, and indicate that the Blanco Trough glasses are, by definition, not tholeiitic, a reasonable petrologic explanation can be found for them. This explanation is not only consistent with the chemistry of the suite, but also with the fact that all of the samples for which thin sections were made contain olivine, and over 60% contain chromian spinel (Table II). In addition, plagioclase is either absent or present only as a minor phenocryst phase in all but two thin sections, unlike other mid-ocean ridge basalts in which it is commonly the dominant phase.

4.4.2 Chemical Variations from the R.P.I. Analyses.

The electron microprobe analyses performed at Rensselaer Polytechnic Institute indicate a petrogenesis for this suite that is quite different from the one described in section 4.4.1. Variation diagrams for the incompatible minor elements once again display negative correlations with MgO, as expected from the other MORB suites, although Na_2O appears to be slightly enriched for a given MgO content (Figs. 31a, 32).

A comparison of variation diagrams for the major elements show that Al_2O_3 is the most consistent between the two data sets. There is a positive correlation with MgO in both cases, an indication that it is behaving as a compatible element. The main difference between the two sets of analyses appears to be the fact that the R.P.I. results show a smaller amount of scatter along the Al_2O_3 axis (Figs. 27b, 31b).

The major difference between the two data sets is shown in the variation diagrams for FeO*

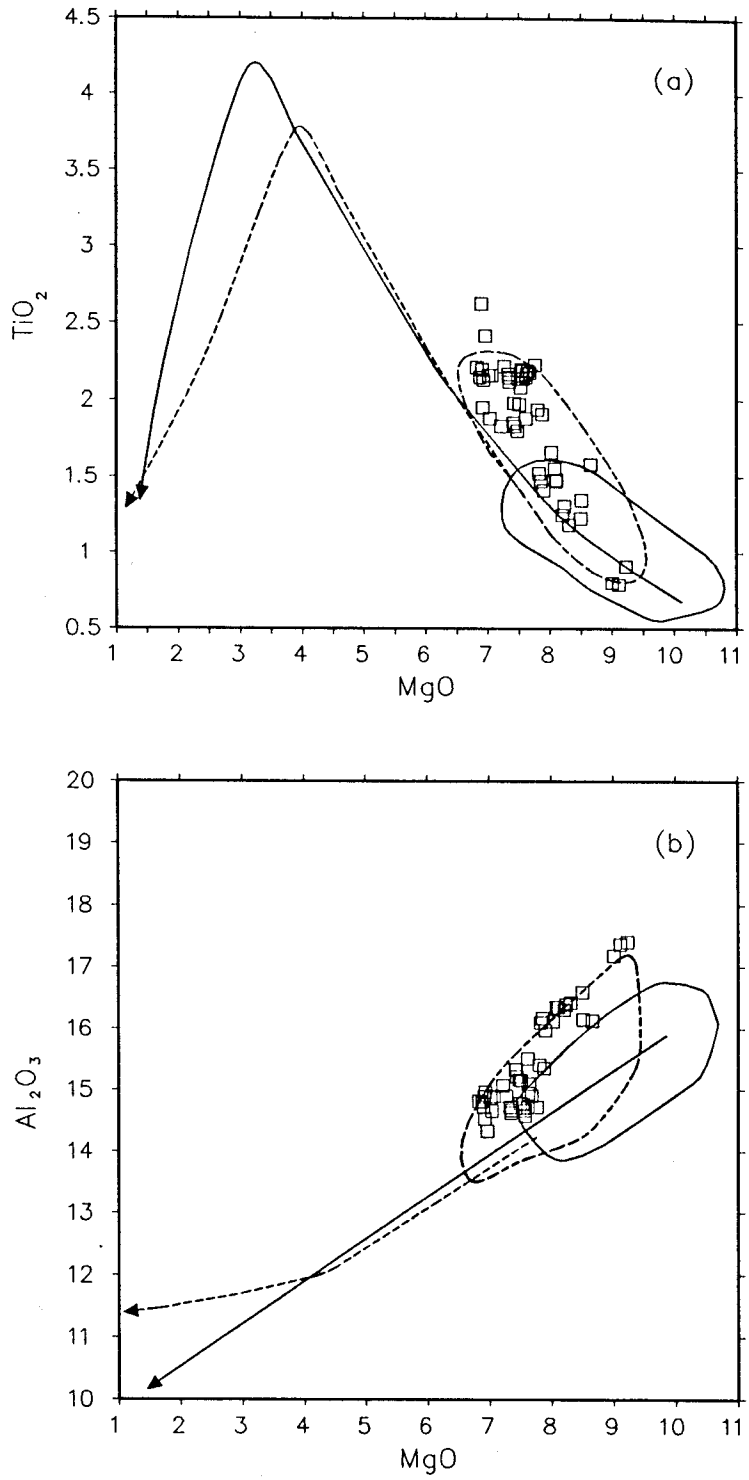

Figure 31. Plots of MgO vs. (a) TiO_2 and (b) Al_2O_3 comparing the R.P.I. analyses of the Blanco Trough glasses with MORB glass compositions from the FAMOUS region (field bounded by solid line), Gorda Ridge and Tamayo Fracture Zone (field bounded by dashed line), Galapagos region (dashed line) and Oceanographer Fracture Zone experiments (solid line).

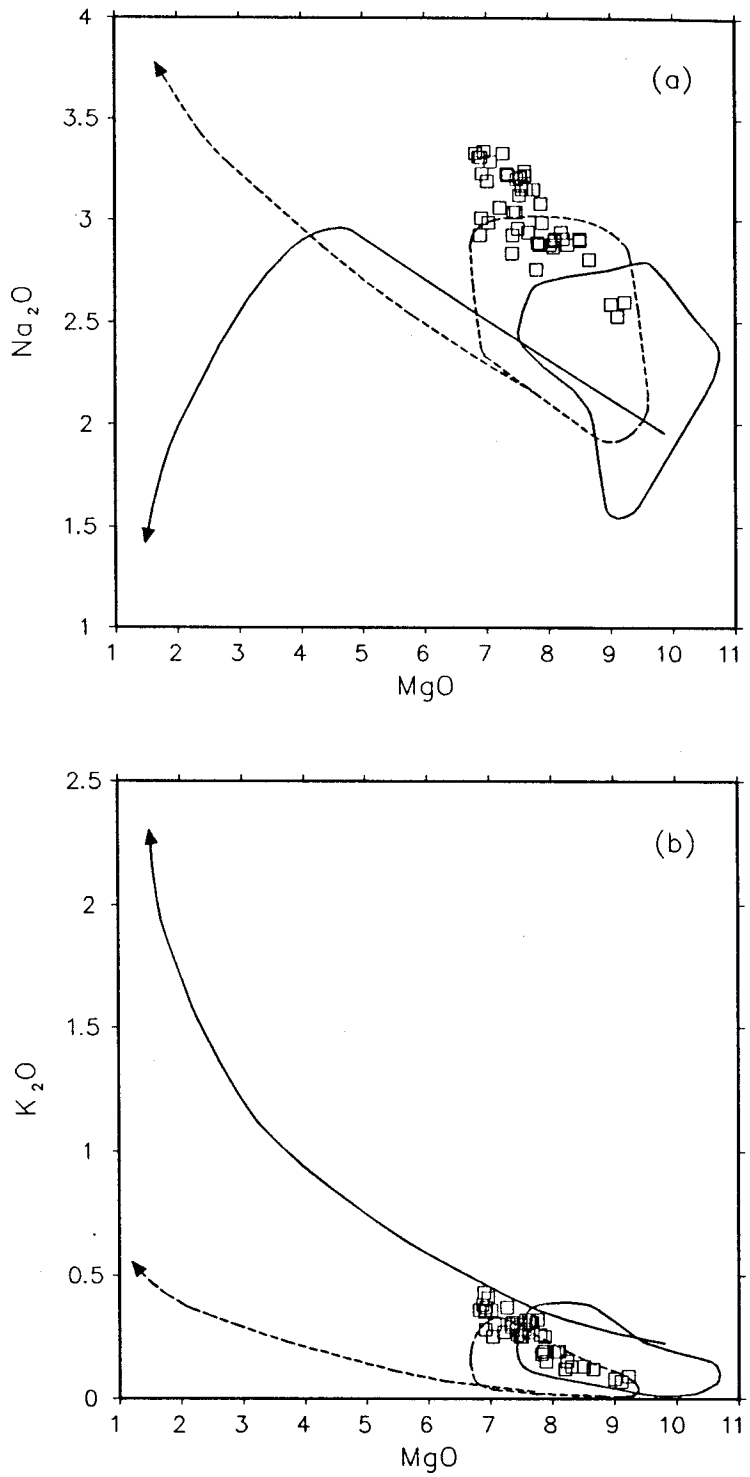

Figure 32. Plots of MgO vs. (a) Na_2O and (b) K_2O comparing the R.P.I. analyses of the Blanco Trough glasses with MORB glass compositions from the FAMOUS region (field bounded by solid line), Gorda Ridge and Tamayo Fracture Zone (field bounded by dashed line), Galapagos region (dashed line) and Oceanographer Fracture Zone experiments (solid line).

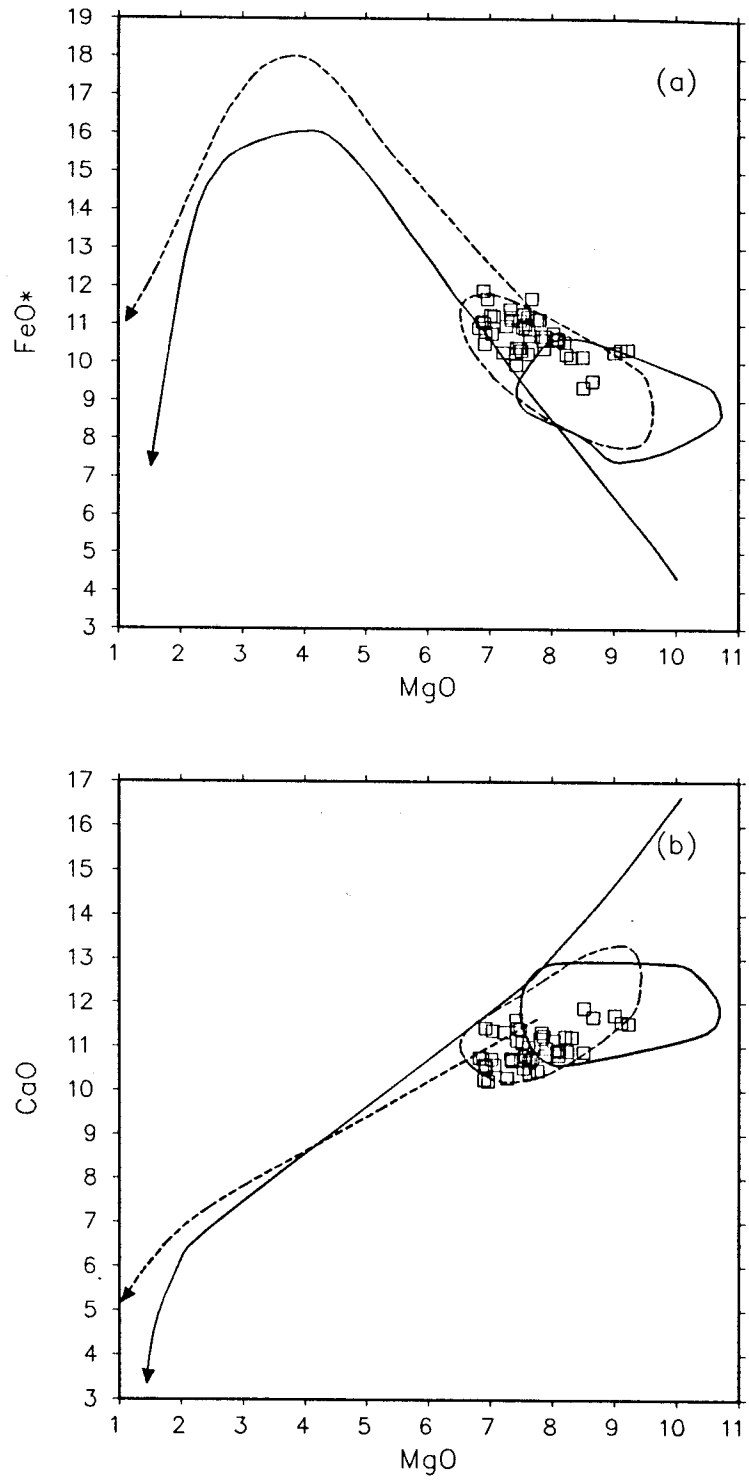

Figure 33. Plots of MgO vs. (a) FeO* and (b) CaO comparing the R.P.I. analyses of the Blanco Trough glasses with MORB glass compositions from the FAMOUS region (field bounded by solid line), Gorda Ridge and Tamayo Fracture Zone (field bounded by dashed line), Galapagos region (dashed line) and Oceanographer Fracture Zone experiments (solid line).

and CaO. The R.P.I. trends contradict the Smithsonian data, in which FeO* appears to be compatible and CaO incompatible. The new analyses indicate that the Blanco Trough glasses are indeed tholeiitic, although slightly enriched in FeO* in the samples with higher MgO (Fig. 33a). In addition, CaO displays a positive correlation with MgO, indicating the contribution of a Ca-bearing phase to the compositional variability, although the suite is slightly depleted in Ca in the MgO rich sabmples (Fig. 33).

The new analyses also appear to be compatible with the phenocryst phases observed in thin section. The fact that the glasses are slightly enriched in Al_2O_3 and slightly depleted in CaO would seem to favor the crystallization of chromian spinel, while causing plagioclase crystallization to be suppressed slightly. Because the range of compositions of these glasses appears to be so similar to those recovered from the Gorda Ridge and the Tamayo fracture zone, it seems reasonable to assume that their petrogenesis also involved some combination of variation in degree of partial melting and fractional crystallization of olivine, chromian spinel and plagioclase. If fractional crystallization is the dominant influence on the compositional variations; the slight enrichments observed in FeO* and Na_2O, and the slight depletion in CaO might be due to smaller than normal degrees of partial melting during formation of the parent liquid. Conversely, if partial melting is the dominant control, then the enrichments and depletions must be the chemical signature of the source region.

4.5 Phase Chemistry of the Blanco Trough Glasses.

The phenocryst phases found in the Blanco Trough glasses tend to be, with a few notable exceptions, euhedral to subhedral and unzoned. This is indicative of a melt that has undergone relatively little magma mixing or assimilation of xenocrystic material. In addition to textural evidence and the presence or absence of zoning, the partitioning of major elements between crystalline and melt phases can be used to indicate the relative importance of these processes, as the composition of xenocrystic material or phenocrysts inherited from a relatively more primitive or evolved magma would be distinct from equilibrium phases. In addition to holding information of petrogenetic significance, the phase chemistry of these glasses should help in discriminating which of the two data sets is in error,

so that the correct petrogenesis for the suite can be discerned.

4.5.1 Olivine-Melt Equilibria.

The partitioning behavior of Fe^{2+} and Mg between olivine and melt has been the focus of phase equilibria studies for the past twenty years because of its importance to the study of basaltic and ultramafic rocks (e.g. Roeder and Emslie, 1970; Mysen, 1975). In their benchmark study Roeder and Emslie found that for basaltic liquids, at one atmosphere total pressure, the distribution coefficient:

$$K_D^{Ol/L} = (X_{FeO}/X_{MgO})^{olivine}(X_{MgO}/X_{FeO})^{liquid}$$

is a constant, independent of temperature, equal to 0.30. Studies of lunar rocks have demonstrated a compositional dependence for $K_D^{Ol/L}$, especially in high-titanium basalts, thought to be caused by TiO_2-induced variations in melt structure (Green et al., 1975; Longhi et al., 1978; Delano, 1980; Jones 1988; Delano, 1990), however this effect has been found to be negligible for terrestrial basalt compositions.

Knowledge of the fugacity of oxygen (f_{O2}) in a basaltic melt is an important intensive parameter in understanding melting and crystallization phenomena. Variations in f_{O2} in a melt or its source region can change the valence state, and thus the partitioning behavior, of several elements, as well as affecting the speciation of any volatiles which may be present (e.g. Morse, 1980; Green et al., 1987). The ratio of ferrous to ferric iron in a basaltic liquid is sensitive to changes of f_{O2} in the range believed to prevail in the Earth's upper mantle so that, although MORB in general are reduced, the $Fe^{3+}/(Fe^{2+} + Fe^{3+})$ ratio is somewhat variable (Christie et al., 1986). The $K_D^{Ol/L}$ of Roedder and Emslie is a measure of the Mg/Fe^{2+} ratio in the melt, so that if all Fe is treated as FeO the effective distribution coefficient:

$$K_D^* = (X_{FeO^*}/X_{MgO})^{olivine}\,(X_{MgO}/X_{FeO^*})^{liquid}$$

will be lowered from the nominal $K_D^{Ol/L}$ value by the presence of Fe^{3+} in the melt. This effect can be used to give an estimate of the $Fe^{3+}/(Fe^{2+} + Fe^{3+})$ ratio for a MORB because the glass is a reasonable representation of the liquid from which the olivine crystallized, assuming that the two phases are in equilibrium.

The K_D* values calculated for the Blanco Trough glasses display distinctly different behavior between the two sets of analyses. The Smithsonian analyses give anomalously low K_D* values in the most Fe-rich samples (e.g. K_D* = 0.181 in VG-345 with 12.57 wt.% FeO*) despite the fact that the olivine microphenocrysts found in this glass are euhedral to subhedral and unzoned (Table VI; App. 3). This may be an indication that a high $Fe^{3+} / (Fe^{2+} + Fe^{3+})$ ratio is causing the Mg#'s to appear lower than they actually are. If K_D* values are calculated for all of the samples from the anomalous group (Table V) for which olivines have been analyzed (Table VI) and plotted against the FeO* values from the Smithsonian analyses, a fairly good linear relationship (r = -0.8945) is found (Fig 34). This means that the K_D* values are approaching Roedder and Emslie's nominal value of 0.30 as a function of decreasing FeO*. Because FeO* shows a positive correlation with MgO in these samples (Fig. 30a), the simplest interpretation for this observation is that Fe_2O_3 is initially very abundant in the melt, and is decreasing with increasing degree of fractional crystallization, or conversely is increasing with increasing degree of partial melting. The highly oxidizing conditions necessary to produce these phenomena have not been found in other MORB, however some alkali basalts from the Revillagigedo Islands have been determined to be in the f_{O2} range necessary to explain the observed phenomena (Carmichael and Ghiorso, 1986).

The K_D* values calculated using the Rensselaer data set for the same 13 samples are much less unusual (Table VI). Although a few give low values (e.g. 0.216 for VG-342), there is not a good correlation between K_D* values and FeO* (r = -0.3309)(Fig. 34). This implies a magma which is far more reducing, especially when comparing those glasses that are the most primitive, which is what would be expected for a normal MORB.

The ferrous iron determinations performed on twelve samples, selected from both the anomalous and normal groups, support this interpretation for the olivine partitioning data (Table VII). Figure 35 shows that if the FeO determined through colorimetry is subtracted from the Smithsonian values for FeO*, large amounts of Fe_2O_3 in the melt are indicated, while the R.P.I. data indicate more reducing conditions. Using the empirically derived relationship of Kilinc et al. (1983) the log f_{O2} for a basaltic glass can be calculated at any given temperature. VG-345, the sample with the highest FeO*

Table VI

Average olivine phenocryst compositions for the Blanco Trough glasses.

Sample	*VG-169*		*VG-172*		*VG-342*	
SiO_2	39.86	±0.22	39.44	±0.19	40.25	±0.12
Al_2O_3	0.04	±0.01	0.05	±0.01	0.06	±0.01
TiO_2	0.01	±0.01	0.03	±0.01	0.01	±0.01
FeO	15.83	±0.84	15.75	±0.21	13.05	±0.08
MnO	0.26	±0.05	0.25	±0.01	0.23	±0.03
MgO	43.73	±0.71	43.78	±0.38	46.06	±0.39
CaO	0.30	±0.02	0.30	±0.02	0.32	±0.02
Cr_2O_3	0.04	±0.01	0.06	±0.01	0.05	±0.01
NiO	0.20	±0.03	0.24	±0.02	0.27	±0.01
Total	100.27		99.90		100.30	
n	7		6		3	
Fo	83.1		83.2		86.3	
K_D*(Sm)	0.217		0.232		0.188	
K_D*(RPI)	0.239		0.256		0.216	

Sample	*VG-345*		*VG-347*		*VG-348*	
SiO_2	39.56	±0.23	39.51	±0.34	39.89	±0.41
Al_2O_3	0.04	±0.02	0.06	±0.02	0.07	±0.02
TiO_2	0.00	±0.00	0.02	±0.02	0.01	±0.01
FeO	13.20	±0.39	14.83	±0.56	13.10	±0.39
MnO	0.22	±0.03	0.24	±0.02	0.20	±0.02
MgO	46.53	±0.25	44.61	±0.47	45.96	±0.21
CaO	0.28	±0.02	0.29	±0.04	0.29	±0.02
Cr_2O_3	0.05	±0.04	0.06	±0.02	0.04	±0.02
NiO	0.24	±0.02	0.26	±0.04	0.28	±0.02
Total	100.12		99.88		99.84	
n	6		13		23	
Fo	86.3		84.3		86.2	
K_D*(Sm)	0.181		0.208		0.202	
K_D*(RPI)	0.258		0.247		0.254	

Table VI

(Continued)

Sample	*VG-356*		*VG-357*		*VG-360*	
SiO_2	39.58	±0.20	39.39	±0.40	38.97	±0.16
Al_2O_3	0.08	±0.10	0.05	±0.01	0.04	±0.01
TiO_2	0.03	±0.02	0.04	±0.01	0.02	±0.02
FeO	15.16	±0.42	16.41	±0.29	17.37	±0.16
MnO	0.25	±0.02	0.30	±0.09	0.28	±0.02
MgO	44.55	±0.64	43.46	±0.28	42.72	±0.20
CaO	0.32	±0.08	0.30	±0.01	0.28	±0.04
Cr_2O_3	0.05	±0.02	0.05	±0.02	0.05	±0.03
NiO	0.24	±0.02	0.22	±0.02	0.23	±0.03
Total	100.26		100.22		99.96	
n	15		13		11	
Fo	84.0		82.5		81.4	
K_D*(Sm)	0.210		0.228		0.241	
K_D*(RPI)	0.246		0.236		0.236	

Sample	*VG-368*		*VG-370*		*VG-373*	
SiO_2	39.86	±0.18	39.21	±0.39	39.75	±0.20
Al_2O_3	0.05	±0.01	0.05	±0.02	0.07	±0.01
TiO_2	0.02	±0.01	0.02	±0.01	0.01	±0.01
FeO	15.36	±0.32	15.96	±0.34	12.91	±0.21
MnO	0.23	±0.03	0.27	±0.03	0.21	±0.02
MgO	44.06	±0.49	43.49	±0.37	46.01	±0.21
CaO	0.29	±0.01	0.31	±0.10	0.28	±0.02
Cr_2O_3	0.04	±0.01	0.06	±0.02	0.05	±0.02
NiO	0.26	±0.02	0.25	±0.03	0.30	±0.03
Total	100.17		99.62		99.59	
n	6		12		9	
Fo	83.6		82.9		86.4	
K_D*(Sm)	0.253		0.252		0.247	
K_D*(RPI)	0.241		0.228		0.232	

Table VI
(Continued)

Sample	*VG-376*		*VG-378*		*VG-380*	
SiO_2	39.42	±0.13	39.10	±0.33	39.54	±0.28
Al_2O_3	0.10	±0.18	0.05	±0.01	0.04	±0.01
TiO_2	0.03	±0.01	0.03	±0.01	0.01	±0.01
FeO	14.60	±0.41	17.16	±0.09	16.27	±0.20
MnO	0.26	±0.03	0.31	±0.11	0.22	±0.05
MgO	44.25	±0.48	42.39	±0.12	43.11	±0.20
CaO	0.34	±0.08	0.28	±0.01	0.29	±0.01
Cr_2O_3	0.08	±0.05	0.04	±0.02	0.05	±0.01
NiO	0.22	±0.03	0.21	±0.03	0.22	±0.03
Total	99.30		99.57		99.75	
n	10		10		8	
Fo	84.4		81.5		82.5	
K_D*(Sm)	0.231		0.236		0.250	
K_D*(RPI)	0.245		0.241		0.264	

Sample	*VG-383*		*VG-384*		*VG-385*	
SiO_2	39.03	±0.25	39.58	±0.18	39.33	±0.30
Al_2O_3	0.04	±0.01	0.04	±0.01	0.09	±0.10
TiO_2	0.02	±0.01	0.02	±0.01	0.02	±0.02
FeO	16.18	±0.31	16.18	±0.11	14.08	±0.38
MnO	0.18	±0.09	0.30	±0.15	0.22	±0.02
MgO	43.99	±0.17	43.45	±0.22	45.53	±0.62
CaO	0.31	±0.02	0.30	±0.01	0.30	±0.08
Cr_2O_3	0.04	±0.01	0.06	±0.02	0.05	±0.02
NiO	0.22	±0.02	0.22	±0.02	0.28	±0.03
Total	100.01		100.15		99.90	
n	5		12		14	
Fo	82.9		82.7		85.2	
K_D*(Sm)	0.244		0.231		0.209	
K_D*(RPI)	0.241		0.232		0.241	

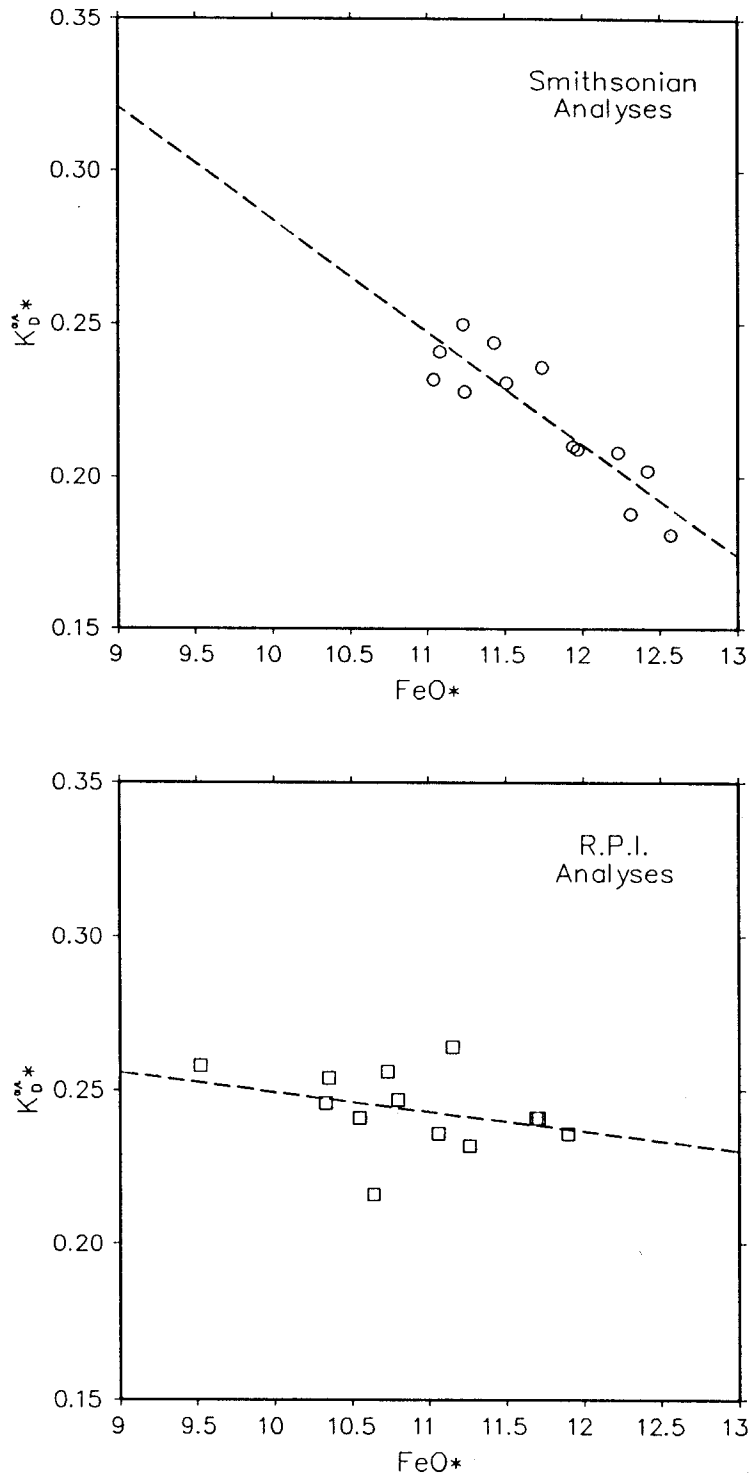

Figure 34. Plots comparing effective olivine/liquid distribution coefficient (K_D^*) vs. FeO* for the Smithsonian and R.P.I. analyses of the anomalous Blanco Trough samples. Dashed line is best straight-line fit to the data.

Table VII

Ferrous iron content for twelve of the glasses from the Blanco Trough as determined using colorimetry by I.S.E. Carmichael at U.C. Berkeley.

Sample	*Wt. % FeO*	*2 σ*	*1*	*2*	*3*	*4*
VG-172	9.90	±0.19	11.04	0.103	10.73	0.077
VG-345	8.66	±0.17	12.57	0.311	9.52	0.090
VG-347	9.98	±0.19	12.23	0.184	10.80	0.076
VG-348	9.56	±0.18	12.42	0.230	10.35	0.076
VG-356	9.52	±0.18	11.94	0.203	10.33	0.078
VG-360	10.36	±0.20	11.08	0.065	11.90	0.129
VG-368	10.02	±0.19	11.02	0.091	10.94	0.084
VG-373	9.67	±0.19	10.63	0.090	10.35	0.066
VG-376	9.14	±0.18	10.24	0.107	9.96	0.082
VG-380	10.29	±0.20	11.23	0.084	11.15	0.077
VG-382	9.89	±0.19	11.44	0.135	11.28	0.123
VG-384	9.91	±0.19	11.51	0.139	11.26	0.120

Stated errors are based on use of the colorimetric technique on a MORB glass (JDFD 2) as reported by I.S.E. Carmichael.

(1) FeO* from Smithsonian data set.

(2) $Fe^{3+} / (Fe^{2+} + Fe^{3+})$ based on Smithsonian FeO*.

(3) FeO* from R.P.I. data set.

(4) $Fe^{3+} / (Fe^{2+} + Fe^{3+})$ based on R.P.I. FeO*.

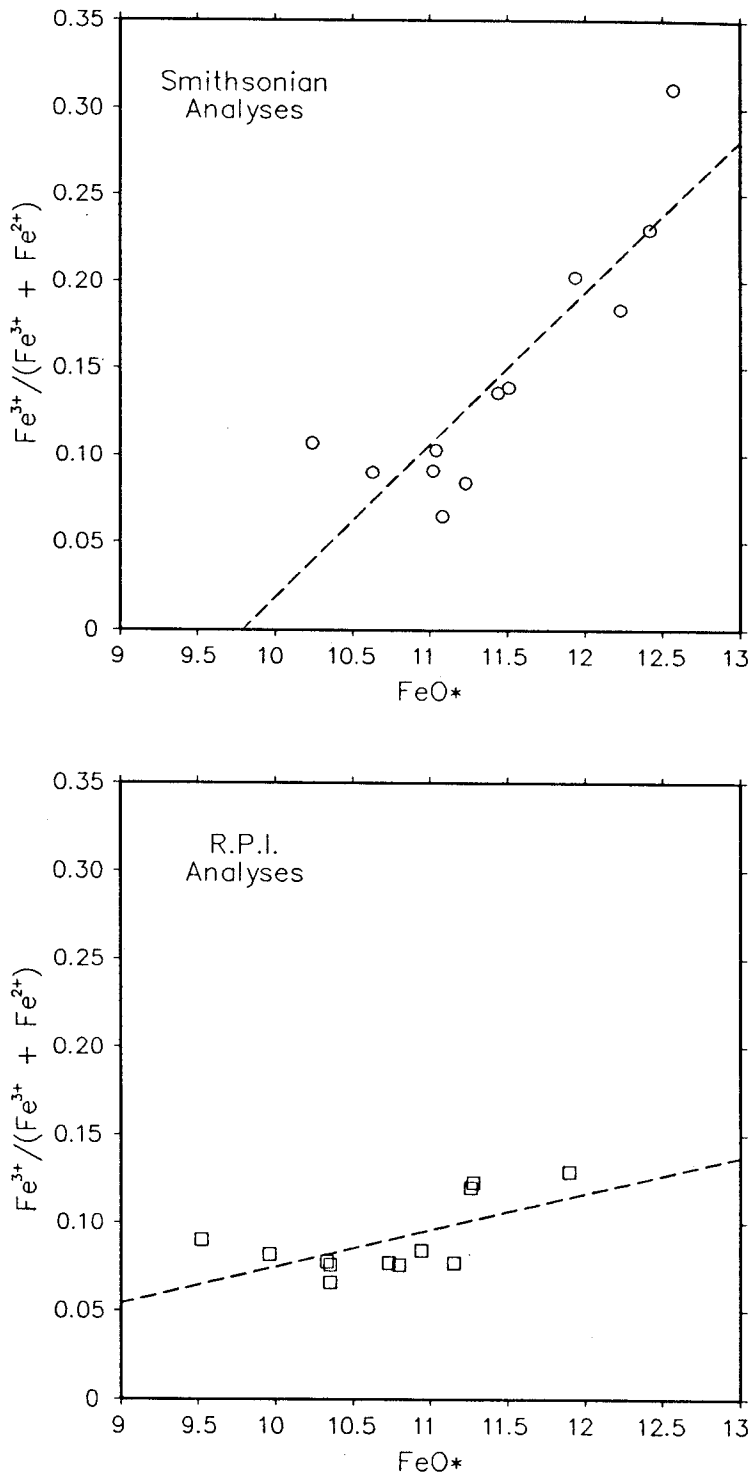

Figure 35. Plots comparing $Fe^{3+}/(Fe^{2+} + Fe^{3+})$ vs. FeO* for the Smithsonian and R.P.I. analyses of the twelve Blanco Trough samples for which FeO has been independently determined by I.S.E. Carmichael. Dashed line is best straight-line fit to the data.

value according to the Smithsonian data, would have a log f_{O2} = -6.02 at 1200° C (ΔNNO = +1.51). Using the R.P.I. value for FeO* VG-345 would have a log f_{O2} = -9.16 at 1200° C (ΔNNO = -1.63), over 3 log units more reduced.

A direct comparison of the K_D* values calculated from both data sets, for all samples for which there are olivine analyses, is shown in Fig 36a. If the FeO* and MgO values were the same for both sets of analyses, the points would fall along a line through the origin with a slope of one. Figure 36b shows the effect of a +5% difference in calibration of the R.P.I. FeO* values, in which case the points would fall along a line with a slope less than one, and a y-intercept of zero. It can be seen from this comparison that the disagreement between the two data sets cannot be a simple inter-laboratory calibration difference, but has to be something more complicated.

The ferrous iron determinations provide a good constraint on the degree of olvine-melt equilibrium. The dashed line in Figure 37a shows the expected change in K_D* as $Fe^{3+}/(Fe^{2+} + Fe^{3+})$ increases in the melt (assuming that $K_D^{Ol/L}$ = 0.30 for $Fe^{3+}/(Fe^{2+} + Fe^{3+})$ = 0). It can be seen that both data sets fall along a trend that is roughly sub-parallel to what would be expected if K_D* varies in a linear way as a function of the $Fe^{3+}/(Fe^{2+} + Fe^{3+})$ ratio of the melt. The reason for this behavior is not clear, as the only two factors known to influence K_D* are Fe^{3+} and TiO_2 concentrations in the melt, neither of which is high enough in these samples to explain the observed K_D* values. Figure 37b is a comparison of $K_D^{Ol/L}$ values calculated with the FeO concentrations determined by I.S.E. Carmichael using colorimetry, and MgO values taken from the two data sets. This plot shows that MgO values from the two laboratories are fairly consistent, with nine out of eleven falling in an area which indicates that the Smithsonian calibration is a few percent lower than at R.P.I.. This is a strong indication that FeO* is responsible for the observed olivine-melt partitioning anomalies, although it is inconclusive as to which data set is in error.

VG-383 contains several olivines that are deeply embayed and display reverse zoning (Fig. 16), an indication that these phenocrysts either represent xenocrystic material or were inherited from a more evolved magma during an episode of mixing. The K_D* values calculated from both data sets for the average core composition of these olivines are closer to 0.30 than the rim K_D*'s (Table VIII), a

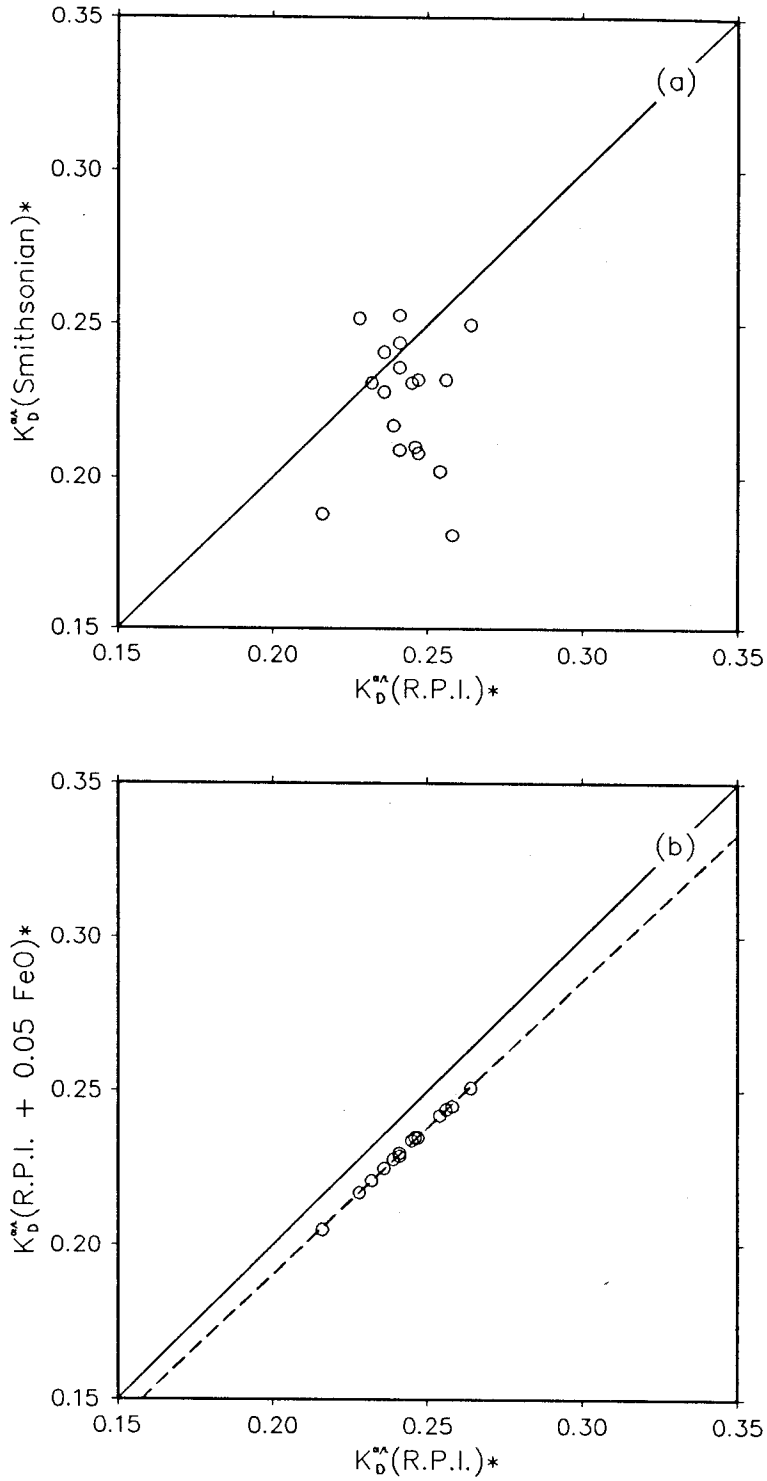

Figure 36. Plots (a) comparing olivine/liquid K_D* values calculated using Smithonian and R.P.I glass data, and (b) illustrating the effect of a +5% calibration difference between the two data sets.

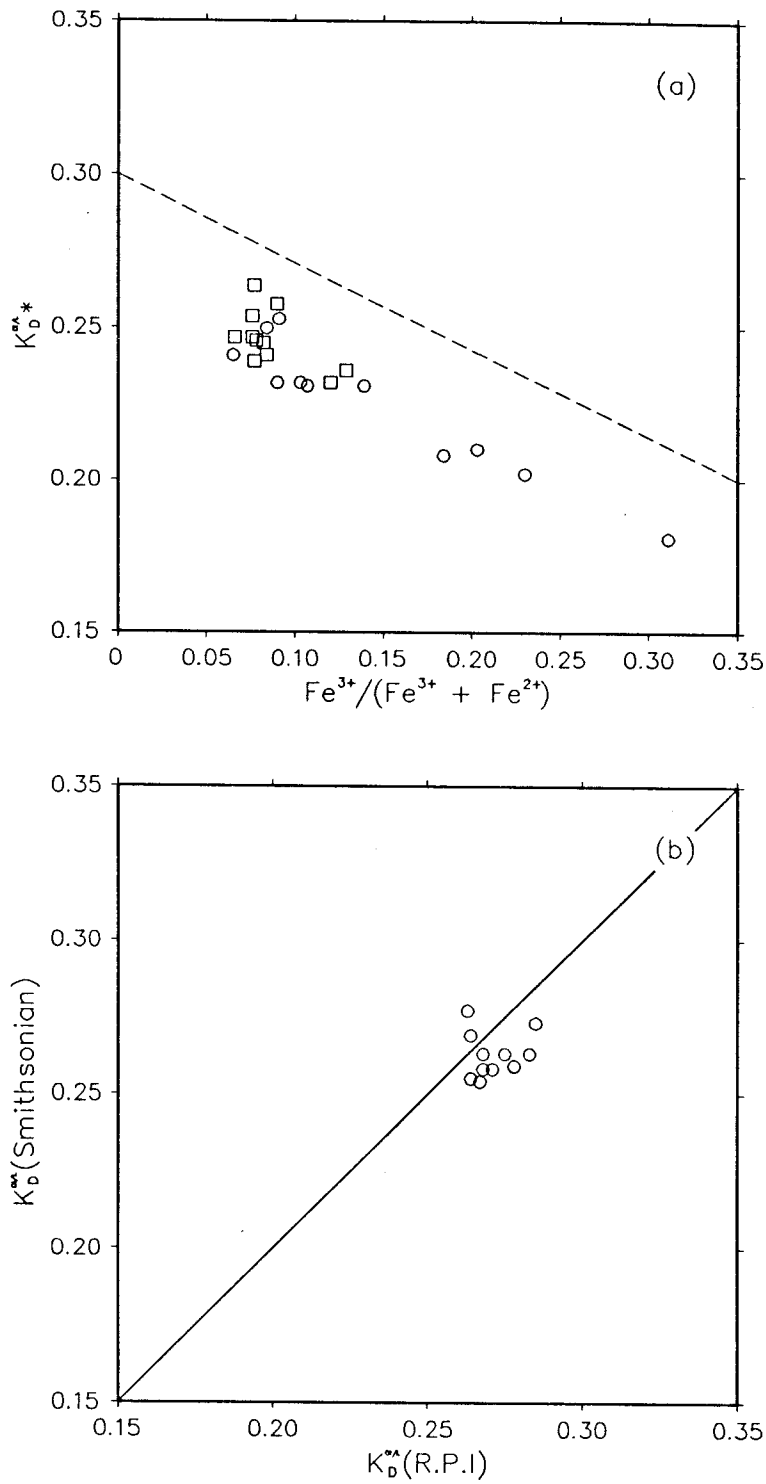

Figure 37. Plots (a) comparing the observed relationship between olivine/liquid K_D* values and $Fe^{3+}/(Fe^{2+} + Fe^{3+})$ in the melt for the Smithsonian (circles) and R.P.I. (squares) Blanco Trough glass analyses with the expected linear relationship (dashed line), and (b) comparing olivine/liquid K_D* values calculated using FeO determined colorimetrically and MgO values from the two glass data sets.

Table VIII

Average core and rim compositions for reversely zoned olivine in VG-383.

	Core	*σ*	*Rim*	*σ*
SiO_2	38.89	±0.24	39.03	±0.25
Al_2O_3	0.04	±0.02	0.04	±0.01
TiO_2	0.01	±0.01	0.02	±0.01
FeO	17.29	±0.08	16.18	±0.31
MnO	0.22	±0.05	0.18	±0.09
MgO	43.26	±0.12	43.99	±0.17
CaO	0.28	±0.03	0.31	±0.02
Cr_2O_3	0.03	±0.01	0.04	±0.01
NiO	0.18	±0.02	0.22	±0.02
Total	100.20		100.01	
n	6		5	
Fo	81.7		82.9	
K_D*(Sm)	0.265		0.244	
K_D*(RPI)	0.261		0.241	

possible indication that the glass has a large $Fe^{3+}/(Fe^{2+} + Fe^{3+})$ component, so that the observed Mg# is considerably lower than the actual Mg#. It is curious, however, that this phenomenon is seen in both data sets, when it has already been established that the R.P.I. glass compositions are consistent with more reducing conditions in the magma. A second possible explanation is that the magma with which these phenocrysts were attempting to equilibrate was a mixture richer in the primitive end-member, and thus more Mg-rich, than VG-383. As the two end-members were homogenized, the composition of the magma began to change back toward the more evolved liquid from which the cores had originally crystallized and the whole package was erupted onto the ocean floor too quickly for the rims to begin reacting again. It is therefore possible that the phenocrysts in VG-383 are recording the history of the mixing event. A third alternative for the origin of these olivines is that they are xenocrystic, in which case the observed reverse zoning has no relevance to the composition of VG-383, and higher K_D*'s for the cores are coincidental.

4.5.2 Chromian Spinel-Melt Equilibria.

Chromian spinel is a common early crystallizing phase in primitive MORB which possess a large range of compositional variability. The crystal structure of spinel group minerals contains both tetrahedral (A) and octahedral (B) sites, and may be of either normal or inverse type. In normal spinels the A site is occupied by divalent cations, while the B site contains trivalent cations. Inverse spinels are characterized by one-half of the trivalent cations in the A site, while the B site is occupied by both divalent and trivalent cations (Deer et al., 1966). The spinel group is represented by the chemical formula $R^{2+}R^{3+}{}_2O_4$, with the dominant constituents of chromian spinels being MgO, FeO, Al_2O_3, Cr_2O_3 and Fe_2O_3, with minor amounts of TiO_2 and MnO, so that they can be thought of as a solid solution among the endmembers:

chromite:	$Fe^{2+}Cr_2O_4$	picrochromite:	$MgCr_2O_4$
hercynite:	$Fe^{2+}Al_2O_4$	spinel:	$MgAl_2O_4$
magnetite:	$Fe^{2+}Fe^{3+}{}_2O_4$	magnesioferrite:	$MgFe^{3+}{}_2O_4$

These six components correspond to a compositional space that can be represented by the triangular

prism shown in Fig. 38. The base of the prism contains the endmembers with normal spinel structure, while the apex contains those with inverse structure. The triangular cross section of the prism is equivalent to a ternary plot showing the relative proportions of the trivalent cations, while its length represents the relative proportions of MgO and FeO. Projections onto the faces of the prism labelled A and B are commonly used to plot chromian spinel compositions, and are shown in the lower part of Fig. 38. The axis representing the relative proportion of trivalent cations in each projection is shown as twice the length of the axis representing the relative proportions of Mg and Fe so that compositional variations can be compared on an atom-for-atom basis (Irvine, 1965; Haggerty, 1976). The Fe2O3 content of spinel can be estimated based on stoichiometry and the assumption that no vacancies are present (Carmichael, 1967).

The compositional range for spinels found in MORB is similar to that of abyssal dunites and peridotites, with a concentration at the Cr-rich end of the dunite-peridotite field. They commonly have Cr/(Cr + Al) ratios (Cr#) between 0.40 and 0.60, and display a moderate range of Mg#. Spinels with Cr# < 0.40 are generally restricted to the most primitive abyssal basalts (Dick and Bullen, 1984).

Partitioning between chromian spinel and melt of Cr and Fe, both essential structural constituents in the crystalline phase, is highly sensitive to changes of temperature and f_{O2} conditions in the melt (Hill and Roeder, 1974; Fisk and Bence, 1980; Barnes 1986; Murck and Campbell, 1986; Delano et al., 1990). This sensitivity to intensive parameters has led many to suggest that spinels potentially hold a great deal of petrogenetic information (e.g. Irvine, 1965; Irvine 1967; Sigurdsson and Schilling, 1976; Sack, 1982; Allan et al., 1988). This complexity makes it difficult to quantitatively evaluate partitioning of major elements between spinel and melt in any simple fashion analogous to the $K_D^{Ol/L}$ of Roeder and Emlsie.

The compositional range of the of the spinels found in the Blanco Trough glasses can be qualitatively evaluated through comparison with analyses of spinel-glass pairs from other suites in the literature. Allan et al. (1988; 1989) reported Cr-rich spinel and glass compositions from a suite of MORB-type lavas recovered from the Lamont seamount chain in the eastern Pacific. The basalts are classified as LREE-depleted N-type MORB, with $Mg/(Mg + Fe^{2+})$ between 0.611 and 0.694, and

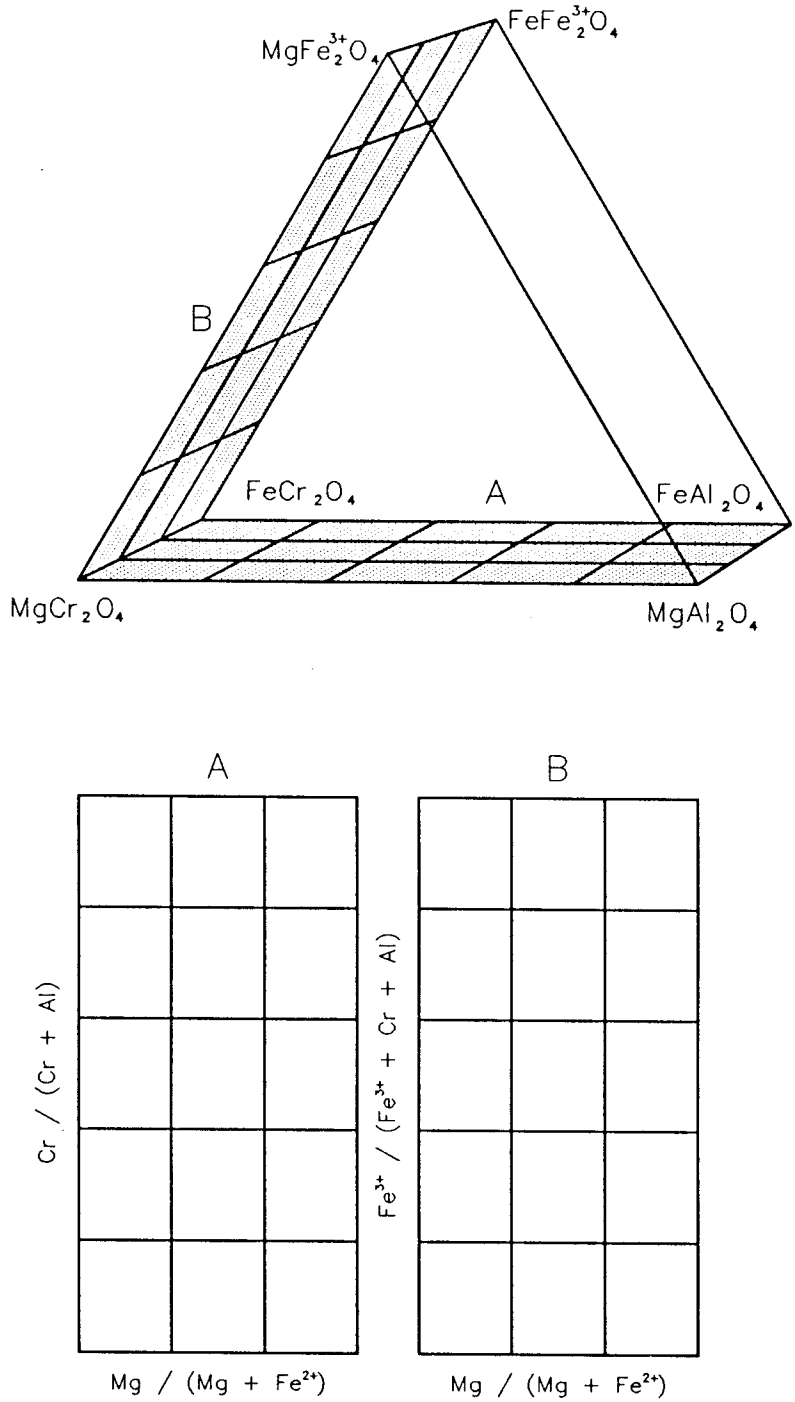

Figure 38. Spinel compositional prism (above) and projections for A and B faces (below). The axes representing the relative proportions of trivalent cations are drawn twice the length of those representing the divalent cations so that compositional variations can be compared on an atom-for-atom basis. After Irvine (1965).

typically contain phenocrysts of unzoned olivine, plagioclase and chromian spinel. They are believed to have experienced generally short crustal residence times, so that episodes of mixing and wall-rock contamination are minimized. The spinel compositions reported by Allan et al. (1988) have been recalculated in this study using the scheme of Carmichael (1967), to allow a more direct comparison with the spinels found in the Blanco Trough samples. The recalculated spinel compositions are characterized by Cr/(Cr + Al) varying from 0.20 to 0.54, Mg/(Mg + Fe^{2+}) from 0.66 to 0.84, and Fe^{3+}/(Cr + Al + Fe^{3+}) from 0.06 to 0.11. This compositional range is similar to that found by Sigurdsson and Schilling (1976) for spinels in MORB from the Mid-Atlantic Ridge, and may be a good estimate for abyssal basalts in general.

Chromian spinel is present in the Blanco Trough glasses as inclusions in olivine, embedded in olivine grain boundaries, and as small microphenocrysts in the glass. Grains are unzoned, with the exception of VG-373, and the intra-sample compositional range is limited, although there is a good deal of variability with respect to Al_2O_3, Cr_2O_3 and FeO* (probably due to the presence of Fe_2O_3) in several samples (Table IX).

A comparison of the compositional ranges of spinels found in the Blanco Trough glasses with those recovered from the Lamont seamounts is shown in Fig. 39. In the projection onto the A face of the prism it can be seen that the range in Cr# is strikingly similar in the two suites. The magnitude of the variation in Mg# is similar, although the Blanco Trough compositions are offset to slightly lower values, consistent with the indication from both sets of glass analyses that these basalts are Fe-enriched. The B projection shows that the Blanco Trough samples have a substantially larger range of Fe^{3+}/(Cr + Al + Fe^{3+}) than the Lamont samples. This could be an indication that there is a larger than normal Fe^{3+} component in the melt, except that the Fe^{3+} / Fe^{2+} ratios for the Lamont samples (0.506 to 0.786) are higher than those for the Blanco Trough spinels (0.339 to 0.638, based on average phenocryst compositions). The larger Fe^{3+} / (Cr + Al + Fe^{3+}) values are therefore probably due to the fact that the Blanco Trough glasses are enriched in total Fe.

Plotting the concentration of MgO, FeO and Al_2O_3 in the glass against the concentration in the crystalline phase can be used to evaluate similarities and differences in partitioning behavior

Table IX

Average chromian spinel phenocryst compositions for the Blanco Trough glasses.

Sample	*VG-169*	σ	*VG-172*	σ	*VG342*	σ
FeO	28.32	±1.47	27.56	±0.20	20.88	±2.34
TiO_2	1.96	±0.29	2.23	±0.11	1.04	±0.59
MnO	0.26	±0.02	0.28	±0.06	0.18	±0.05
MgO	11.74	±0.32	13.21	±0.01	14.95	±0.77
Al_2O_3	20.94	±1.74	21.70	±0.01	29.67	±4.00
SiO_2	0.00	±0.00	0.00	±0.00	0.00	±0.00
Cr_2O_3	35.11	±0.55	34.49	±0.05	32.27	±1.81
NiO	0.12	±0.02	0.16	±0.01	0.16	±0.02
Total	98.45		99.63		99.15	
n	6		2		3	
Fe_2O_3	10.91		11.79		7.27	
FeO	18.49		16.94		14.33	
Total	99.53		100.80		99.87	

Sample	*VG-345*	σ	*VG-347*	σ	*VG-348*	σ
FeO	19.46		22.21	±0.31	16.14	±0.44
TiO_2	0.69		0.87	±0.09	0.27	±0.03
MnO	0.19		0.22	±0.02	0.15	±0.04
MgO	15.61		14.83	±0.18	17.49	±0.59
Al_2O_3	32.16		32.23	±0.71	43.87	±3.38
SiO_2	0.00		0.00	±0.00	0.00	±0.00
Cr_2O_3	31.94		29.21	±0.68	21.99	±3.54
NiO	0.17		0.20	±0.02	0.24	±0.02
Total	100.23		99.77		100.15	
n	1		15		12	
Fe_2O_3	6.39		8.11		4.36	
FeO	13.71		14.90		12.21	
Total	100.85		100.57		100.58	

Table IX

(Continued)

Sample	*VG-356*	*σ*	*VG-357*	*σ*	*VG-360*	*σ*
FeO	25.57	±0.32	30.22	±0.90	32.36	±0.64
TiO_2	1.62	±0.06	2.39	±0.30	3.23	±0.26
MnO	0.26	±0.02	0.20	±0.08	0.29	±0.03
MgO	12.88	±0.13	12.03	±0.11	10.80	±0.15
Al_2O_3	22.70	±0.38	20.49	±0.68	18.05	±0.50
SiO_2	0.00	±0.00	0.05	±0.12	0.00	±0.00
Cr_2O_3	35.77	±0.49	33.49	±0.36	33.46	±0.60
NiO	0.16	±0.04	0.17	±0.02	0.18	±0.03
Total	98.96		99.04		98.37	
n	14		6		13	
Fe_2O_3	9.71		12.83		13.12	
FeO	16.82		18.66		20.54	
Total	99.92		100.31		99.67	

Sample	*VG-370*	*σ*	*VG-373*	*σ*	*VG-376*	*σ*
FeO	29.32	±0.42	16.07	±0.30	26.31	±2.43
TiO_2	2.34	±0.17	0.27	±0.03	2.03	±0.74
MnO	0.27	±0.03	0.15	±0.04	0.21	±0.04
MgO	11.96	±0.11	17.58	±0.28	12.95	±0.25
Al_2O_3	21.10	±0.22	44.77	±1.31	22.76	±1.97
SiO_2	0.03	±0.08	0.01	±0.01	0.04	±0.09
Cr_2O_3	33.17	±0.80	20.37	±1.21	33.85	±1.12
NiO	0.18	±0.02	0.25	±0.03	0.16	±0.02
Total	98.37		99.47		98.31	
n	6		14		5	
Fe_2O_3	12.02		4.51		10.34	
FeO	18.49		12.00		17.00	
Total	99.56		99.92		99.33	

Table IX

(Continued)

Sample	*VG-378*	*σ*	*VG-384*	*σ*	*VG-385*	*σ*
FeO	32.33	±0.17	29.83	±0.30	19.26	±0.15
TiO_2	3.00	±0.07	2.25	±0.09	0.60	±0.04
MnO	0.29	±0.05	0.31	±0.09	0.16	±0.01
MgO	11.17	±0.06	12.10	±0.07	15.53	±0.28
Al_2O_3	18.17	±0.39	20.83	±0.32	34.75	±0.46
SiO_2	0.00	±0.00	0.00	±0.00	0.02	±0.04
Cr_2O_3	33.03	±0.69	33.73	±0.21	29.20	±0.38
NiO	0.18	±0.02	0.16	±0.03	0.22	±0.03
Total	98.17		99.21		99.73	
n	5		4		3	
Fe_2O_3	13.98		12.72		5.84	
FeO	19.74		18.37		14.00	
Total	99.56		100.47		100.32	

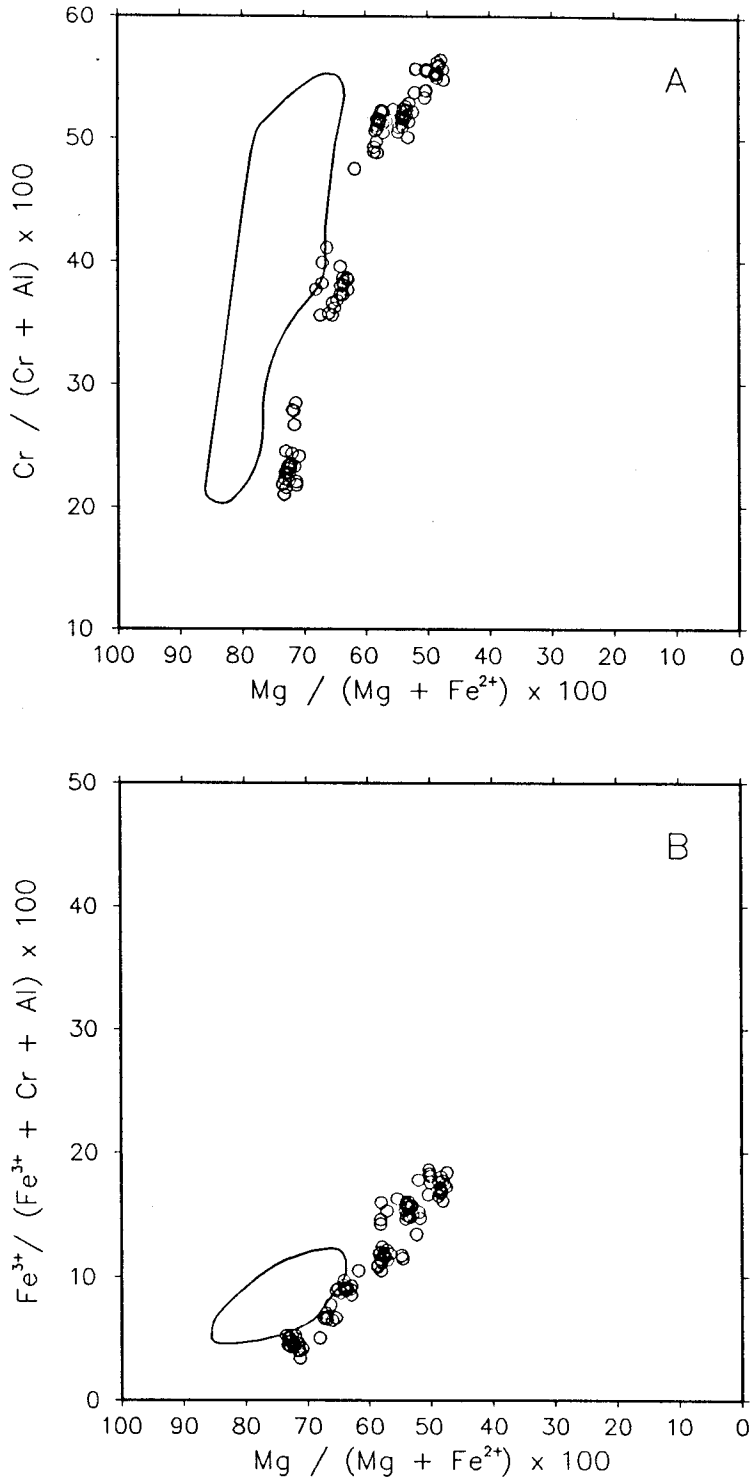

Figure 39. Comparison of the compositional fields for chromian spinels found in MORB-type glasses from the Lamont seamounts (field bounded by solid line) and the Blanco Trough glasses (circles) as seen in the projections onto the A and B faces of the spinel prism.

between the two suites. Cr_2O_3 is an additional essential structural constituent in chromian spinel, but because it is only present in the glass as a trace element the approach used for major elements is difficult to apply. Figure 40 demonstrates that using the average phenocryst compositions a good linear relationship between MgO in spinel and MgO in the glass is obtained using both the Smithsonian glass data:

$$MgO_{sp} = 2.89\ MgO_{liq} - 8.00$$
$$r = 0.95607$$

and the glass data collected at R.P.I.:

$$MgOsp = 2.63\ MgO_{liq} - 6.59$$
$$r = 0.98204$$

These plots agree with the olivine data in suggesting that the Smithsonian MgO calibration is slightly lower than tha R.P.I. calibration. The best-fit line to the Lamont data is surprisingly similar to the first two, although the fit is not quite as good:

$$MgOsp = 2.63\ MgO_{liq} - 5.76$$
$$r = 0.81202$$

Many of the spinels from this data set are zoned , however, and the necessity of using rim compositions for the plot may explain the poor fit.

Figure 41 shows plots of Al_2O_3 in the glass against Al_2O_3 in chromian spinel, and again a good linear fit is obatined for the Smithsonian glass compositions:

$$Al_2O_{3sp} = 8.05\ Al_2O_{3liq} - 101.15$$
$$r = 0.94888$$

as well as those from R.P.I.:

$$Al_2O_{3sp} = 8.75\ Al_2O_{3liq} - 109.29$$
$$r = 0.97832$$

even though the standard deviation for the average Al_2O_3 content is quite large for VG-373 and VG-376 (Table IX). The best-fit line for the data of Allan et al. has a much lower slope, and the fit is poor:

$$Al_2O_{3sp} = 6.54\ Al_2O_{3liq} - 76.58$$
$$r = 0.74768$$

but spinel zonation has a large effect on Al_2O_3 content, so that this result is not surprising. A positive correlation for Al_2O_3 has also been noted for spinels found in samples collected from the Mid-Atlantic

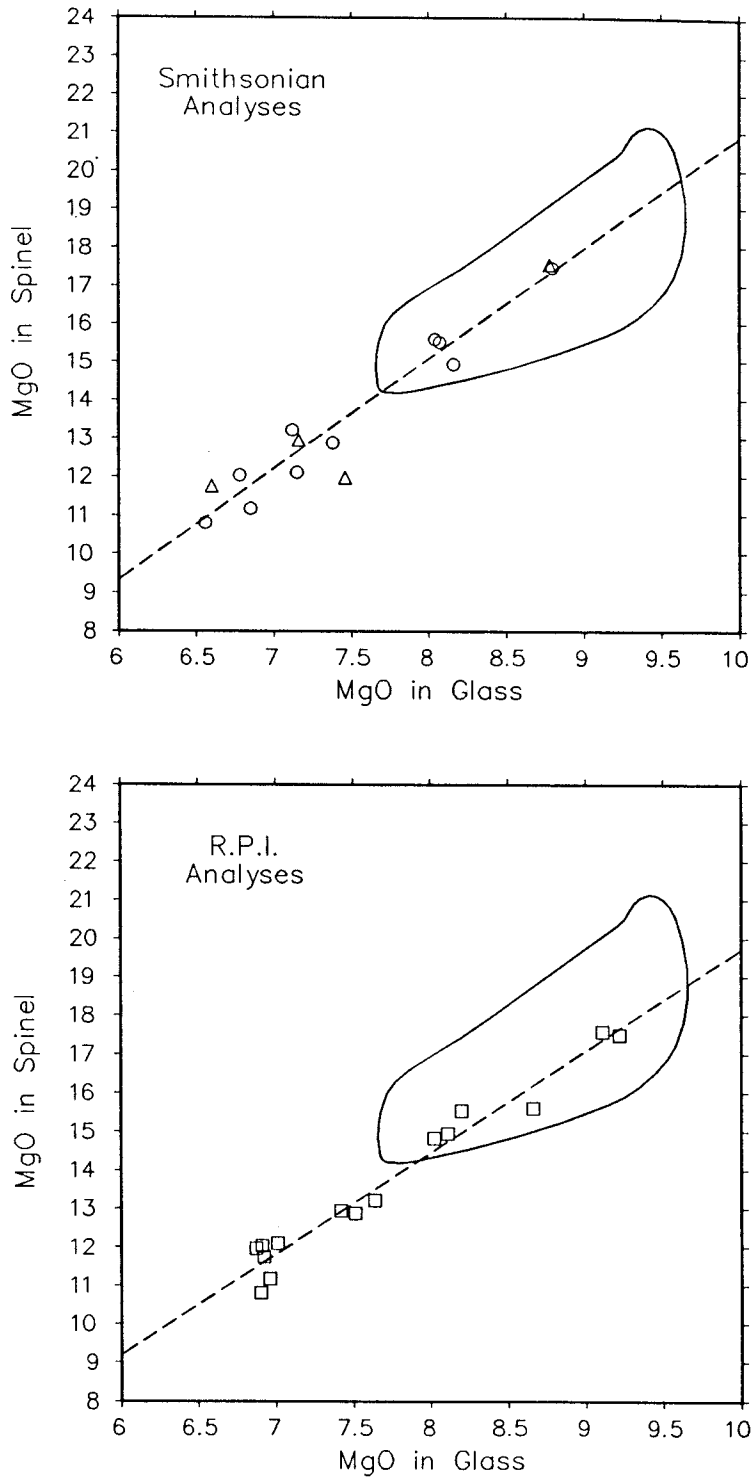

Figure 40. Comparison of partitioning of MgO between chromian spinel and melt based on "anomalous" (circles) and "normal" (triangles) Smithsonian analyses of the Blanco Trough glasses, and those performed at R.P.I. Note that the Smithsonian MgO calibration is slightly lower than the R.P.I. calibration. Dashed line is best straight-line fit to the data. Field bordered by solid line is for Lamont seamount spinels.

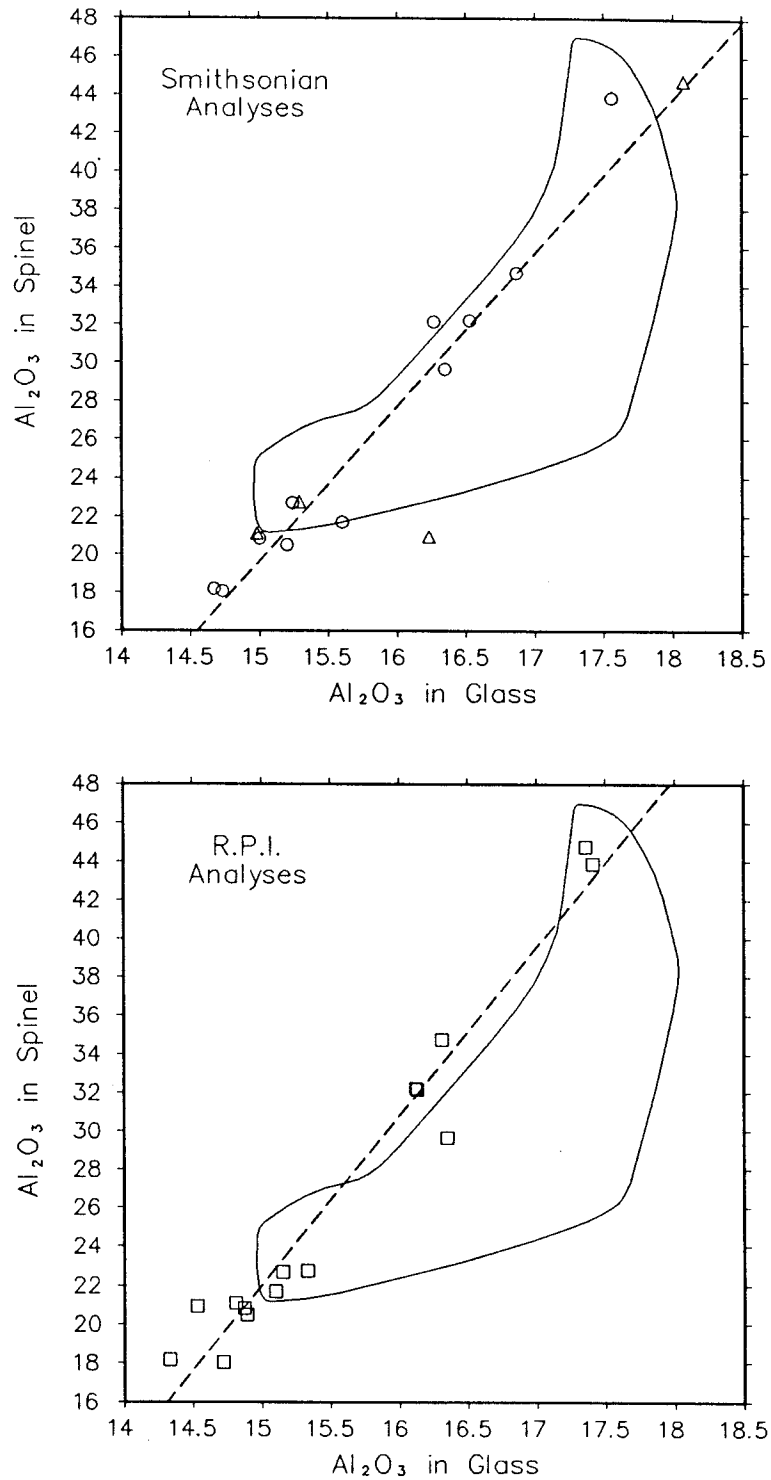

Figure 41. Comparison of partitioning of Al_2O_3 between chromian spinel and melt based on "anomalous" (circles) and "normal" (triangles) Smithsonian analyses of the Blanco Trough glasses, and those performed at R.P.I. Note that the Smithsonian Al_2O_3 calibration is slightly higher than the R.P.I. calibration. Dashed line is best straight-line fit to the data. Field bordered by solid line is for Lamont seamount spinels.

Ridge (Sigurdsson and Schilling, 1976).

In contrast to the good agreement between the two data sets for MgO and Al_2O_3, there is considerable disagreement with regard to the partitioning of FeO* between spinel and melt. Figure 42 shows that even though there is a good deal of scatter for the data set as a whole, if the anomalous samples are considered alone there is a negative correlation between the concentration of FeO* in the glass and in the spinel phase:

$$FeO^*_{sp} = -8.77\ FeO^*_{liq} + 128.77$$
$$r = -0.82827$$

This relationship seems to be consistent with the abnormal partitioning behavior observed for FeO* between olivine and melt for the Smithsonian data. A large Fe_2O_3 component in the most Fe-rich samples could drastically change the behavior of FeO* if the partition coefficient for Fe_2O_3 between spinel and melt were very small for the conditions in the melt (i.e. if the paritition coefficient is strongly dependent on melt composition, temperature, f_{O2}, etc.). The negative correlation could then be explained by a decreasing Fe_2O_3 component, coupled with an increasing FeO component, gradually changing the melt toward a more normal MORB. The negative correlation would eventually have to "turn over" and become positive, however, or the result would be an extremely Fe-rich spinel in a melt with no FeO* (the y-intercept is > 100 wt. % !).

The R.P.I. glass compositions display a positive correlation between the concentration of FeO* in the glass and in the spinel phase in Figure 42. A single straight line fit would seem to be insufficient to describe the observed relationship, however, due to 5 points that fall along a trend different from both the Lamont seamount spinels and the remainder of the samples from the Blanco Trough. The majority of the samples seem to be in good agreement with the trend of the Lamont samples, although they define an extension to more Fe-rich compositions.

Figure 43 shows the relationship between the $Fe^{3+}/(Fe^{2+} + Fe^{3+})$ ratios in the chromian spinels and in the melt. The anomalous Smithsonian analyses show a weak negative correlation, not what would be expected if the Fe_2O_3 component in the melt were being removed by the spinel phase. The R.P.I. analyses show a positive correlation, and plot in the same area as the Lamont spinel-glass

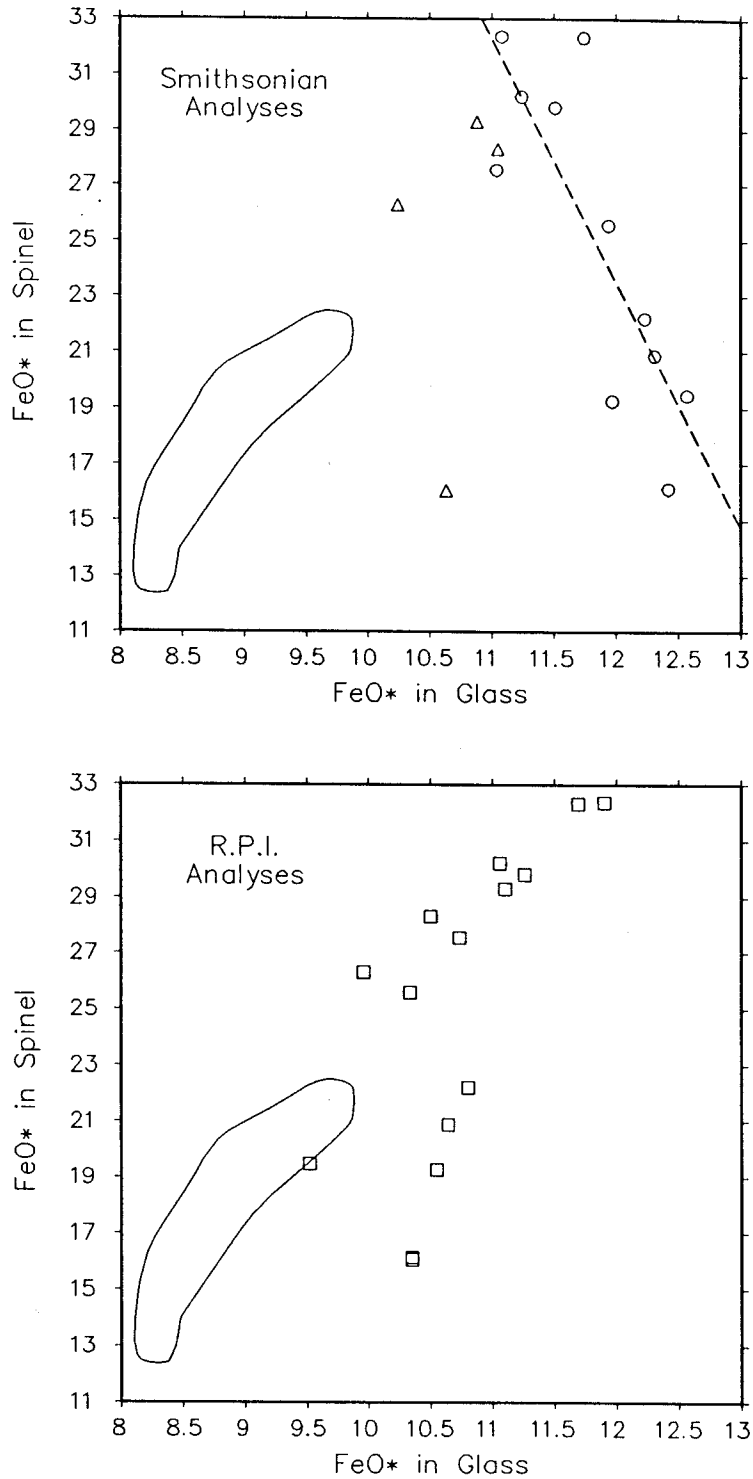

Figure 42. Comparison of partitioning of FeO* between chromian spinel and melt based on "anomalous" (circles) and "normal" (triangles) Smithsonian analyses of the Blanco Trough glasses, and those performed at R.P.I. Dashed line is best straight-line fit to the "anomalous" Smithsonian compositions only. Field bordered by solid line is for Lamont seamount spinels.

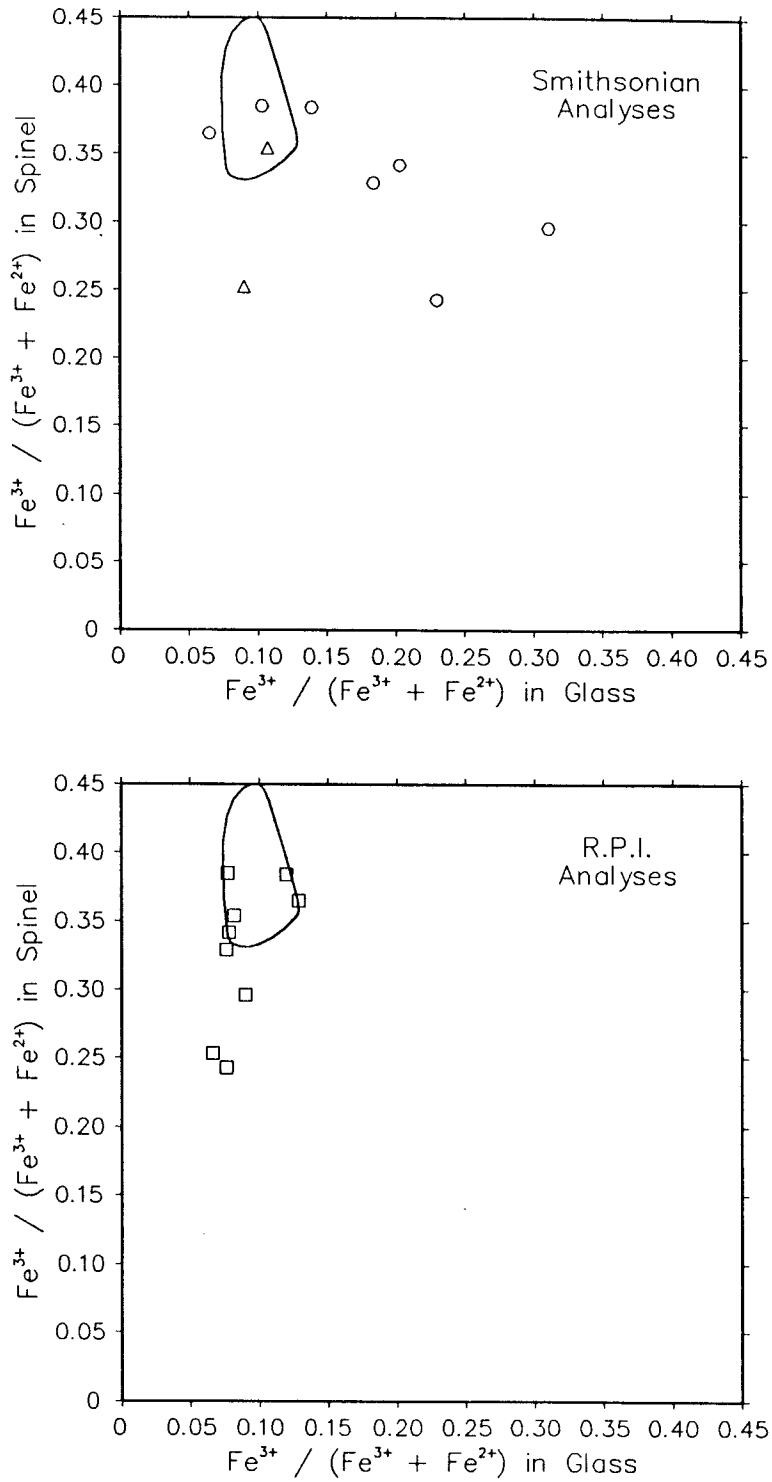

Figure 43. Comparison of the relationship between $Fe^{3+}/(Fe^{2+} + Fe^{3+})$ in chromian spinel and melt observed for "anomalous" (circles) and "normal" (triangles) Smithsonian analyses of the Blanco Trough glasses, and those performed at R.P.I. Field bordered by solid line is for Lamont seamount spinels.

pairs, at slightly lower $Fe^{3+}/(Fe^{2+} + Fe^{3+})$ values for the spinels.

Table X contains the average composition for both zoned and homogeneous spinel from VG-373, the only sample in which zoning was observed. Spinel zoning is a common feature in MORB, with examples of both Al-Mg rich cores coupled with Cr-Fe rich rims (normal zoning) and Cr-Fe rich cores with Al-Mg rich rims (reverse zoning) having been reported in other suites in the literature. Sigurdsson and Shilling (1976) reported both reverse and normal zoning in spinels found in MORB from the Mid-Atlantic Ridge, with the latter being the more common of the two types. The normal zoning was interpreted to be the result of early high-pressure crystallization followed by re-equilibration at low pressure. They based this on the experiments performed by Green et al. (1971) on Apollo 12 basalt compositions, where an increase in Al_2O_3 in spinels on or near the liquidus as a function of increasing pressure was found. Allan et al. (1988) reported zoning, commonly either reverse or complex, in the spinels found in some of the samples recovered from the Lamont seamounts. They attributed the zonation to magma mixing or wall rock assimilation, feeling that the effect of pressure on spinel composition is minor compared with the effects of melt composition.

The spinels found in VG-373 are either unzoned or display reverse or complex zoning, with the former being the most common. The boundary between core and rim is generally quite distinct, although the cores tend to be rounded. The rim compositions are very similar to the compositions of the unzoned spinels, indicating that they have both equilibrated with the same liquid composition. In addition, no change in TiO_2 content is observed from core to rim, an important observation because there appears to be a strong compositional dependence of TiO_2 partitioning between spinel and melt. The dashed line in Figure 44 is an exponential curve fit for chromian spinel-basaltic glass pairs from Evans (1987), and the fit to both sets of Blanco Trough glass analyses is fairly good. This implies that for MORB parameters other than composition may have little effect on the partitioning of TiO_2 between spinel and melt. Based on the Cr# and Mg# of the cores, and the assumption that the intensive parameters of the melt did not change, the composition of the liquid from which the zoned spinels originally crystallized should have been similar to VG-342. The TiO_2 content of the cores are too low for them to have crystallized from VG-342 (0.33 wt. % TiO_2 as compared to 1.04 in VG-342

Table X

Average compositions for zoned and unzoned spinels in VG-373.

	Unzoned	σ	*Core*	σ	*Rim*	σ
FeO	16.07	±0.30	17.74	±0.54	16.44	±0.86
TiO_2	0.27	±0.03	0.33	±0.03	0.27	±0.05
MnO	0.15	±0.04	0.18	±0.03	0.14	±0.05
MgO	17.58	±0.28	15.27	±0.68	17.17	±0.75
Al_2O_3	44.77	±1.31	31.83	±3.32	42.85	±4.72
SiO_2	0.01	±0.01	0.04	±0.08	0.00	±0.00
Cr_2O_3	20.37	±1.21	33.44	±3.57	21.90	±4.40
NiO	0.25	±0.03	0.19	±0.05	0.22	±0.04
Total	99.47		99.02		98.99	
n	14		5		6	
Fe_2O_3[a]	4.51		4.73		4.70	
FeO	12.00		13.48		12.21	
Total	99.92		99.49		99.46	
Cr#[b]	0.2338		0.4133		0.2552	
Mg#[c]	0.7230		0.6687		0.7148	
Fe^{3+}#[d]	0.0470		0.0527		0.0496	

(a) Fe_2O_3 recalculated based on stoichiometry after Carmichael (1967).
(b) Cr# = Cr / (Cr + Al).
(c) Mg# = Mg / (Mg + Fe^{2+}).
(d) Fe^{3+}# = Fe^{3+} / (Cr + Al + Fe^{3+}).

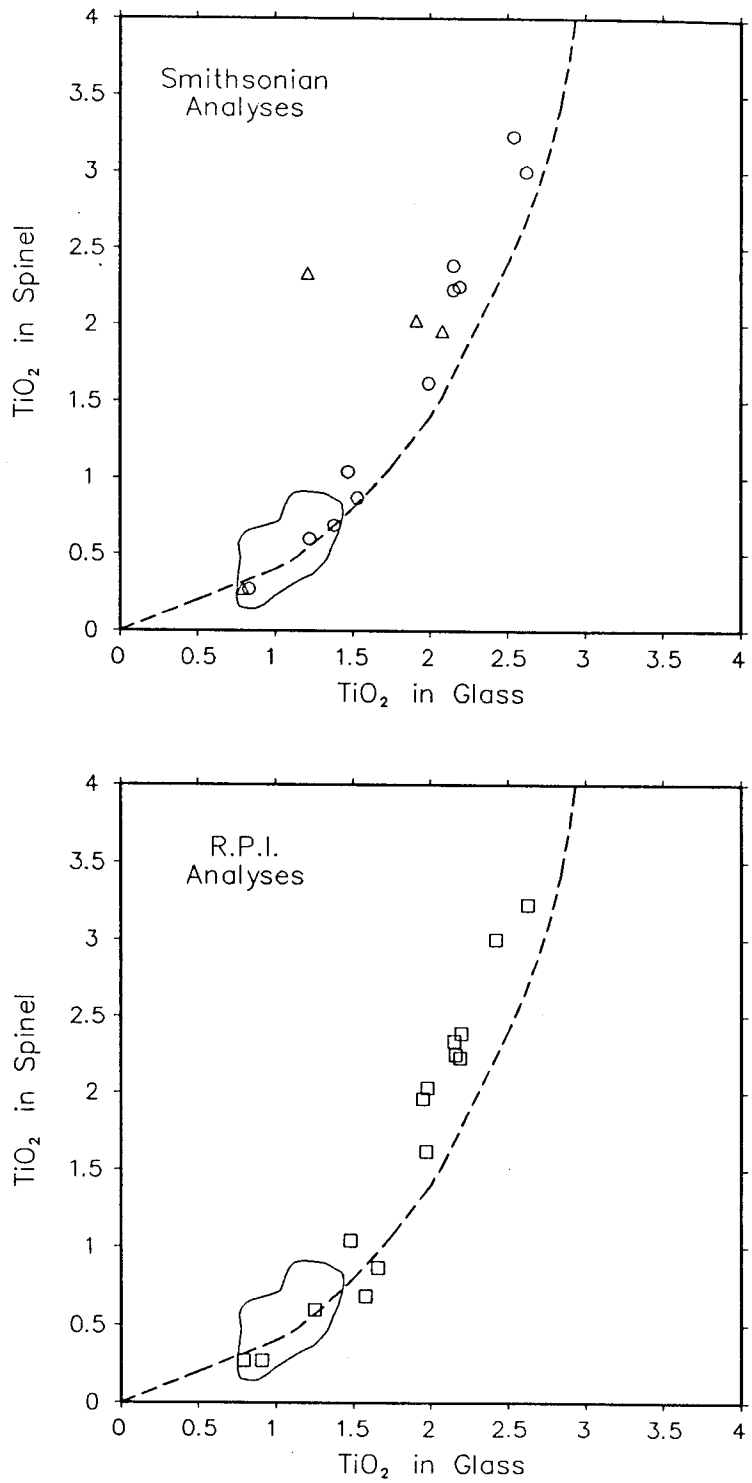

Figure 44. Comparison of partitioning of TiO_2 between chromian spinel and melt based on "anomalous" (circles) and "normal" (triangles) Smithsonian analyses of the Blanco Trough glasses, and those performed at R.P.I. Dashed line is exponential curve fit for spinel-glass pairs from Evans (1987). Field bordered by solid line is for Lamont seamount spinels.

spinels). The Blanco Trough glasses have normal TiO_2 content for their range of MgO (Figs. 27, 31), so that the melt from which the cores crystallized would have to be relatively TiO_2-depleted (0.79 as compared to 1.48 in VG-342). Rapid re-equilibration of the cores with respect to TiO_2 is a possibility, but this reaction is probably sluggish due to the necessity of a coupled substitution in order to maintain the charge balance (e.g. $FeO + TiO_2 = Al_2O_3$). A second consideration is the fact that the presence of TiO_2 in spinel requires inverse structure, while the chromian spinels in MORB are dominated compositionally by endmembers with normal structure.

The alternative to a magma mixing or xenocrystic origin for the Cr-rich cores would be a change in the intensive parameters in the melt leading to a change in spinel composition. Because the partitioning of Cr^{3+} and Fe^{3+} is sensitive to such parameters as temperature and f_{O2}, it is possible that changing melt conditions, particularly during ascent, could lead to changes in the equilibrium spinel composition for a relatively static melt composition, similar to the pressure effect observed in the experiments of Green et al. The lack of zoned olivines in VG-373, like those seen in VG383, is further circumstantial evidence against magma mixing.

4.5.3 Plagioclase-Melt Equilibria.

Plagioclase is either absent or present only as a minor phenocryst phase in the majority of the Blanco Trough samples. Due to the small grain size of the plagioclase laths that are present, as well as the fact that the early focus of this study was olivine and chromian spinel chemistry, microprobe analyses of plagioclase grains were only obtained for six samples (Table XI). Laths appear homogeneous in backscattered electron images, indicating that any zoning which may be present is minor. Figure 45 shows that the range of plagioclase compositions found in the samples which were analysed is between An_{77} and An_{66}. Phase equilibria studies have shown that the composition of plagioclase is dependent on such parameters as temperature and the partial pressure of H_2O (Kudo and Weill, 1970; Mathez, 1973; Drake, 1976). In light of these complications, it is not surprising that the distribution coefficient:

$$K_D^{Pl/L} = (X_{Ca}/X_{Na})^{plagioclase}(X_{Na}/X_{Ca})^{liquid}$$

Table XI

Average plagioclase phenocryst compositions for the Blanco Trough glasses.

Sample	*VG-169*	*σ*	*VG-347*	*σ*	*VG-356*	*σ*
SiO_2	50.82	±0.34	50.53	±0.56	51.54	±0.29
Al_2O_3	30.03	±0.16	30.68	±0.59	29.49	±0.25
FeO	0.49	±0.03	0.68	±0.19	0.89	±0.07
CaO	14.86	±0.29	14.52	±0.23	13.69	±0.22
K_2O	0.06	±0.01	0.04	±0.01	0.07	±0.01
Na_2O	3.24	±0.15	3.23	±0.11	3.73	±0.10
Total	99.50		99.68		99.41	
n	6		4		6	
An	71.5		71.1		66.7	
Ab	28.2		28.6		32.9	
Or	1.2		0.8		1.2	
$K_D^{Pl/L}$(Sm)	1.19		1.18		1.50	
$K_D^{Pl/L}$(RPI)	1.21		1.16		1.34	

Sample	*VG-373*	*σ*	*VG-376*	*σ*	*VG-385*	*σ*
SiO_2	49.25	±0.48	50.94		49.73	±0.17
Al_2O_3	30.93	±0.15	29.98		31.13	±0.15
FeO	0.67	±0.02	0.87		0.57	±0.13
CaO	15.69	±0.33	13.95		14.74	±0.09
K_2O	0.02	±0.01	0.07		0.03	±0.01
Na_2O	2.87	±0.27	3.57		3.20	±0.06
Total	99.43		99.38		99.40	
n	2		1		3	
An	75.0		68.1		71.7	
Ab	24.8		31.5		28.2	
Or	0.5		1.3		0.6	
$K_D^{Pl/L}$(Sm)	1.14		1.00		1.24	
$K_D^{Pl/L}$(RPI)	1.20		1.03		1.21	

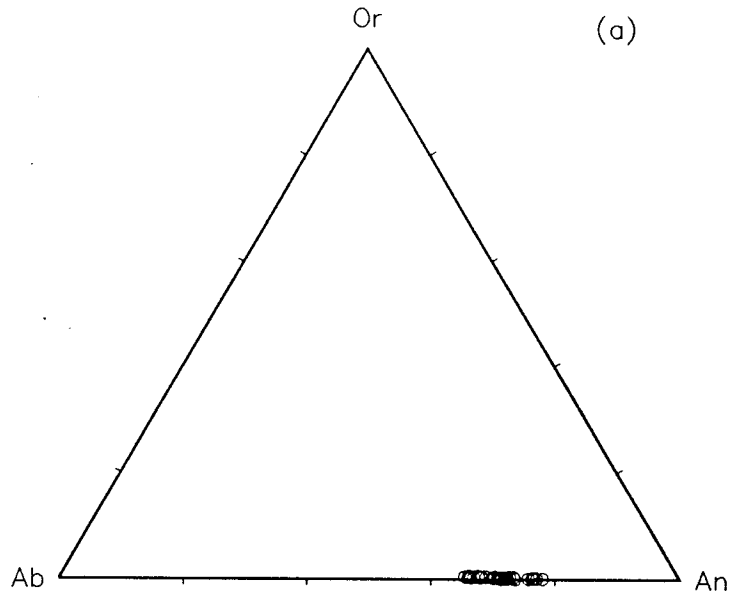

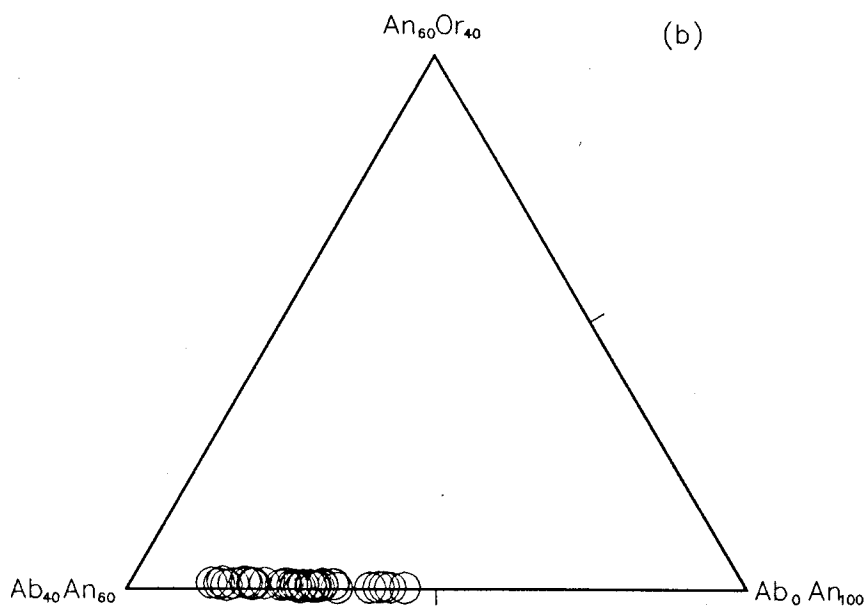

Figure 45. Composition of plagioclase phenocrysts found in the Blanco Trough glasses (a) plotted in the anorthite-albite-orthoclase ternary, and (b) detail of lower right corner of ternary.

found in low pressure experimental studies is not a single value, but displays a range of values (1.2-1.4)(Eissen et al., 1989). The resolution on the estimate of the degree of plagioclase-liquid equilibrium is, therefore, not as good as for olivine-liquid. $K_D^{Pl/L}$ values calculated using both glass data sets are similar, and none are very far from the expected range (Table XI).

Figure 46 demonstrates that for both sets of analyses, the An content of the plagioclase increases as a function of Ca/(Ca + Na) in the melt, as would be expected, although the slopes of the two lines are quite different. The significance of this difference is difficult to estimate due to the small size of the database.

4.6 Reconciling the Two Data Sets.

The disagreement between the Smithsonian analyses of the Blanco Trough glasses and those performed at Rensselaer Polytechnic Institute appears to come primarily from FeO* and CaO. Table XII lists the VG-2 normalized compositions for VG-348, which is at the primitive end of the suite, and VG-360 at the evolved end. The analyses match very well, with the exception of FeO*, which is considerably higher, and CaO, which is considerably lower in the Smithsonian VG-348. The opposite relationship holds for the two analyses of VG-360. Figure 47 is a plot of Mg# against Ca#, in which it can be seen that the R.P.I. glass compositions display the expected positive correlation between these two parameters, while the Smithsonian data shows a distribution which cannot be explained in a cogenetic suite, even given oxidizing conditions and large amounts of chromian spinel crystallization. This is a very strong indication that the Smithsonian FeO* and CaO numbers are in error, and that the conditions in the magma are more reducing, as implied by the R.P.I. analyses in Figure 35. The difference between the two sets of data has already been shown to be something other than a calibration error (Fig. 36), and the coherence of the FeO* and CaO variations in Figure 30 does not seem to indicate that the numbers are random, as might be the case if the microprobe spectrometers measuring these two elements had simply failed, so that a satisfactory explanation is still lacking.

Figure 48a is a plot of the FeO* values measured at the Smithsonian against those measured at R.P.I. and, with the exception of a few samples that plot close to the one-to-one line, the majority of the analyses fall along a trend at a high angle to the expected trend. A similar plot for CaO (Fig. 48b)

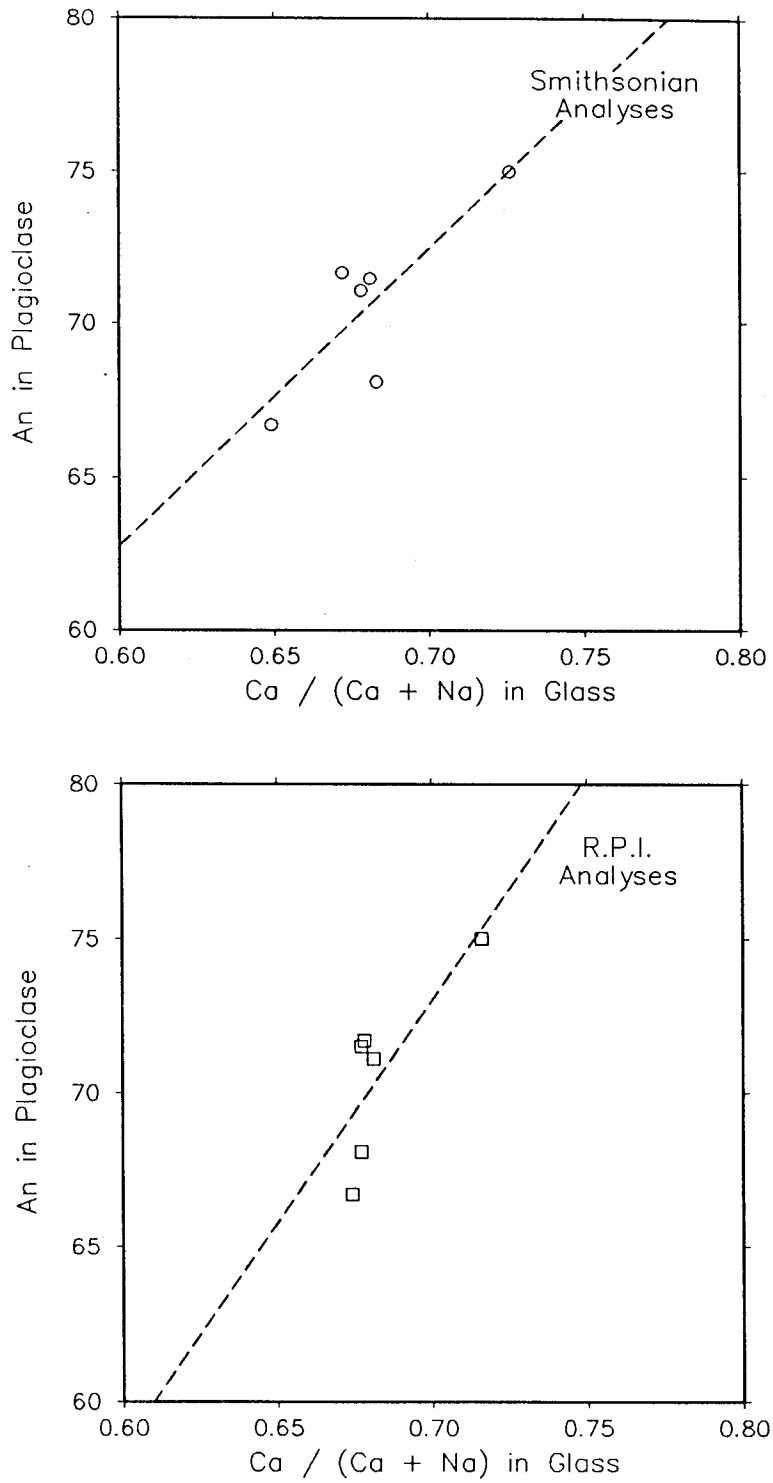

Figure 46. Comparison of anorthite in plagioclase as a function of Ca/(Ca + Na) in the melt based on Smithsonian and R.P.I. Blanco Trough glass analyses. Dashed line is best straight-line fit to the data.

Table XII

Comparison of VG-2 normalized analyses of primitive and evolved glasses from the Blanco Trough performed by the Smithsonian and at Rensselaer Polytechnic Institute.

Sample	*1*	*2*	*3*	*4*
SiO_2	48.34	48.01	50.15	50.33
TiO_2	0.83	0.89	2.54	2.56
Al_2O_3	17.56	17.73	14.73	14.99
FeO*	12.42	10.41	11.08	11.97
MgO	8.80	8.80	6.56	6.59
CaO	9.71	11.59	11.27	10.25
Na_2O	2.37	2.42	2.98	2.73
K_2O	0.06	0.09	0.39	0.41
Total	100.15	99.94	99.99	99.83
Mg#	55.8	60.1	51.3	49.5
Ca#	69.4	72.6	67.6	67.5
CaO/Al_2O_3	0.553	0.654	0.765	0.684

(1) Smithsonian analysis of VG-348.
(2) RPI analysis of VG-348.
(3) Smithsonian analysis of VG-360.
(4) RPI analysis of VG-360.

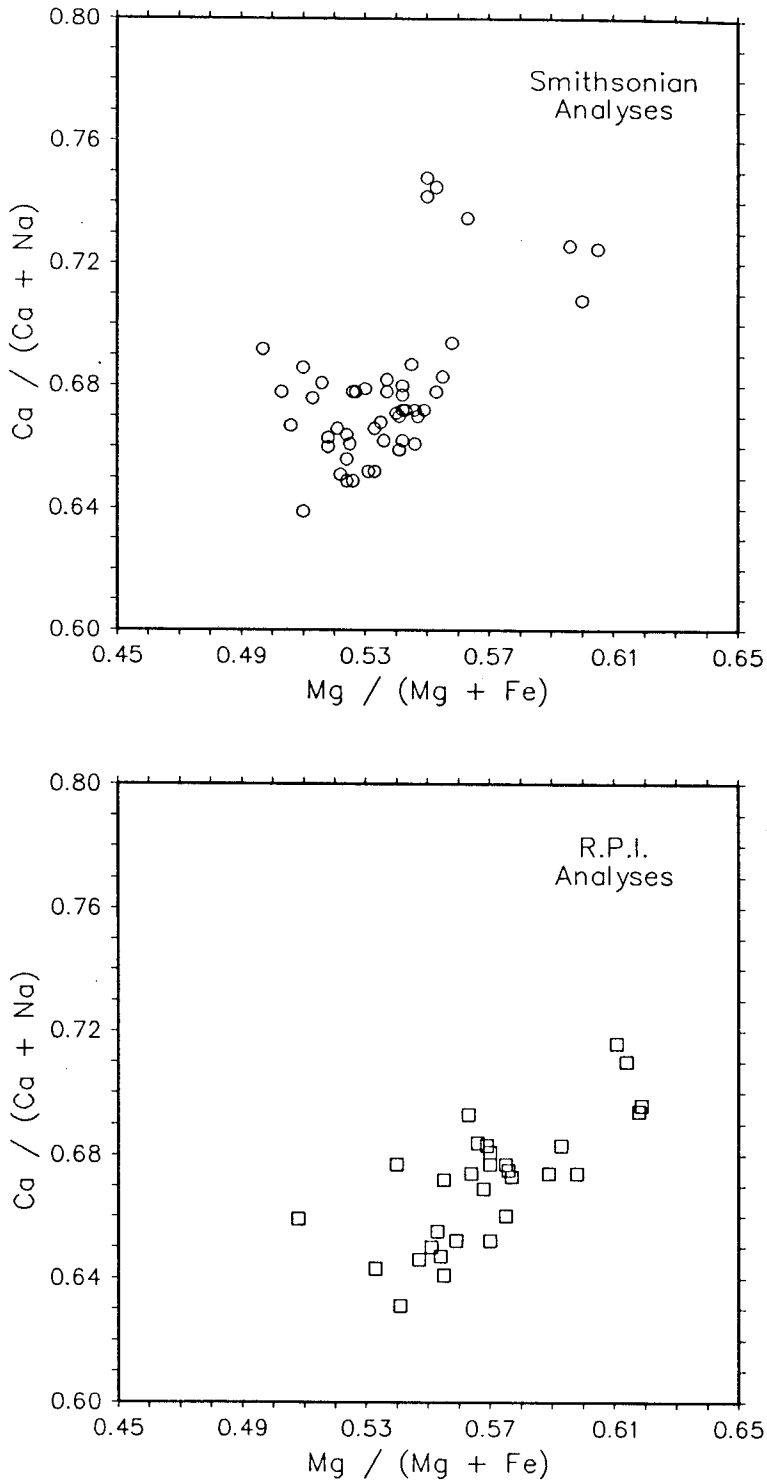

Figure 47. Comparison of Ca/(Ca + Na) vs. Mg/(Mg + Fe) in the melt based on Smithsonian and R.P.I. analyses of the Blanco Trough glasses.

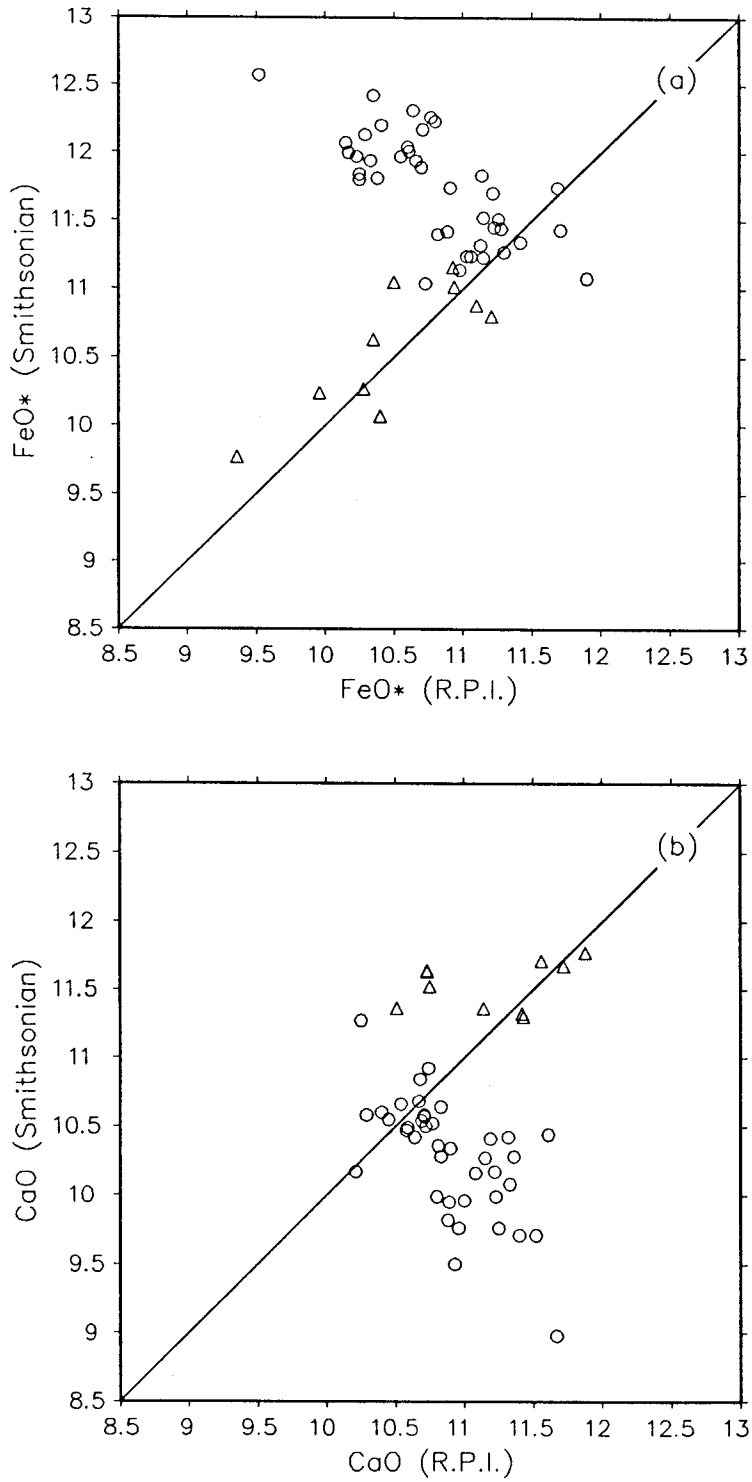

Figure 48. Plots comparing Smithsonian and R.P.I. values for (a) FeO* and (b) CaO in the Blanco Trough glasses. Note that there are two different trends apparent in each plot, one representing the "normal" (triangles) and one the "anomalous" (circles) Smithsonian analyses.

gives similar results, but with the majority of samples falling in the lower-right half of the diagram. This suggests that what has been reported as FeO* in the Smithsonian analyses is actually another oxide, and the same with CaO. Figure 49 shows the result of switching the Smithsonian FeO* and CaO values from Figure 48. In these plots it becomes apparent that the what originally seemed to be anomalies are actually the result of transposing the values for the two oxides, along with slight differences in calibration. The higher abundance of CaO relative to FeO* in the more primitive samples explains the suggestion from the partitioning data that the melt contains a large Fe_2O_3 component. Because the general abundances of these two oxides tends to be so similar in MORB, switching their values would not become obvious upon examining a few analyses, however for a relatively large set of closely related basalts the result is a seemingly anomalous suite of rocks.

4.7 Summary.

The two sets of electron microprobe analyses that exist for the suite of basaltic glasses recovered from the Blanco Trough disagree in their FeO* and CaO values, with each suggesting a very different petrogenesis. The Smithsonian analyses plot in a region of the Ol-Di-Pl-SiO_2 tetrahedron which suggests that they represent a high pressure trend, possibly in equilibrium with olivine + orthopyroxene. The major element variations imply that the phases dominating the observed trends are olivine and chromian spinel. The crystal/melt partitioning data are consistent with an unusually large Fe_2O_3 component in the melt, which could explain the variation in liquidus phases, and thus the suite's position in Ol-Di-Pl-SiO_2 space.

The analyses performed on the microprobe at R.P.I. plot in the region expected for primitive MORB in the Ol-Di-Pl-SiO_2 tetrahedron. The major element variations are consistent with other MORB suites, implying that they may be the product of a combination of variation in degree of partial melting of a peridotitic source and fractional crystallization of olivine + plagioclase ± chromian spinel ± clinopyroxene. Partitioning data are consistent with more reducing conditions in the melt, similar to what has been reported for other MORB suites, with a slight degree of Fe-enrichment in the more primitive samples.

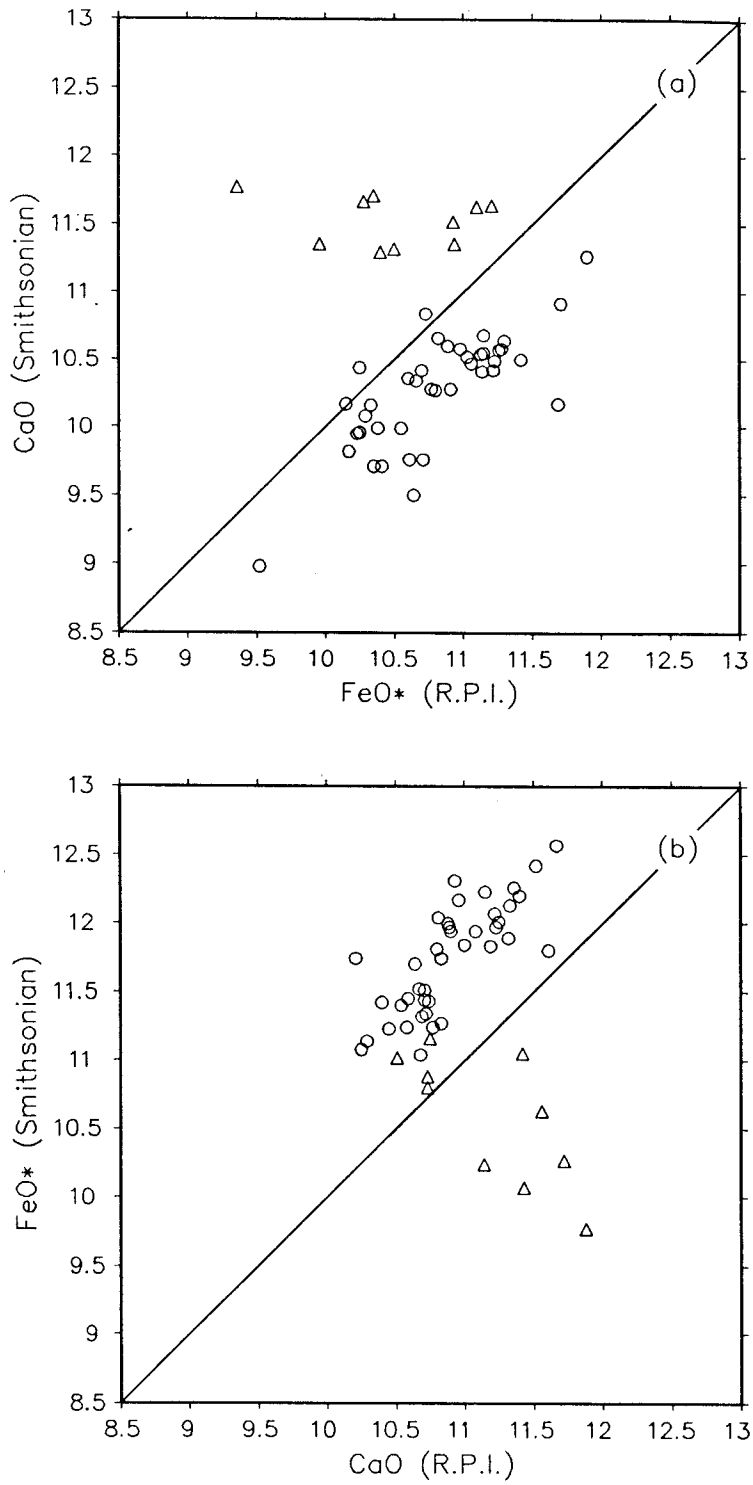

Figure 49. Plots showing the effect of transposing the Smithsonian values for (a) FeO* and (b) CaO in the Blanco Trough glasses with respect to the R.P.I. values. Note that in these plots the "anomalous" Smithsonian analyses (circles) fall close to the one-to-one line, while the "normal" analyses (triangles) do not.

The disagreement between the two data sets appears to be the result of a transposition of the FeO* and CaO abundances in the Smithsonian analyses, in addition to minor differences in calibration between the two laboratories.

5. Discussion and Conclusions.

5.1 Discussion.

The original electron microprobe analyses of basaltic glasses recovered from the Blanco Trough plot in a region of Ol-Di-Pl-SiO_2 space that is indicative of liquids in equilibrium with olivine + orthopyroxene ± clinopyroxene at high pressure (Fig. 50a). Given the present state of controversy surrounding the nature of primary MORB (e.g. Fujii, 1989; Elthon, 1989), a suite of MORB glasses that had equilibrated with harzburgite or lherzolite at 10-15 kb, and was not subsequently modified by low pressure processes, would be very important. Although thin sections of the glasses contain no orthopyroxene, olivine and chromian spinel are abundant and plagioclase is either absent or sparse, consistent with the primitive nature of these samples.

A re-analysis of the original mounts indicates that the Smithsonian analyses are in error, and that the Blanco Trough glasses represent ordinary primitive MORB. The new glass analyses plot along the olivine-diopside join in the plagioclase projection onto the olivine-diopside-silica plane (Fig. 50b), a common region for primitive MORB glasses. The source of the error in the Smithsonian data is a transposition of the FeO* and CaO values at some point prior to their publication by Melson et al. (1977). This causes the suite to appear quite anomalous, due to the fact that FeO* behaves incompatibly and CaO behaves compatibly during the early stages of tholeiite crystallization. Because the two oxides are present in similar abundances in most MORB glasses, switching their values in an analysis might not be apparent unless a relatively large number of closely related samples were involved.

CaO is more abundant than FeO* in the more primitive glasses, so that calculation of iron-magnesium $K_D^{Ol/L}$ values based on the Smithsonian analyses gives the impression that there is a large Fe_2O_3 component in the melt. As the actual abundance of FeO* increases and CaO decreases in the melt, their ratio approaches one, and the Smithsonian K_D* values approach the nominal value of 0.30 found by Roeder and Emslie (1970). This gives the impression that Fe_2O_3 is decreasing in the melt, thus increasing the Fe^{2+}/Fe^{3+} ratio drastically.

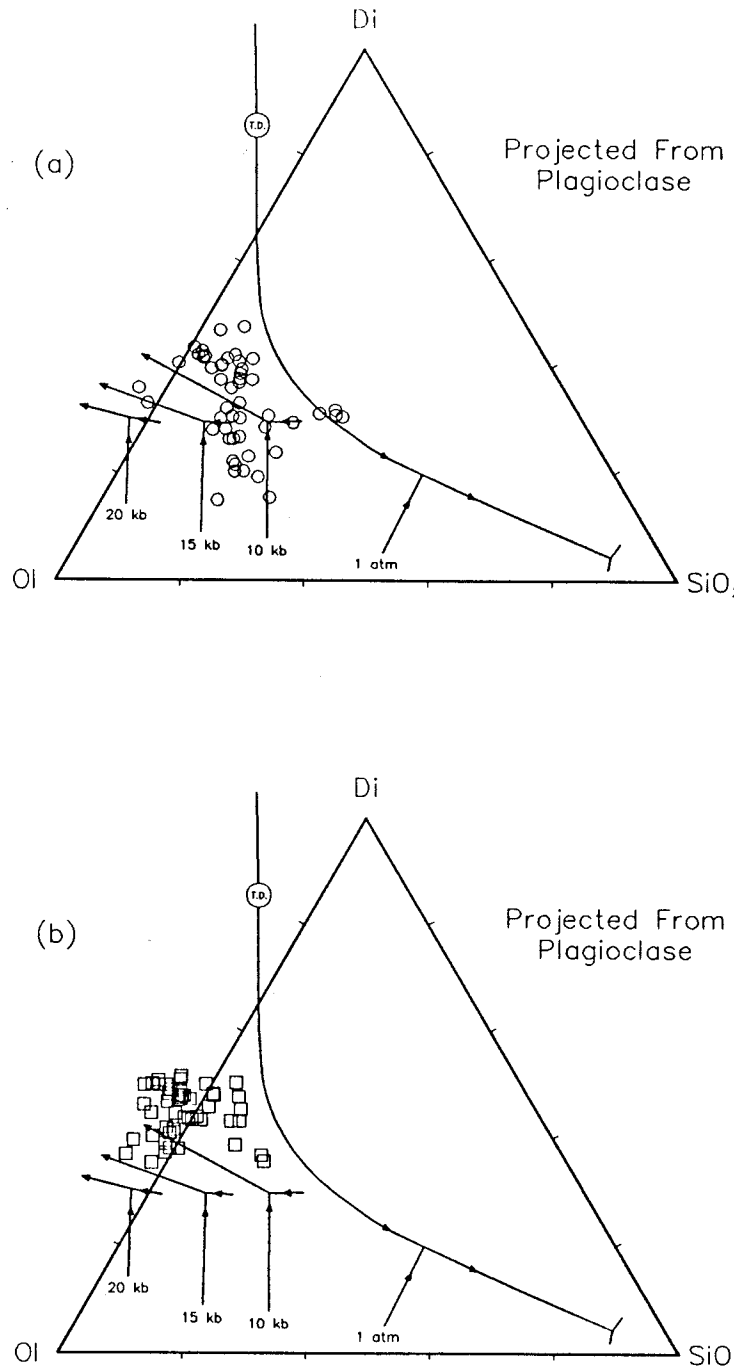

Figure 50. Comparison of (a) Smithsonian and (b) Rensselaer Polytechnic Institute analyses of the Blanco Trough glasses in the projection from plagioclase onto the olivine-diopside-olivine plane.

Recognition of the importance of glass compositions to the study of MORB petrogenesis has grown rapidly over the past 15 years. Studying the glass rind on pillow basalts allows the petrologist to get a clearer picture of the liquid composition, as well as the partitioning of elements between crystalline phases and the melt. Because acquiring new MORB samples is relatively difficult, the entire database of Melson et al. (1977) needs to be re-examined to insure that all analyses are accurate, although the number of samples involved in the FeO*/CaO transposition is likely to be small. Determining which of the analyses are incorrect will be difficult, given the similarity in the abundance of CaO and FeO* in most MORB.

The new glass analyses have been divided into three groups, based on Mg/(Mg + Fe) ratio, and plotted in Ol-Di-Pl-SiO_2 space in Figure 51. The triangles represent the most primitive samples ($Mg/(Mg + Fe) \geq 0.59$), the circles are slightly more evolved ($0.58 \geq Mg/(Mg + Fe) \geq 0.55$), and the squares are the most evolved samples ($Mg/(Mg + Fe) \leq 0.54$). It can be seen that in a qualitative way, the relative positions of the three groups are not inconsistent with a parental magma near Stolper's 15 kb olivine + clinopyroxene cotectic, that crystallizes olivine ± chromian spinel until reaching plagioclase saturation, and subsequently follows a cotectic which is sub-parallel to that of Walker et al. (1979). There is a great deal of overlap between the three groups, however, so that this interpretation is far from unique. Presnall and Hoover (1984) showed that microprobe analytical uncertainties, especially in SiO_2, can cause significant uncertainty in the position of analyses relative to the quartz apex in the normative plot used here. Figure 52 shows the 15 analyses of the VG-2 basaltic glass standard that were performed while re-analyzing the Blanco Trough samples (App. 1) plotted on the plagioclase and diopside projections. It is evident that a single sample analyzed many times in the same laboratory can indeed show a considerable range of locations. Given this type of uncertainty, it is difficult to quantitatively evaluate the relative positions of the samples in the Blanco Trough suite.

The least-squares mixing model of Bryan, Finger and Chayes (1968) was used in an attempt to quantify the petrogenesis of the suite. Three of the most primitive samples (VG-345, VG-348, and VG-373) were chosen as possible parental compositions for the rest of the suite. Olivine, chromian

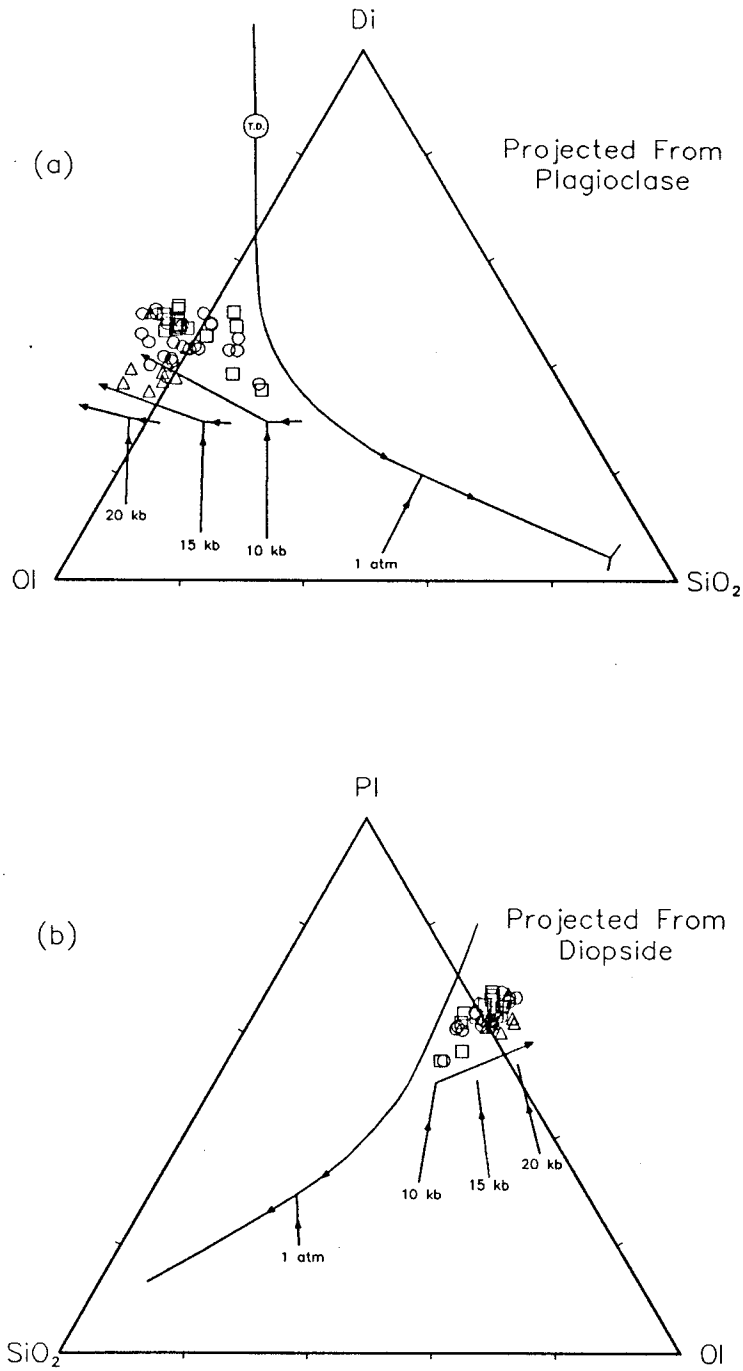

Figure 51. R.P.I. analyses of the Blanco Trough glasses grouped by Mg/(Mg + Fe) and projected from (a) a plagioclase onto the olivine-diopside-silica plane, and (b) diopside onto the olivine-plagioclase-silica plane. Groups consist of samples with Mg/(Mg + Fe) ≥ 0.59 (triangles), 0.58 ≥ Mg/(Mg + Fe) ≥ 0.55 (circles) and Mg/(Mg + Fe) ≤ 0.54 (squares).

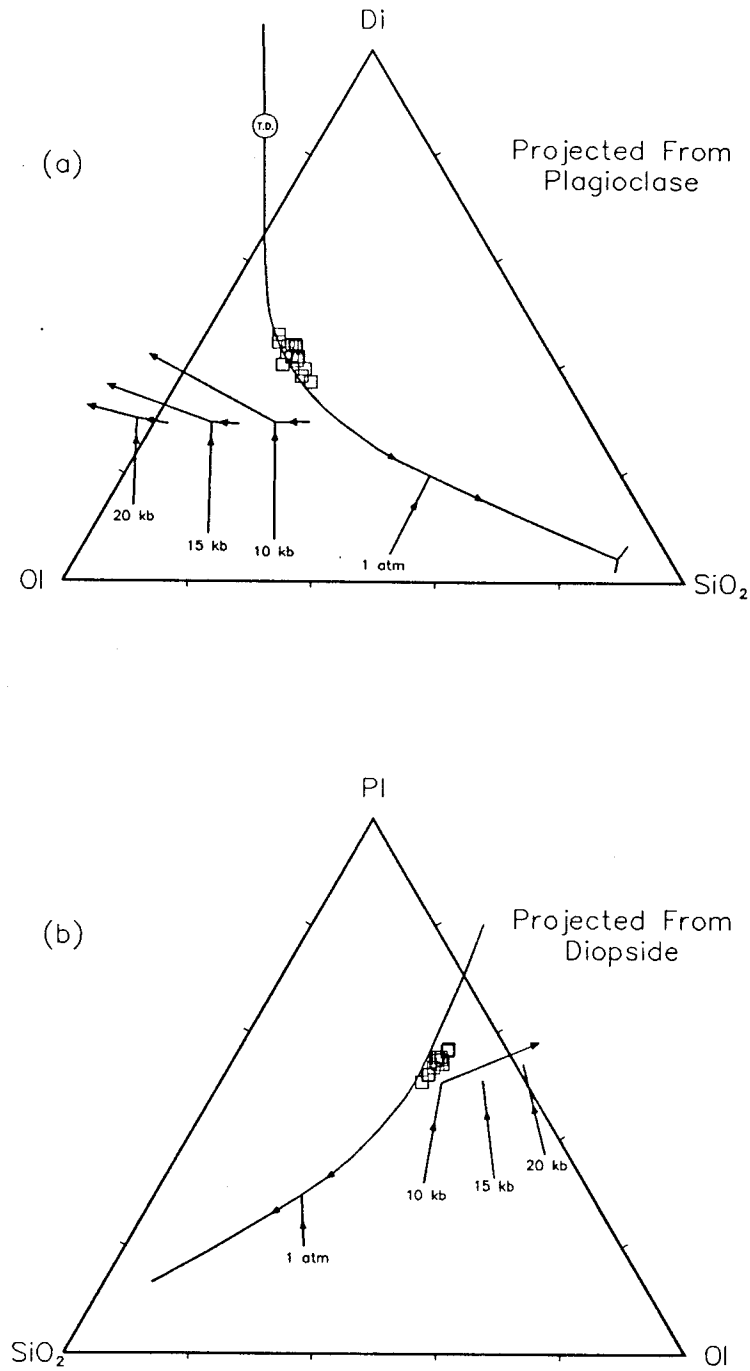

Figure 52. 15 analyses of the VG-2 basaltic glass standard performed during analysis of the Blanco Trough glass at R.P.I. projected (a) from plagioclase onto the olivine-diopside-silica plane, and (b) from diopside onto the olivine-plagioclase-silica plane.

spinel and plagioclase of various compositions (Tables VI, IX, XI) were added to two of the most highly evolved samples to try and reproduce the parental compositions. The best fit (App. 4) was achieved using VG-345 as the parental magma and VG-384 as the evolved end-member. A considerable mismatch was found for CaO, however, using a model that requires crystallization of 9.44 wt.% olivine with 21.72 wt.% plagioclase, and the *addition* of 1.69 wt.% chromian spinel to the magma, a petrogenesis which seems unlikely based on petrographic evidence. When clinopyroxene is added to the model a good fit is obtained, requiring crystallization of 4.98 wt.% olivine, 0.81 wt. % chromian spinel, 15.73 wt. % plagioclase and 8.20 wt.% clinopyroxene. Crystallization in these proportions might be a reasonable if clinopyroxene were present as a phenocryst phase in any of the samples. The need for clinopyroxene crystallization to model the petrogenesis of a MORB suite which contains no clinopyroxene phenocrysts is a paradox that is not new to MORB petrology (e.g. Francis, 1986). It is clear that the basalts in this suite are related by processes more complex than simple fractional crystallization in a shallow magma chamber, probably involving polybaric fractional crystallization of several batches of parental magma followed by mixing in a shallow level chamber prior to eruption.

5.2 Conclusions.

(1) The Blanco Trough glasses do not represent liquids in equilibrium with an assemblage of olivine + orthopyroxene at 10-15 kb as implied by the Smithsonian analyses. Their presence in an unusual region of the Ol-Di-Pl-SiO_2 tetrahedron is due to a transposition of FeO* and CaO values at some point prior to publication of the data by Melson et al. (1977).

(2) The oxidation state of the Blanco Trough glasses is similar to that of other mid-ocean ridge basalts, with an f_{O2} approximately 2 $\log_{10}$ units more reduced than NNO at 1200° C (Christie et al., 1986). The apparently large Fe_2O_3 component in the melt indicated by the Smithsonian analyses is due to the higher abundance of CaO relative to FeO* in the primitive samples.

(3) Based on the electron microprobe analyses performed at Rensselaer Polytechnic Institute, the Blanco Trough glasses represent primitive MORB that are slightly enriched in FeO* and Al_2O_3, while being slightly depleted in CaO.

(4) All of the Blanco Trough glasses are saturated in olivine (Fo_{86} - Fo_{81}), 62% are saturated in chromian spinel, and 62% contain some plagioclase. The abundance of plagioclase ranges from sparse in the majority of samples, to very abundant in VG-169. Most olivine phenocrysts are unzoned, and are close to being equilibrium with the liquid based on the R.P.I. data (for $K_D^{Ol/L} = 0.30$).

(5) Large subhedral olivines which display deformation bands occur in several samples, and are xenocrystic. They are likely to be cumulate in origin, based on a few microprobe analyses. Further work is needed to determine the compositions of all of these grains, and to better characterize the deformation bands. Because the slip system responsible for plastic deformation in olivine is dependent on temperature and pressure (Carter, 1976), the deformation bands can help to constrain the origin of the xenocrysts.

(6) Least-squares mixing models show that the primitive and evolved ends of the suite cannot be related by simple fractional crystallization of olivine, chromian spinel and plagioclase. A model incorporating clinopyroxene crystallization gives a good fit, but clinopyroxene was not found in any of the samples. This implies that a number of processes must have been involved in the petrogenesis of the suite, such as polybaric fractional crystallization of several batches of parental magma followed by mixing in a shallow level magma chamber.

(7) Given the importance of glass compositions to the study of MORB petrogenesis, the database of Melson et al. (1977) needs to be re-examined. Although the majority of the analyses are accurate, a relatively small number have had their FeO* and CaO values switched. Recognizing the analyses that are erroneous will not be a simple task because the abundances of FeO* and CaO are so similar in most MORB.

References.

Allan, J.F., Batiza, R., Perfit, M.R., Fornari, D.J. and Sack, R.O., 1989, Petrology of lavas from the Lamont seamount chain and adjacent East Pacific Rise, 10° N: *Journal of Petrology*, v. 30, 1,245-1,298.

Allan, J.F., Sack, R.O., and Batiza, R., 1988, Cr-rich spinels as petrogenetic indicators: MORB-type lavas from the Lamont seamount chain, eastern Pacific: *American Mineralogist*, v. 73, p. 741-753.

Atwater, T.M., 1970, Implications of plate tectonics for the Cenozoic tectonic evolution of western North America: *Geological Society of America Bulletin*, v. 81, p. 3,513-3,536.

Atwater, T.M., 1989, Plate tectonic history of the northeast Pacific and western North America, in, Winterer, E.L., Hussong, D.M., and Decker, R.W., eds., *The Eastern Pacific Ocean and Hawaii*, Geological Society of America, The Geology of North America, v. N, p. 21-72.

Atwater, T.M., and Menard, H.W., 1970, Magnetic lineations in the northeast Pacific: *Earth and Planetary Science Letters*, v. 7, p. 445-450.

Atwater, T.M., and Mudie, J.D., 1968, Block Faulting on the Gorda rise: *Science*, v. 159, p.729-731.

Atwater, T.M., and Mudie, J.D., 1973, Detailed near-bottom geophysical study of the Gorda rise: *Journal of Geophysical Research*, v. 78, p. 8,665-8,686.

Barnes, S.J., 1986, The distribution of chromium among orthopyroxene, spinel and liquid at atmospheric pressure: *Geochimica et Cosmochimica Acta*, v. 50, p. 1,889-1,909.

Basaltic Volcanism Study Project, 1981, *Basaltic Volcanism on the Terrestrial Planets*. Pergammon press, Inc., 1,286 pp.

Bender, J.F., Hodges, F.N., and Bence, A.E., 1978, Petrogenesis of basalts from the project FAMOUS area: experimental study from 0 to 15 kbars: *Earth and Planetary Science Letters*, v. 41, p. 277-302.

Bender, J.F., Langmuir, C.H., and Hanson, G.N., 1984, Petrogenesis of basalt glasses from the Tamayo region, East Pacific Rise: *Journal of Petrology*, v. 25, p. 213-254.

Bryan, W.B., 1972, Morphology of quench crystals in submarine basalts: *Journal of Geophysical Research*, v. 77, p. 5,812-5,819.

Bryan, W.B., 1983, Systematics of modal phenocryst assemblages in submarine basalts: petrologic implications: *Contributions to Mineralogy and Petrology*, v. 83, p. 62-74.

Bryan, W.B., Finger, L.W., and Chayes, F., 1969, Estimating proportions in petrographic mixing equations by least-squares mixing approximation: *Science*, v. 163, p. 926-927.

Bryan, W.B., and Moore, J.G., 1977, Compositional variations of young basalts in the Mid-Atlantic Ridge rift valley near lat 36° 49′ N: *Geological Society of America Bulletin*, v. 88, p. 556-570.

Bryan, W.B., Thompson, G., and Ludden, J.N., 1981, Compositional variation in Normal MORB from 22′ - 25° N: Mid-Atlantic Ridge and Kane Fracture Zone: *Journal of Geophysical Research*, v. 86, p. 11,815-11,836.

Byerly, G.R., 1980, The nature of differentiation trends in some volcanic rocks from the Galapagos spreading center: *Journal of Geophysical Research*, v. 85, p. 3,797-3,810.

Byerly, G.R., Melson, W.G., Nelen, J.A. and Jarosewich, E., 1977, Abyssal basaltic glasses as indicators of magma compositions: *Smithsonian Contributions to the Earth Sciences*, v. 19, p. 22-30.

Byerly, G.R., Melson, W.G., and Vogt. P.R., 1976, Rhyodacites, andesites, ferrobasalts, and oceanic tholeiites from the Galapagos spreading center: *Earth and Planetary Science Letters*, v. 30, p. 215-221.

Byrne, T., 1979, Late Paleocene demise of the Kula-Pacific spreading center: *Geology*, v. 7, p. 341-344.

Carmichael, I.S.E., 1967, The iron-titanium oxides of salic volcanic rocks and their associated ferromagnesian silicates: *Contributions to Mineralogy and Petrology*, v. 14, p. 36-64.

Carmichael I.S.E., and Ghiorso, M.S., 1986, Oxidation-reduction relations in basic magma: a case for homogeneous equilibria: *Earth and Planetary Science Letters*, v. 78, 200-210.

Carmichael, I.S.E, Turner, F.J., and Verhoogen, J., 1974, *Igneous Petrology*. McGraw-Hill Book Company, 739 pp.

Carter, N.L., 1976, Steady state flow of rocks: *Reviews of Geophysics and Space Physics*, v. 14, p. 301-360.

Christie, D.M., Carmichael, I.S.E., and Langmuir, C.H., 1986, Oxidation state of mid-ocean ridge basalt glasses: *Earth and Planetary Science Letters*, v. 79, p. 397-411.

Christie D.M., and Sinton, J.M., 1981, Evolution of abyssal lavas along propagating segments of the Galapagos spreading center: *Earth and Planetary Science Letters*, v. 56, p. 321-335.

Clague, D.A., Frey, F.A., Thompson, G., and Rindge S., 1981, Minor and trace element geochemistry of volcanic rocks dredged from the Galapagos spreading center: role of crystal fractionation and mantle heterogeneity: *Journal of Geophysical Research*, v. 86, p. 9,469-9,482.

Coney, P.J., 1978, Mesozoic-Cenozoic Cordilleran plate tectonics, in, Smith, R.B., and Eaton, G.P., eds., *Cenozoic Tectonics and Regional Geophysics of the Western Cordillera,* Geological Society of America Memoir, v. 152, p. 33-50.

Cooper, A.W., Scholl, D.W., and Marlow, M.S., 1976, Plate tectonic model for the evolution of the eastern Bering Sea Basin: *Geological Society of America Bulletin*, v. 87, p. 1,119-1,126.

Czamanske, G.K., and Moore, J.G., 1977, Composition and phase chemistry of sulfide globules in basalt from the Mid-Atlantic Ridge rift valley near 37°N lat: *Geological Society of America Bulletin*, v. 88, p. 587-599.

Davis, A.S., and Clague, D.A., 1987, Geochemistry, mineralogy and petrogenesis of basalts from the Gorda Ridge: *Journal of Geophysical Research*, v. 92, p. 10,467-10,483.

Deer, W.A., Howie, R.A., and Zussman, J., 1966, *An Introduction to the Rock-Forming Minerals.* Longman Group Limited, 528 pp.

Delaney, J.R., Johnson, H.P., Karsten, J.L., 1981, The Juan de Fuca ridge-hot spot-propogating rift system: new tectonic, geochemical, and magnetic data: *Journal of Geophysical Research*, v. 86, p. 11,747-11,750.

Delaney, J.R., Karsten, J.L., and Clague, D.A., 1982, Geochemistry of Juan de Fuca Ridge basaltic glass [abs.]: *EOS, Transactions of the American Geophysical Union*, v. 63, p. 1,147.

Delano, J.W., 1980, Chemistry and liquidus phase relations of Apollo 15 red glass: Implications for the deep lunar interior: *Proceedings of the Lunar and Planetary Science Conference, 11th,* p. 251-288.

Delano, J.W., 1990, Buoyancy-driven melt segregation on the Earth's Moon, I. Numerical results: *Proceedings of the Lunar and Planetary Science Conference, 20th,* p. 3-12.

Delano, J.W., Gaetani, G.A., and DeLong, S.E., 1990, Partitioning of Cr and Fe between spinel and basaltic melt as a function of temperature and oxygen fugacity [abs.]: *V.M. Goldschmidt Conference, Program and Abstacts*, p. 40.

Dick, H.J.B., and Bullen, T., 1984, Chromian spinel as a petrogenetic indicator in abyssal lavas and

alpine-type peridotites and spatially associated lavas: *Contributions to Mineralogy and Petrology*, v. 86, p. 54-76.

Drake, M.J., 1976, Plagioclase-melt equilibria: *Geochimica et Cosmochimica Acta*, v. 40, p. 457-465.

Dungan, M.A., and Rhodes, J.M., 1978, Residual glasses and melt inclusions in basalts from DSDP Legs 45 and 46: evidence for magma mixing: *Contributions to Mineralogy and Petrology*, v. 67, p. 417-431.

Eissen, J.-P., Juteau, T., Joron, J.-L., Dupre, B., Humler, E., and Al'Mukhamedov, A., 1989, Petrology and geochemistry of basalts from the Red Sea Axial Rift at 18° North: *Journal of Petrology*, v. 30, p. 791-839.

Elthon, D., 1989, Pressure of origin of primary mid-ocean ridge basalts, in, Saunders, A.D., and Norry, M.J., eds., *Magmatism in the Ocean Basins*, Geological Society Special Publications No. 42, p. 125-136.

Engebretson, D.C., 1982, *Relative motions between oceanic and continental plates in the Pacific basin*, Ph.D. thesis, Stanford University, 218 pp.

Engebretson, D.C., Cox, A., and Gordon, R.G., 1985, *Relative motions between oceanic and continental plates in the Pacific Basin,* Geological Society of America Special Paper No. 206.

Engel, A.E.J., Engel, C.G., and Havens, 1965, Chemical characteristics of oceanic basalts and the upper mantle: *Geological Society of America Bulletin*, v. 76, p. 719-734.

Evans, C.A., 1987, Oceanic magmas with alkalic characteristics; evidence from basal cumulate rocks in the Zambales ophiolite, Luzon, Philippine Islands, in, Morris, E.M., and Pasteris, J.D., *Mantle Metasomatism and Alkaline Magmatism*, Geological Society of America Special Paper No. 215, p. 139-150.

Falloon, T.J., and Green, D.H., 1987, Anhydrous partial melting of MORB pyrolite and other peridotite compositions at 10 kbar: implications for the origin of primitive MORB glasses: *Mineralogy and Petrology*, v. 37, p. 181-219.

Falloon, T.J., and Green, D.H., 1988, Anhydrous partial melting of peridotite from 8 to 35 kb and the petrogenesis of MORB, in, Menzies, M.A., and Cox, K.G., eds., *Oceanic and Continental Lithospheres: Similarities and Differences*, Journal of Petrology Special Volume, p. 379-414.

Falloon, T.J., Green, D.H., Hatton, C.J., and Harris, K.L., 1988, Anhydrous partial melting of a fertile and depleted peridotite from 2 to 30 kb and application to basalt petrogenesis: *Journal of Petrology*, v. 29, p. 1,257-1,282.

Fisk, M.R., and Bence, A.E., 1980, Experimental crystallization if chrome spinel in FAMOUS basalt 527-1-1: *Earth and Planetary Science Letters*, v. 48, p. 111-123.

Fornari, D.J., Perfit, M.R., Malahoff, A., and Embley, R., 1983, Geochemical studies of abyssal lavas recovered by DSRV *Alvin* from eastern Galapagos Rift, Inca Transform, and Ecuador Rift 1. Major element variations in natural glasses and spacial distribution of lavas: *Journal of Geophysical Research*, v. 88, p. 10,519-10,529.

Francis, D., 1986, The pyroxene paradox in MORB glasses - a signature of picritic parental magmas?: *Nature*, v. 319, p. 586-558.

Fujii, T., 1989, Genesis of mid-ocean ridge basalts, in, Saunders, A.D., and Norry, M.J., eds., *Magmatism in the Ocean Basins*, Geological Society Special Publications No. 42, p. 137-146.

Fujii, T., and Bougault, H., 1983, Melting relations of a magnesian abyssal tholeiite and the origin of MORBs: *Earth and Planetary Science Letters*, v. 62, p. 283-295.

Fujii, T., and Scarfe, C.M., 1985, Composition of liquids coexisting with spinel lherzolite at 10 kb and the genesis of MORBs: *Contributions to Mineralogy and Petrology*, v. 90, p. 18-28.

Green, D.H., Falloon, T.J., and Taylor, W.R., 1987, Mantle-derived magmas - roles of variable source peridotite and variable C-H-O fluid compositions, in, Mysen, B.O., ed., *Magmatic Processes: Physicochemical Principles*, The Geochemical Society Special Publication No. 1, p. 139-154.

Green, D.H., Hibberson, W.O., and Jacques, A.L., 1979, Petrogenesis of mid-ocean ridge basalts, in McElhinney, M.W., ed., *The Earth: Its Origin, Structure and Evolution*, p. 265-299.

Green, D.H., Ringwood, A.E., Hibberson, W.O. and Ware, N.G., 1975, Experimental petrology of Apollo 17 mare basalts: *Proceedings of the Lunar and Planetary Science Conference, 6th*. p. 871-893.

Green, D.H., Ringwood, A.E., Ware, N.G., Hibberson, W.O., and Major, A., 1971, Experimental petrology and petrogenesis of Apollo 12 basalts: *Proceedings of Lunar and Planetary Science Conference, 2nd*, p. 601-615.

Grow, J.A., and Atwater, T., 1970, Mid-Tertiary tectonic transition in the Aleutian Arc: *Geological Society of America Bulletin*, v. 81, p. 3,715-3,722.

Haggerty, S.E., 1976, Opaque mineral oxides in terrestrial igneous rocks rocks, in, Rumble, D., ed., *Oxide Minerals,* Mineralogical Society of America, Washington D.C., Short Course Notes v. 3.

Hey, R., 1977, A new class of "pseudofaults" and their bearing on plate tectonics: a propogating rift

model: *Earth and Planetary Science Letters*, v. 37, p.321-325.

Hey, R.N., Sinton, J.M., and Duennebier, F.K., 1989, Propogating rifts and spreading centers, in, Winterer, E.L., Hussong, D.M., and Decker, R.W., eds., *The Eastern Pacific Ocean and Hawaii*, Geological Society of America, The Geology of North America, v. N, p. 161-176.

Hey, R., and Wilson, D.S., 1982, Propogating rift explanation for the tectonic evolution of the northeast Pacific - the pseudomovie: *Earth and Planetary Science Letters*, v. 58, p. 167-188.

Hill, R., and Roeder, P., 1974, The crystallization of spinel from basaltic liquid as a function of oxygen fugacity: Journal of Geology, v. 82, p. 709-729.

Irvine, T.N., 1965, Chromian spinel as a petrogenetic indicator. Part 1. Theory: *Canadian Journal of Earth Sciences,* v. 2, p. 648-672.

Irvine, T.N., 1967, Chromian spinel as a petrogenetic indicator. Part 2. Petrologic applications: *Canadian Journal of Earth Sciences*, v. 4, p. 71-103.

Jaques, A.L., and Green, D.H., 1980, Anhydrous melting of peridotite at 0-15 kb pressure and the genesis of tholeiitic basalts: *Contributions to Mineralogy and Petrology*, v. 73, p. 287-310.

Johnson, H.P., and Holmes, M.L., 1989, Evolution in plate tectonics; The Juan de Fuca Ridge, in Winterer, E.L., Hussong, D.M., and Decker, R.W., eds., *The Eastern Pacific Ocean and Hawaii*, The Geology of North America, v. N, p. 73-91.

Johnson, H.P., Karsten, J.L., Delaney, J.R., Davis, E.E., Currie, R.G., and Chase, R.L., 1983, A detailed study of the Cobb offset of the Juan de Fuca ridge: evolution of a propogating rift: *Journal of Geophysical Research*, v. 88, p. 2,297-2,315.

Jones, J.H., 1988, Partitioning of Mg and Fe between olivine and liquids of lunar compositions: the roles of composition, pressure and Ti speciation [abs.]: *Abstracts of Papers Submitted to the Nineteenth Lunar and Planetary Science Conference*, p. 561-562.

Karsten, J.L., and Delaney, J.R., 1985, Comparison of glass geochemistry from seamount and adjacent ridge crest lavas [abs.]: *EOS, Transactions of the American Geophysical Union*, v. 66, p. 1,109.

Kilinc, A., Carmichael, I.S.E., Rivers, M.L., and Sack, R.O., 1983, Ferric-ferrous ratio of natural silicate liquids at 1 bar: *Contributions to Mineralogy and Petrology*, v. 83, p. 136-140.

Kirkpatrick, R.J., 1981, Kinetics of crystallization of igneous rocks, in Lasaga, A.C., and Kirkpatrick, R.J., eds., *Kinetics of Geochemical Processes,* Mineralogical Society of America, Washington, D.C., Reviews in Mineralogy, v. 8, p. 321-398.

Kirkpatrick, R.J., 1978, Processes of crystallization in pillow basalts, Hole 396B, DSDP Leg 46, in, *Initial Reports of the Deep Sea Drilling Project*, v. 46, p. 271-282.

Kudo, A.M., and Weill, D.F., 1970, An igneous plagioclase thermometer: *Contributions to Mineralogy and Petrology*, v. 25, p. 52-65.

Lange, R.A., and Carmichael, I.S.E., 1989, Ferric-ferrous equilibria in Na_2O-FeO-Fe_2O_3-SiO_2 melts: effects of analytical techniques on derived partial molar volume: *Geochimica et Cosmochimica Acta*, v. 53, p. 2,195-2,204.

Langmuir, C.H., and Bender, J.F., 1984, The geochemistry of oceanic basalts in the vicinity of transform faults: observations and implications: *Earth and Planetary Science Letters*, v. 69, p. 107-127.

Le Roex, A.P., 1987, Source regions of mid-ocean ridge basalts: evidence for enrichment processes, in, Menzies, M.A., and Hawkesworth, C.J., eds., *Mantle Metasomatism*, Academic Press, p. 389-422.

Longhi, J., Walker, D., and Hays, J.F., 1978, The distribution of Fe and Mg between olivine and lunar basaltic liquids: *Geochimica et Cosmochimica Acta*, v. 42, p. 1,545-1,558.

Mathez, E.A., 1973, Refinement of the Kudo-Weill plagioclase thermometer and its application to basaltic rocks: *Contributions to Mineralogy and Petrology*, v. 41, p. 61-72.

Mathez, E.A., 1976, Sulfur solubility and magmatic sulfides in submarine basalt glass: *Journal of Geophysical Research*, v. 81, p. 4,269-4,276.

Melson, W.G., 1969, Preliminary results of a geophysical study of portions of the Juan de Fuca Ridge and Blanco Fracture Zone. *Environmental Science Services Administration Technical Memorandum C & GSTM 6.*

Melson, W.G., Byerly, G.R., Nelen, J.A., O'Hearn, T., Wright, T.L., and Vallier, T., 1977, A catalog of the major element chemistry of abyssal volcanic glasses: *Smithsonian Contributions to the Earth Sciences*, v. 19 p. 31-60.

Menard, H.W. and Atwater, T.M., 1968, Changes in direction of sea floor spreading: *Nature*, v. 219, p. 463-467

Morse, S.A., 1980, *Basalts and Phase Diagrams: An Introduction to the Quantitative Use of Phase Diagrams in Igneous Petrology.* Springer-Verlag, 493 pp.

Murck, B.W., and Campbell, I.H., 1986, The effects of temperature, oxygen fugacity and melt composition on the behavior of chromium in basic and ultrabasic melts: *Geochimica et*

Cosmochimica Acta, v. 50, p. 1,871-1,887.

Mysen, B.O., 1975, Partitioning of Iron and Magnesium between crystals and partial melts in peridotite upper mantle: *Contributions to Mineralogy and Petrology*, v. 52, p. 69-76.

O'Hara, M.J., 1968, Are ocean floor basalts primary magma?: *Nature*, v. 220, p. 683-686.

Presnall, D.C., Dixon J.R., O'Donnell, T.H., and Dixon, S.A., 1979, Generation of mid-ocean ridge tholeiites: *Journal of Petrology*, v. 20, p. 3-35.

Presnall, D.C., and Hoover, J.D., 1984, Composition and depth of origin of primary mid-ocean ridge basalts: *Contributions to Mineralogy and Petrology*, v. 87, p. 170-178.

Presnall, D.C., and Hoover, J.D., 1986, Composition and depth of origin of primary mid-ocean ridge basalts - reply to D. Elthon: *Contributions to Mineralogy and Petrology*, v. 94, p. 257-261.

Presnall, D.C., and Hoover, J.D., 1987, High pressure phase equilibrium constraints on the origin of mid-ocean ridge basalts, in, Mysen, B.O., ed., *Magmatic Processes: Physicochemical Principles*, The Geochemical Society Special Publication No. 1, p. 75-89.

Raff, A.D., and Mason, R.G., 1961, Magnetic survey off the west coast of North America, 40° N. latitude to 52° N. latitude: *Geological Society of America Bulletin*, v. 72, p. 1,267-1,270.

Rhodes, J.M., Dungan, M.A., Blanchard, D.P., and Long, P.E., 1979, Magma mixing at mid-ocean ridges: evidence from basalts drilled near 22° N on the Mid-Atlantic Ridge: *Tectonophysics*, v. 55, p. 35-62.

Riddihough, R.P., 1982, One hundred million years of plate tectonics in western Canada: *Geoscience Canada*, v. 9, p. 28-34.

Riddihough, R.P., 1988, The northeast Pacific Ocean and margin, in, Nairn, A.E.M., Stehli, F.G., and Uyeda, S., eds., *The Pacific Ocean*, The Ocean Basins and Margins. v. 7B, p. 85-118.

Roeder, P.L., and Emslie, R.F., 1970, Olivine-liquid equilibrium: *Contributions to Mineralogy and Petrology*, v. 29, p. 275-289.

Sack, R.O., 1982, Spinels as petrogenetic indicators: Activity-composition relations at low pressures: *Contributions to Mineralogy and Petrology*, v. 79, p. 169-186.

Sigurdsson, H., and Shilling, J.-G., 1976, Spinels in Mid-Atlantic Ridge basalts: Chemistry and

occurence: *Earth and Planetary Science Letters*, v. 29, p. 7-20.

Sinton, J.M., Wilson, D.S., Christie, D.M., Hey, R.N., and Delaney, J.R., 1983, Petrologic consequences of rift propogation on oceanic spreading ridges: *Earth and Planetary Science Letters*, v. 62, p. 193-207.

Staudigel, H., and Bryan, W.B., 1981, Contrasted glass-whole rock compositions and phenocryst redistribution, IPOD sites 417 and 418: *Contributions to Mineralogy and Petrology*, v. 78, p. 255-262.

Stoddard, P.R., 1987, A kinematic model for the evolution of the Gorda plate: *Journal of Geophysical Research*, v. 92, p. 11,524-11,532.

Stolper, E., 1980, A phase diagram for mid-ocean ridge basalts: preliminary results and implications for petrogenesis: *Contributions to Mineralogy and Petrology*, v. 74, p. 13-27.

Stolper, E., and Walker, D., 1980, Melt density and the average composition of basalt: *Contributions to Mineralogy and Petrology*, v. 74, p. 7-12.

Stone, D.B., 1977, Plate tectonics, paleomagnetism and the tectonic history of the N.E. Pacific: *Geophysical Surveys*, v. 3, p. 3-37.

Takahashi, E., and Kushiro, I., 1983, Melting of a dry peridotite at high pressures and basalt magma genesis: *American Mineralogist*, v. 68, p. 859-879.

Thompson, R.N., 1987, Phase-equilibria constraints on the genesis and magmatic evolution of oceanic basalts: *Earth Science Reviews*, v. 24, p. 161-210.

Vacquier, V., 1959, Measurement of horizontal displacement along faults in the ocean floor: *Nature*, v. 183, p. 452-453.

Vacquier, V., Raff, A.D., and Warren, R.E., 1961, Horizontal displacements in the floor of the northeastern Pacific Ocean: *Geological Society of America Bulletin*, v. 72, p. 1,251-1,258.

Vine, F.J., 1966, Spreading of the ocean floor: new evidence: *Science*, v. 154, p. 1,405-1,415.

Vine, F.J., and Matthews, D.H., 1963, Magnetic anomalies over ocean ridges: *Nature*, v. 199, p. 947-949.

Vine, F.J., and Wilson, T.J., 1965, Magnetic anomalies over a young ridge off Vancouver Island: *Science*, v. 150, p. 485-489.

Vogt, P.R., and Byerly, G.R., 1976, Magnetic anomalies and basalt composition in the Juan de Fuca-Gorda ridge area: *Earth and Planetary Science Letters*, v. 33, p. 185-207.

Walker, D., DeLong, S.E., and Shibata, T., 1980, Crystal-ring microstructures in Oceanographer Fracture Zone basalts: *Contributions to Mineralogy and Petrology*, v. 74, p.1-6.

Walker, D., Shibata, T., and DeLong, S.E., 1979, Abyssal tholeiites from the Oceanographer Fracture Zone II: phase equilibria and mixing: *Contributions to Mineralogy and Petrology*, v. 70, p. 111-125.

Wilson, A.D., 1960, The micro-determination of ferrous iron in silicate minerals by a volumetric and colorimetric method: *Analyst*, v. 85, p. 823-827.

Wilson, D.S., Hey, R.N., and Nishimura, C., 1984, Propogation as a mechanism of reorientation of the Juan de Fuca ridge: *Journal of Geophysical Research*, v. 89, p. 9,215-9,225.

Wilson, J.T., 1965, Transform faults, oceanic ridges, and magnetic anomalies southwest of Vancouver Island: *Science*, v. 150, p. 482-485.

Yeats, R.S., and Mathez, E.A., 1976, Decorated vesicles in deep-sea basalt glass, eastern Pacific: *Journal of Geophysical Research*, v. 81, p. 4,277-4,284.